Evaluation of EMG, Force and Joystick as Control Interfaces for Active Upper-Extremity Movement-Assistive Devices

MSc. Thesis Dissertation

Joan Lobo Prat

TU Delft Delft University of Technology

Student Number: 4111958
Degree Program: Biomedical Engineering (BME)
Specialization: Biomechatronics (BM)

MSc. Thesis Advisors: Dr. ir. Arno H.A. Stienen
Prof. Dr. ir. Just L. Herder

PREFACE

Patients with Duchenne Muscular Dystrophy (DMD) gradually lose their ability to use their muscles as they grow older. Consequently, arm function decreases to the point that no movement is possible. The disease affects approximately 1 in every 3,500 live male births and with increasing life expectancy, the preservation of functional arm abilities in boys with DMD becomes crucial. Although some devices aiming to compensate for the loss of muscle function exist, they are only useful during the early stages of the disease and are highly stigmatizing.

The Flextension A(bility)-Gear project aims to develop an inconspicuous body-bound assistive device that can be worn underneath clothing and supports the arm for the independent execution of essential activities of daily living, adapting the support to the needs and capabilities of the user. In order to achieve this goal, several subprojects have been defined, one of them focusing on the control of the active orthosis, which must allow adaptive, intuitive and safe operation of the assistive device. The present work is one of the first steps to accomplish the goal of these subproject.

In March 2012, I was hired to work on the Flextension A-Gear project at the Department of Biomechanical Engineering from the University of Twente (Enschede, The Netherlands), while still carrying out my MSc. degree in Biomedical Engineering at the Delft University of Technology. This dissertation describes one of the research studies I carried out at the aforementioned department which holds a very close collaboration with the Delft University of Technology. The different parties involved in my supervision decided that I could carry out my MSc. graduation project in the framework of the Flextension project in order to accomplish both tasks.

The aim of the work described in this Dissertation was to evaluate different control interfaces to identify their limitations and capabilities. This knowledge will be used on the selection of the most suitable control interface for operating the aforementioned A-Gear. This work gave me the opportunity to become familiar with several sensors, data acquisition systems and signal processing methods as well as applying a significant part of the theory given during my MSc. degree.

Overall, I think I have provided to the scientific community relevant knowledge on the area of control interfaces for active upper-extremity movement-assistive devices that complement the existing literature. However, the reader should judge on his own. What I do know for sure is that the success of this work is the result of the collaboration with a multidisciplinary team. Therefore, I would like to express my deepest gratitude to my advisors, Dr. Arno Stienen, Edsko E.G. Heckman, Prof. Peter H. Veltink, Prof. (Bart) H.F.J.M. Koopman and Prof. Just L. Herder. I would equally like to thank my office-mates especially Arvid Q.L. Keemink, Serdar Ates, Israel Mora Moreno and Claudia J.W. Haarman, and all the memebers of the Flextnesion Research Group, for their support and encouragement. I would also like to thank Dr. Alfred Schouten, for his advice on system identification and Dr. Edwin van Asseldonk for his support on the statistical analysis. Grateful thanks as well to subjects 01, 02, 03, 04, 05, 06, 07 and 08 for their patience, predisposition and interest. Thanks to Diana Pavia Moreira and Joao Ramalhinho who provided crucial help for the development of the experimental set-up and assisted me during the measurements. Last but not least, thanks to Sara Busquets and my family for their help and moral support.

Joan Lobo Prat

10th July 2013

TABLE OF CONTENTS

Evaluation of EMG, Force and Joystick as Control Interfaces for Active Upper-Extremity Movement-Assistive Devices

Joan Lobo-Prat, Arno H. A. Stienen and Just L. Herder

***Abstract*— Currently, many different control interfaces for the operation of active movement-assistive device exist but their respective performance capabilities and limitations remain unclear. The goal of this study was to quantitatively evaluate the performance and learning characteristics of EMG-, force- and hand joystick-based interfaces. The human operator abilities were assessed in 8 healthy subjects using a screen-based one-dimensional position-tracking task, where the interface signal was mapped to the velocity of the cursor and the target was moving according to a multi-sine signal with a flat velocity spectrum. The performance of the control interfaces was evaluated in terms of tracking error, human-operator bandwidth, information transmission rate and effort. Results showed significant differences between the control interfaces in all the performance descriptors: the joystick-based interface presented significantly higher tracking error compared to EMG- (p<0.001) and force-based (p<0.005) interfaces; the EMG-based control interface showed a significantly higher bandwidth (p<0.001) than the force- and the joystick-based interfaces; the force- and joystick-based interfaces provided significantly higher information transmission rates (p<0.001) than the EMG-based interface; the force-based interface presented significantly lower effort than EMG- (p<0.001) and joystick-based (p<0.005) interfaces. None of the evaluated interfaces was superior in all four performance descriptors, but the force-based interface presented more positive results than the EMG- and joystick-based interfaces. However, in practice, the performance descriptors should be weighted according to the requirements of the specific application to determine which interface is the most suitable for the control of a particular active upper-extremity movement-assistive device.**

***Index Terms*— control interface, electromyography, force, joystick, performance evaluation, learning curve, human-operator.**

I. Introduction

Several active upper-extremity movement-assistive devices are currently available and used to increase the independence and the quality of life for patients suffering from severe neuromusculoskeletal disorders [1], [2], [3]. The operation of these active devices is mediated by a control interface. The design of the control interface in response to specific user needs and capabilities – which may change over time – is crucial for the usability and success of the device.

Electromyography-based interfaces are by far the most common method used for the control of active prostheses and orthoses. Myoelectric prostheses are controlled by measuring electromyographic (EMG) signals from two independent residual muscles or by distinguishing different activation levels of one residual muscle. Switching techniques such as muscle co-contraction or the use of mechanical switches or force-sensitive resistors are implemented for the sequential operation of several degrees of freedom (DOF) [4]. In the case of active orthoses, these are controlled trough proportional myoelectric control using the EMG signals from the muscles that are associated with the supported motion [5]. Recently, innovative pattern recognition algorithms [6] and surgical procedures such as targeted muscle reinnervation [7] are being developed in order to improve the functionality of EMG-based interfaces.

Force-based interfaces have been used in assisted-powered wheelchairs [8] where the wheelchair detects and amplifies the force applied by the user. Additionally, recent studies implemented six-DOF force-torque sensors or simple force sensor resistors for the control of active upper-extremity orthoses [9], [10], [11], [12] and prosthesis [13]. Force-based interfaces generally implement admittance control strategies where the input is force and the output is velocity or position [14].

Joysticks are used for the control of powered wheelchairs [15] and external robotic arms [16], [17]. Recent studies also investigated the performance of controlling prosthetic arms with the residual shoulder motion measured with a two-DOF joystick [13], [18]. Furthermore, Johnson et al. [2] developed a five-DOF upper-extremity orthoses, in which the position of the end point was controlled with a joystick operated by the contralateral hand.

While there is a large variety of control interfaces under development, only a few studies have focused on their formal performance evaluation and comparison. As a consequence, there is a considerable confusion as to which one is the most suitable for each type of impairment and task. Currently, there is no consensus on how to evaluate the performance of control interfaces which prevents their objective evaluation and comparison (see *Appendix A* for further information on existing non-invasive control interfaces).

This work was supported in part by the Flextension Foundation through the Dutch Technology Foundation (STW), the Duchenne Parent Project, Spieren voor Spieren, Prinses Beatrix Fonds, Johanna Kinderfonds and Rotterdams Kinderrevalidatie Fonds Adriaanstichting, Focal Meditech, OIM Orthopedie and Ambroise.

J. Lobo-Prat and Arno H. A. Stienen are with the Department of Biomechanical Engineering, University of Twente, Drienerlolaan 5, 7522 NB, Enschede, The Netherlands (e-mail: j.loboprat@utwente.nl, arnostienen@gmail.com). Arno H. A. Stienen is also research associate at the Department of Physical Therapy and Human Movement Sciences, Northwestern University, Chicago (IL), USA.

Just L. Herder is with the Department of Department of Precision and Microsystems Engineering, Delft University of Technology, Mekelweg 2, 2628 CD Delft, The Netherlands (e-mail j.l.herder@tudelft.nl). He is also part-time full professor at the Departemnt of Automation, University of Twente, Enschede, The Netherlands.

We think that a better understanding of the limitations and capabilities of the different control interfaces, through objective and quantitative evaluations during functional tasks, can provide relevant information for the selection of the most suited control interface for a specific application. One example of this approach was the study by Corbett et al. [19], which evaluated the performance of EMG-, force- and position-based control interfaces in terms of tracking error, information transmission rate and human-operator bandwidth during a one-dimensional screen-based position-tracking task. Moreover, Guo et al. [20] compared sonomyography-, EMG-, force- and wrist angle-based interfaces during a series of screen-based discrete tracking tasks with and without a simultaneous auditory attention task. Even though these two studies do not evaluate the interface performance during functional tasks, they can provide a first insight on their potential value as control interfaces for active movement-assistive devices.

The goal of our study was to quantitatively evaluate the performance and the learning characteristics of force-, EMG- and hand joystick-based interfaces. The human operator abilities were tested in 8 healthy subjects using a screen-based one-dimensional position-tracking task. The performance of the control interface was evaluated in terms of tracking error, human-operator bandwidth and information transmission rate. The learning characteristics were evaluated by analyzing the tracking error along a series of training trials. The eight participants were also asked to list the control interfaces in order of preference. Finally a model of the human-interface system was fitted to its estimated frequency response function to evaluate the delay and gain parameters of each control interface.

II. Methods

A. Subjects

A total of eight healthy males aged between 22 to 29 years participated in this study. All participants gave written informed consent, were right-arm dominant and had no experience with EMG- or force-based control interfaces (see *Appendix B* for an example of the information letter and consent form). The experimental protocol was in accordance with the Research Ethical Guidelines of the Department of Biomechanical Engineering from the University of Twente (Enschede, The Netherlands).

B. Experimental Setup

A one-dimensional position-tracking task was presented to the subjects on a computer screen by means of a MATLAB (MathWorks Inc; Natick, Massachusetts) graphical user interface. The subjects remained in a sitting position during all the experiment with the arm immobilized as shown in Fig. 1. With the elbow flexed at 90 degrees, the forearm was securely strapped to a rigid structure using a padded brace around the styloid processes. During the experiment, the participants were asked to keep the cursor (yellow circumference in Fig. 1) as close as possible to the center of a dynamic target (magenta square in Fig. 1), which moved according to a predefined

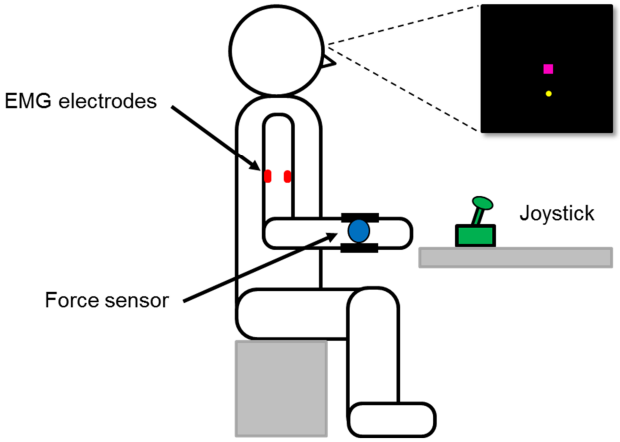

Fig. 1. Experimental Setup. The forearm of the participants was securely strapped to a rigid structure using a padded brace around the styloid processes. The EMG electrodes were placed at the biceps and triceps muscles. The resulting forces from the biceps and triceps activation where measured at the wrist. The joystick was located in front of the subject.

multi-sine signal with a flat velocity spectrum. The experimental task is represented in a block diagram form in Fig. 2. The subject visually perceived the error (e) between the target (w) and cursor (x) position. In order to minimize this error, the human generated a control signal (u), using one of the control interfaces, which was mapped to the velocity of the cursor and subsequently integrated to obtain the cursor position (x).

C. Experimental Protocol

Before starting the tracking task, subjects were asked to perform three maximal voluntary contractions (MVC) of three seconds for both biceps and triceps muscles. Both EMG and force signals were measured simultaneously during the MVCs and their mean values were used to normalize the EMG and force signals respectively. Normalizing the signals with the subject specific MVC provided a relative measure of muscle activation and force that made possible intra-subject comparison.

After performing the three MVCs, the subjects were asked to execute the tracking task with the three different control interfaces. The order in which the subjects tested each interface was randomized. For each interface, 10 training trials of 30 seconds and 3 evaluation trials of 3 minutes were performed. Training trials allowed the subjects to become familiar with the control interface and to get as close to their maximum performance as possible before starting the evaluation trials. A performance plateau was identified before the 10^{th} training trial for all subjects. The researchers informed the participants after each training trial about the tracking error and encouraged him/her to improve it (see *Appendix C* for further information on the experimental protocol).

D. Signals Acquisition and Conditioning

The input signal of the moving target was generated from 10 sinusoidal signals with (i) logarithmically distributed frequencies between 0.1 and 3 Hz; (ii) amplitudes logarithmically decreasing with frequency; (iii) and randomly

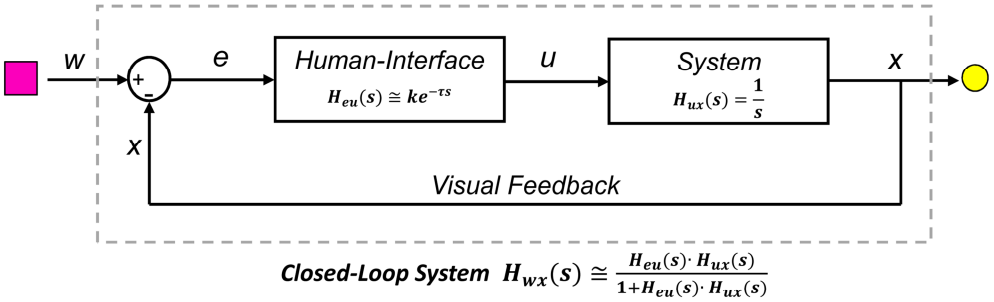

Fig. 2. Block Diagram of the position-tracking task. The subject visually perceived the error (*e*) between the target (*w*) and cursor (*x*) position. In order to minimize this error, the human generated a control signal (*u*), using one of the control interfaces, which was mapped to the velocity of the cursor and subsequently integrated to obtain the cursor position (*x*).

assigned phases for each trial (Fig. 3). The design of the input signal was adapted from the early work by D. McRuer [21] who did extensive research on the modeling of human-machine systems. The multi-sine signal was designed with a duration of 30 s.

The isometric EMG signals were measured from the biceps and the triceps brachii, where the activation of the biceps moved the cursor up and the activation of the triceps moved the cursor down. Two single differential-surface EMG electrodes (Bangoli DE-2.1., Delsys; Boston, Massachusetts) were placed parallel to the muscle fibers according to the European SENIAM recommendations [22]. The signals were amplified with a sixteen-channel Delsys Bagnoli-16 Main Amplifier and Conditioning Unit with a bandwidth of 20 to 450 Hz and a gain of 100.

Force was measured at the wrist, using a custom made one DOF load cell attached between the padded brace and the ground. Subjects were asked to use biceps and triceps muscles, avoiding the generation of force from shoulder or trunk movements. A force upwards moved the cursor up and a force downwards moved the cursor down. For each subject, the offset force resulting from the weight of the arm was corrected at the beginning of the experiment.

Both analog EMG and force signals were sent to a real-time computer (XPC Target 5.1, MathWorks Inc; Natick, Massachusetts) by means of a National Instruments card (PCI-6229; Austin, Texas), which performed the analog-to-digital conversion with a sampling frequency of 1000 Hz with 16-bits signal resolution.

For the joystick-based control interface we used the joystick of the PlayStation 3 controller (Sony Computer Entertainment; Miniato, Tokyo, Japan). A forward tilt of the joystick moved the cursor up and a backward tilt of the joystick moved the cursor down. The digital signal was sent to the real-time computer by means of a USB interface.

E. Signal Processing

In order to obtain the EMG envelope, a full wave rectification was performed by filtering the signal with a second order low-pass Butterworth filter with a cutoff frequency of 5 Hz.

For the tracking task, the velocity of the cursor was set to zero if the EMG or force signals were below a threshold of 2.5 % of the MVC. This threshold prevented that measurement noise could move the cursor. In the case of the EMG-based control interface, after the envelope detection and normalization of each EMG signal, the channel that presented higher amplitude was used to control the cursor. Therefore, when the most active channel was the one corresponding to the biceps muscle, the cursor moved up, whereas a higher activation of triceps muscle moved the cursor down. In the case of the force-based control interface, positive forces (upward forces) where normalized using the mean measured force during the MVC of the biceps and negative forces (downward forces) were normalized using the mean measured force during the MVC of the triceps.

To ensure appropriate velocity control of the cursor and to prevent fatigue, the EMG and force signals were amplified by a fixed gain of 20 after all the aforementioned signal processing. The value of this fixed gain was chosen to ensure that the subjects had to produce a maximum of 25% of their MVC at the peak velocity of the target. In the case of the joystick-based interface the angle signal was normalized to its maximum output and amplified with a gain of 5. With these gain settings the subjects were able to reach the target at its peak velocity without experiencing fatigue.

F. Data Analysis

A quasi-linear model of the human-interface system for the performance analysis of the control interfaces was assumed. The control interfaces were evaluated analyzing the characteristics of the closed-loop system which can be approximated by a linear transfer function. These characteristics will vary according to the operator's ability to adapt to the dynamic characteristics of the controlled elements, influencing the stability and performance of the entire closed-loop system. The target (*w*) and cursor (*x*) position signals were used to evaluate performance of the three control interfaces. The Frequency Response Functions (FRF) of the closed-loop system (H_{wx}) were estimated for the frequencies (f_k) of the aforementioned 10 sinusoidal signals (Fig. 5) using the following formula [23]:

$$\hat{H}_{wx}(f_k) = \frac{\hat{S}_{wx}(f_k)}{\hat{S}_{ww}(f_k)}, \qquad (1)$$

where S_{wx} is the estimated cross-spectral density of the cursor position signal (*x*) and target position signal (*w*), and S_{ww} is the estimated auto-spectral density of the target position signal.

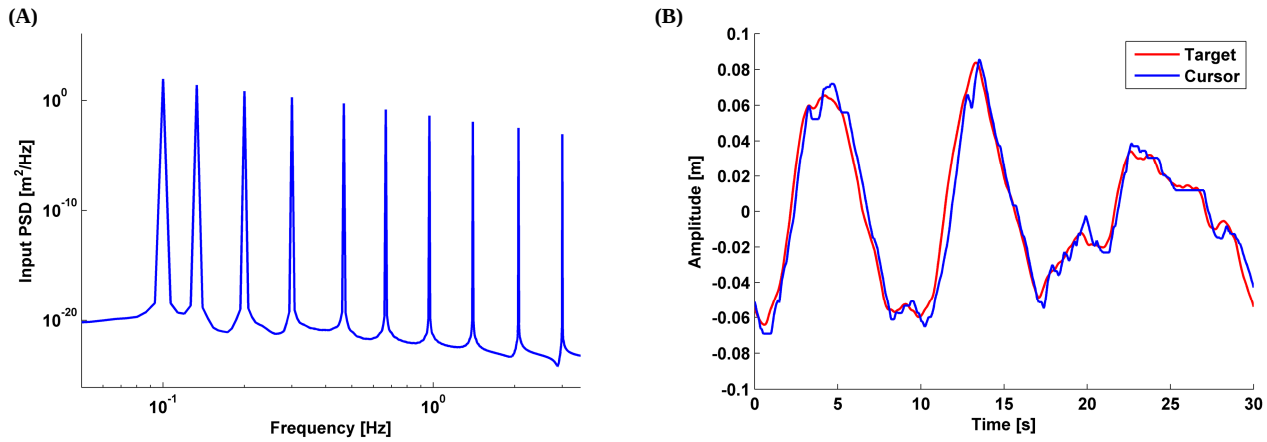

Fig. 3. Input and output signals. (A) Power spectral density (PSD) of the target position signal. The multi-sine signal was generated with 10 frequencies logarithmically distributed between 0.1 and 3 Hz and with amplitudes logarithmically decreasing with frequency. For each trial, a random phase was computed. (B) Target and cursor position along time. The subject was asked to track the target with a cursor that was controlled either with EMG-, force- or joystick-based interfaces.

As a measure of linearity and presence of noise, the coherence function of the closed-loop system (Fig. 5) was estimated according to [23]:

$$\hat{\gamma}^2_{wx}(f_k)=\frac{\left|\hat{S}_{wx}(f_k)\right|^2}{\hat{S}_{ww}(f_k)\hat{S}_{xx}(f_k)}\,, \qquad (2)$$

where S_{xx} is the estimated auto-spectral density of the cursor position signal.

Four performance descriptors were chosen to evaluate the control interfaces: tracking error, human-operator bandwidth, effort and information transmission rate. Furthermore, a model of the human-interface system was fitted to its estimated frequency response functions to evaluate the delay and gain parameters of each control interface. The reader is referred to *Appendix D* for further information on the Matlab functions used for the data analysis.

1) Tracking Error

The tracking error was calculated as the area under the auto-spectral density of the error signal (S_{ee}) from 0 Hz to 10 Hz using the following equation:

$$\hat{F}_{ee}(f)=\sum_{f=0}^{10}\hat{S}_{ee}(f)\,. \qquad (3)$$

A high value of F_{ee} indicates that the frequency content of the target and the cursor signals are different, while a low value of F_{ee} indicates that the frequency content of the target and the cursor signals are similar. This measure of tracking error is independent of any assumptions about the human-interface system. The tracking error was also used to study the learning characteristics during the training trials.

2) Information Transmission Rate

The information transmission rate quantifies the amount of information that is contained in the output signal of a communication channel, relative to the input signal [24]. In this study the human-interface system can be conceived as a communication channel where the human has to transmit a movement intention through the interface. We calculated the information transmission rate ($\dot{I}$) of the human-interface system for each evaluation trial by integrating Shannon's channel capacity over the perturbed frequencies (f_k) using the following equation:

$$\hat{\dot{I}}=\frac{1}{NT}\sum log_2\left(\frac{\hat{S}_{xx}(f_k)}{\hat{S}_{xx}(f_k)-|\hat{H}_{wx}(f_k)|^2\,\hat{S}_{ww}(f_k)}\right), \qquad (4)$$

where N is the number of samples, T is the sampling time, S_{xx} is the auto-spectral density of the cursor position signal (x), S_{ww} is the auto-spectral density of the target position signal (w) and S_{wx} is the cross-spectral density of the cursor and target position. A similar method to calculate the information transmission rate was used in [19], [25], [26].

3) Human-Operator Bandwidth

The human-operator bandwidth indicates the maximum frequency at which the human can properly track the target. The human-operator bandwidth was defined as the first frequency where the gain of H_{wx} dropped below -3dB from its maximum value. We calculated the maximum value as the mean value between 0.1 and 1.5 Hz of the FRF of H_{wx}. A similar method to calculate the human-operator bandwidth was used in [19].

4) Effort Measure

The root-mean-squared (RMS) of the velocity signal (u) was used to compare the required average velocity signal during the control task between interfaces. The RMS value was interpreted as a measure of effort assuming that if the subject had to produce less EMG, force or joystick movements the effort was lower. The increase in RMS of EMG in relation to the level of effort has been reported in several studies [27], [28]. This measure of effort is also independent of any assumptions about the human-interface system.

5) Learning Characteristics

The learning characteristics were analyzed calculating the tracking error for each training trial. An exponential function was fitted to the mean tracking error values. We selected the 1st training trial as a reference to identify significant reduction of the tracking error and a performance plateau was identified when no significant reduction of the tracking error was found in subsequent trials.

6) Human-Interface Model

According to the models proposed by McRuer [21] the human-interface system (H_{eu}), during a velocity-controlled task, can be modeled with the following equation:

$$H_{\mathrm{mod}} = k\, \mathrm{e}^{-\tau s}, \qquad (5)$$

where k and τ represent a gain and a delay respectively, and s is the Laplace transform variable. The values of these two parameters were estimated for each subject and interface from the mean FRF of the human-interface system by solving a non-linear squares optimization problem using the following error cost function [23]:

$$E = \hat{\gamma}^2 \,|\ln\left(\frac{\hat{H}_{eu}(f_k)}{H_{\mathrm{mod}}(f_k)}\right)|, \text{ where } \hat{H}_{eu} = \frac{\hat{S}_{wu}}{\hat{S}_{eu}} \qquad (6)$$

and where $\hat{\gamma}^2$ is the coherence squared, S_{wu} is the cross-spectral density of the velocity signal (u) and target position signal (w), and S_{eu} is the cross-spectral density of the error signal (e) and velocity signal.

The fidelity of the model of each interface was evaluated calculating the variance accounted for (VAF; eq. 7) in the time domain using the mean estimated parameters of each interface.

$$VAF = \left(1 - \frac{\mathrm{var}(y - \hat{y})}{\mathrm{var}(y)}\right)\cdot 100\%, \qquad (7)$$

where var(i) indicates variance of i, y indicates the measured output and $\hat{y}$ indicates the simulated output using the model [23].

G. Statistical Analysis

We carried out a two-way repeated measures analysis of variance (RMANOVA) for each performance measure, defining the interface and the order in which the control interfaces were tested as fixed factors. The order was not significant for any of the performance descriptors (p>0.78) suggesting that the training protocol was effective. The influence of the order was further investigated with a correlation analysis between EMG and force signals during EMG and force tasks. The correlation coefficients showed a mean value of 23% (±10% SD) which suggested that the EMG and force tasks were considerably different.

Since the order did not show significant influence on the evaluation, one-way RMANOVAs were performed for each performance measure. A Benferroni test was applied for pairwise comparisons. We used α=0.05 (probability of Type I error) as the level of significance in all statistical comparisons.

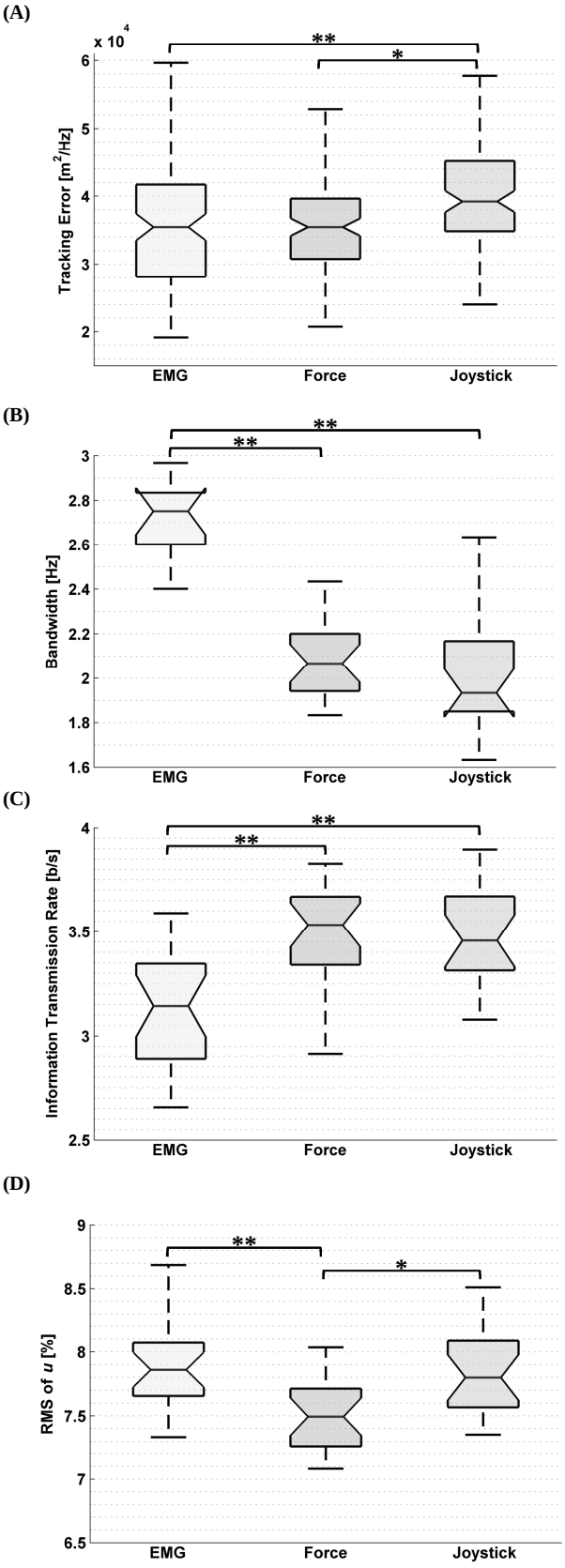

Fig. 4. Performance Evaluation. (A) Boxplots of the tracking error for each interface. (B) Boxplots of the human-operator bandwidth for each interface. (C) Boxplots of the information transmission rate for each interface. (D) Boxplots of the RMS of velocity signal (u) for each interface. Stars indicate statistically significance differences. (*) indicates p<0.05, and (**) indicates p<0.001.

III. Results

A. Performance Evaluation

All the performance descriptors presented significant differences for the RMANOVA test. However, not all pairwise comparisons between interfaces were significant (fig. 4). The joystick-based interface presented significantly higher tracking error compared to EMG- (p<0.001) and force-based (p<0.005) interfaces (Fig. 4A). Furthermore, the EMG-based control interface showed a significantly higher (p<0.001) bandwidth than the force- and the joystick-based interfaces (Fig. 4B). We also found that force- and joystick-based interfaces provided significantly higher information transmission rates (p<0.001) than the EMG-based interface (Fig. 4C). Finally, we found that the force RMS values were significantly lower than the RMS values of the EMG- (p<0.001) and the joystick based control interfaces (p<0.005; Fig. 4D). Table 1 summarizes the results of the performance evaluation.

B. Learning Characteristics

In order to evaluate the learning characteristics, we performed a one-way RMANOVA where each training trial was defined as a fixed factor. The influence of the order was tested for the first training trial in a similar way than in the performance evaluation and did not show any significant difference. Figure 7 shows the learning curves obtained from fitting an exponential function to the mean values of the tracking error for each training trial. For the EMG-based control interface there was a significant improvement in tracking error relative to the 1st training trial at the 6th trial, while the force-based interface presented a significant improvement in the 3rd trial. The joystick-based interface did not show any significant improvement of the tracking error. Finally, the same figure shows that all interfaces reached a performance plateau before the end of the training.

C. Human-interface Model

The results of the parameter estimation of k and τ are shown in fig. 6. While we did not find a significant difference between the gains, the EMG-based interface presented significantly lower delay than the force- and the joystick-based interfaces (p<0.001). We found a VAF of 98.8%, 96.7% and %82.9 for the EMG-, force- and joystick- based interfaces respectively.

D. Subject's Opinion

At the end of the experiment the participants were asked to list the control interfaces in order of overall preference. The results from the questionnaire show that six out of eight subjects preferred the force-based interface followed by EMG- and joystick-based interfaces. The other two subjects preferred EMG-based interface the most, followed by force- and joystick based interfaces.

The reader is referred to *Appendix E* and F which compiles the results of the pilot study and the output of the statistical analysis respectively.

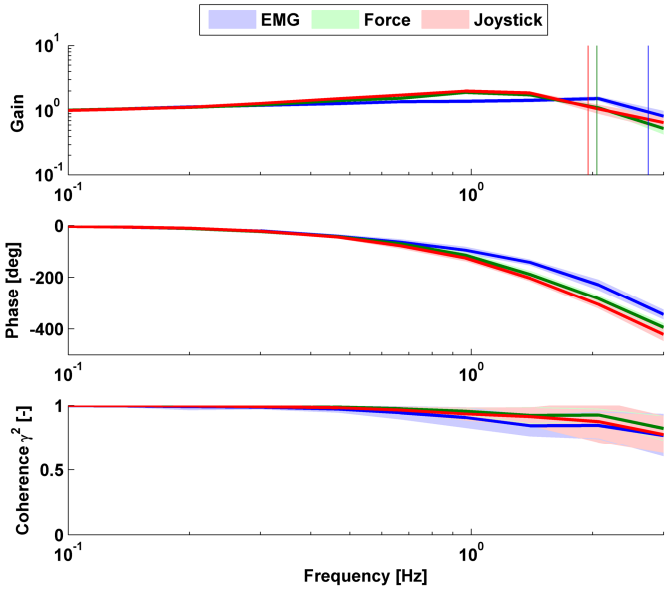

Fig. 5. Estimated Frequency Response Functions of the Closed-Loop System (H_{wx}) for the EMG- (blue), force- (green) and joystick-based (red) control interfaces. The solid lines indicate the mean values and the area in faded colors indicate ±1 SD. The vertical lines in the gain plot indicate the mean estimated bandwidths of each interface.

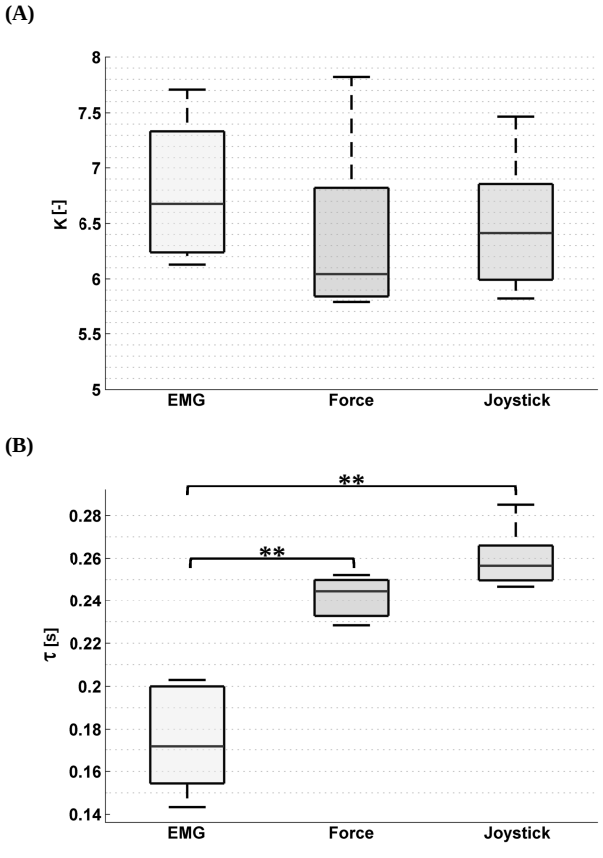

Fig. 6. Estimated parameters of the human-interface model (H_{eu}) for the EMG-, force- and joystick-based control interfaces. (A) Boxplots of the gain parameter. (B) Boxplot of the delay parameter. Stars indicate statistically significance differences. (**) indicates p<0.001.

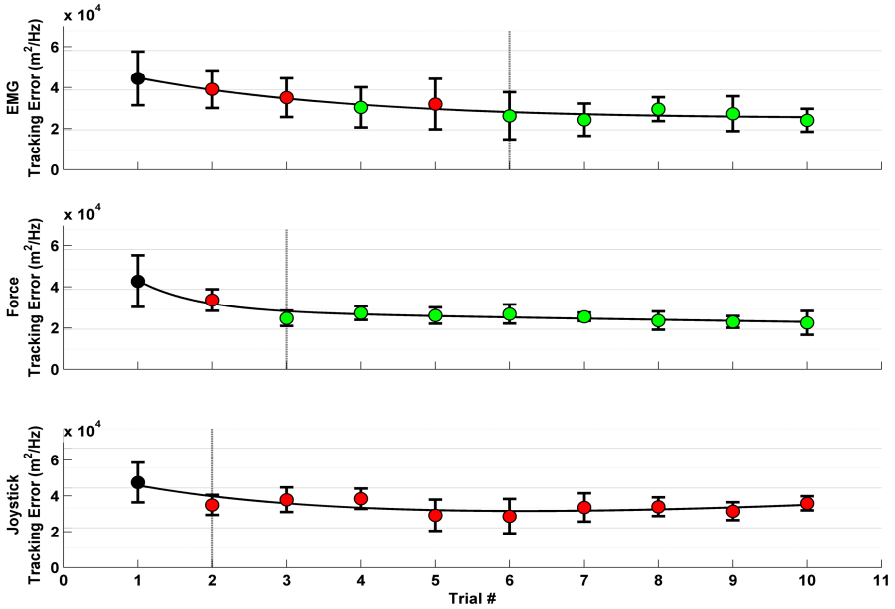

Fig. 7. Learning curve of each interface. An exponential function was fitted to the mean tracking error of each training trial. The first training trial was used as a reference to identify significant reductions of tracking error. The grey markers indicate significant reduction of tracking error relative to the first trial. The black markers indicate non-significant reduction of tracking error relative to the first training trial. The vertical lines indicates the trial in which the performance plateau was identified. The error bars indicate ± 1 SD.

IV. Discussion

Researchers have explored a wide variety of invasive and non-invasive control interfaces for active movement-assistive devices. In order to identify which interface is the most suitable for a specific application it is necessary to know the limitations and capabilities of each method. The present evaluation provides objective and quantitative information in terms of performance and learning characteristics that is relevant when selecting a control interface for active upper-extremity movement-assistive devices.

We found that the tracking error of the joystick-based interface was higher compared to the one of the EMG- and force-based interfaces (Fig. 4A). Additionally, the results from the questionnaire showed that the joystick was the least preferred interface for all subjects. We think that the smaller amplitude of the joystick interface compared to the other two interfaces, for which the amplitude limits where set according to the maximum force or EMG signal that the subject could generate, is the cause of its poor accuracy and user acceptance. Note that, in studies where larger movement amplitudes were used as control signal, the authors report very low tracking errors [19], [29]. Our motivation behind testing an interface with small input range, such as the hand-joystick, is that in general, people with severe movement impairments cannot perform larger displacements than those that are possible with a small hand-joystick. It should be noted, that the importance of the tracking error is task dependent and that one can improve precision by decreasing the reaching velocity [30]. We conjecture that subjects with movement impairments might actually have a different opinion about the hand-joystick than the healthy individuals of this study.

Regarding the measure of human-operator bandwidth, we found that the participants were able to track frequencies up to 2.8 Hz when using the EMG-based control interface, while they were able to track frequencies up to 2 Hz only with the other two interfaces (Fig. 4B). From the parameters estimation of the human-interface system we can conclude that the larger bandwidth of the EMG interface is due to its low delay (Fig. 6B). Note that the EMG interface is bypassing the muscle and skeleton dynamics and therefore it can be detected earlier than its resultant force or motion. Despite having a higher bandwidth, the EMG-based interface presented lower information transmission rate (Fig. 4C) due to its low signal to noise ratio, which is also reflected by its lower coherence in Fig. 5.

TABLE I
Performance Evaluation

Interface	Tracking Error	Bandwidth	ITR	Effort
EMG	-	+	-	+
Force	-	-	+	-
Joystick	+	-	+	+

(+) and (-) indicate significantly higher and lower values of each performance descriptor. ITR: Information Transmission Rate.

The results of the effort comparison show that the force-based interface requires a significantly lower RMS value compared to the EMG- and joystick-based interfaces (Fig. 4D). Further analyzing the EMG data we could conclude that this difference was caused by the presence of co-contraction. Moreover, EMG presented a higher variability of the RMS between subjects than the force- and joystick-based interfaces due to the fact that EMG signals are highly susceptible to sensor placement, changes on skin impedance and fatigue among others factors.

The VAF measures indicate that the parameters found for the EMG- and force-based interfaces describe the human-interface system with high fidelity. However, this is not the case for the joystick-based interface, for which the model can only explain 83% of the measured data. This results suggest

that a different model should be used to describe the joystick-based interface more precisely.

With regard to the learning curves, we can observe, as expected, that as the training proceeded, the subjects learned and F_{ee} became smaller indicating that the frequency content of the target and the cursor became increasingly similar. The results show that despite the fact that the EMG-based interface is far from the natural means to interact with the environment while the force-based interface is closer, the difference in terms of learning cost was small: the participants were able to reach a performance plateau with the EMG-based interface after the 6^{th} training trial, which is only three trials after the same plateau was reached with the force-based interface. (Fig. 7). Regarding the joystick-based interface, we did not find any significant improvement of the tracking error after the 10^{th} training trials. We conjecture that the lack of learning gain with the joystick could be a consequence of the extensive prior experience of the participants with these type of devices, thus no further detectable improvement was achieved during the experiment.

While the methodological approach of this study is similar to the one of Corbett et al. [19], the specific methods present notable differences which leaded to significantly different results. The frequency content of the input signal, the visual feedback, or the gain settings of the control signals are some critical differences of the experimental method, which added to the typical nonlinearities of the human movement control system might have been the cause of the different results.

None of the evaluated interfaces was superior in all four performance descriptors. However, the force-based interface presents more positive results than the EMG- and joystick-based interfaces. In general, the performance descriptors should be weighted according to the requirements of the specific application to find out which interface is the most suitable in a particular case. It is also worth noting that apart from the performance criteria evaluated in this study, additional requirements, such as ease of use or portability, should be taken into account when identifying the most suitable control interface.

There are some limitations in this study that must be acknowledged and addressed in the future. The first limitation concerns the fact that all the participants of this study were healthy subjects. Considering that clear differences exist between healthy individuals and patients with movement impairments in terms of motor control capabilities, the evaluation of control interfaces with specific patient's groups would provide more *ad hoc* results. The second limitation relates to the fact that the control task used in this study is too simple compared to the upper-extremity movements during activities of daily living. Nevertheless it must be noted that a simple experimental task was required for an initial robust analysis providing a first practical insight on the potential value of the control interfaces for active movement-assistive devices. Once this stage has been completed, our future work will involve testing the interfaces within a more realistic context, with patients suffering movement impairments, and using a functional task closer to the activities of daily living, such as two- or three-dimensional reaching-retrieving task.

V. Conclusions

This study evaluated and compared three control interfaces that derived the motion intention of the user from signals measured at three different levels of the human movement control system. We found significant performance differences in terms of tracking error, human-operator bandwidth, information transmission and effort between EMG- force- and joystick-based control interfaces using a one-dimensional screen-based position-tracking task. None of the evaluated interfaces was superior in all four performance descriptors. The precision and acceptance of the joystick-based interface appears to be limited by the small amplitude of movement. The force-based interface presents high accuracy, high information transmission rate, low effort and is the most preferred interface by the users. The EMG-based interface presents high accuracy and bandwidth despite the low information transmission rate.

The analysis of the tracking error along the training trials provided relevant information on the learning characteristics of the tested control interfaces. While EMG- and force-based interfaces present a clear learning curve, the joystick- based interface did not find any significant improvement along the training trials.

The modeling of the human-interface system revealed significant differences in terms of delay between interfaces. The lower delay found in the EMG-based interface should be considered in interfaces where high bandwidths are required.

Finally, we can conclude that the force-based interface presents more positive results than the EMG- and joystick-based interfaces. However, in practice the performance descriptors should be weighted according to the requirements of the specific application to determine which interface is the most suitable for the control of the particular active upper-extremity movement-assistive device.

Acknowledgment

The authors would like to thank Diana P.M. Batista and Arvid Q.L. Keemink for their contributions to the experimental setup and protocol. The authors would also like to thank Dr. Alfred Schouten, for his advice on the system identification and Dr. Edwin van Asseldonk for his support on the statistical analysis.

References

[1] R. A. R. C. Gopura and K. Kiguchi, "Development of a 6DOF Exoskeleton Robot for Human Upper-Limb Motion Assist," in *4th International Conference on Information and Automation for Sustainability, 2008. ICIAFS 2008*, 2008, pp. 13 –18.

[2] G. R. Johnson, D. A. Carus, G. Parrini, Ss. Marchese, and R. Valeggi, "The design of a five-degree-of-freedom powered orthosis for the upper limb," *Proc. Inst. Mech. Eng. [H]*, vol. 215, no. 3, pp. 275–284, Mar. 2001.

[3] A. E. Schultz and T. A. Kuiken, "Neural Interfaces for Control of Upper Limb Prostheses: The State of the Art and Future Possibilities," *PM&R*, vol. 3, no. 1, pp. 55–67, gener 2011.

[4] A. Muzumdar, *Powered Upper Limb Prostheses: Control, Implementation and Clinical Application*. Springer, 2004.

[5] T. Lenzi, S. M. M. De Rossi, N. Vitiello, and M. C. Carrozza, "Intention-based EMG control for powered exoskeletons," *IEEE Trans. Biomed. Eng.*, vol. 59, no. 8, pp. 2180–2190, Aug. 2012.

[6] A. Fougner, O. Stavdahl, P. J. Kyberd, Y. G. Losier, and P. A. Parker, "Control of Upper Limb Prostheses: Terminology and Proportional Myoelectric Control #x2014;A Review," *Ieee Trans. Neural Syst. Rehabil. Eng.*, vol. 20, no. 5, pp. 663 –677, Sep. 2012.

[7] T. A. Kuiken, G. Li, B. A. Lock, R. D. Lipschutz, L. A. Miller, K. A. Stubblefield, and K. Englehart, "Targeted Muscle Reinnervation for Real-Time Myoelectric Control of Multifunction Artificial Arms," *Jama J. Am. Med. Assoc.*, vol. 301, no. 6, pp. 619–628, Feb. 2009.

[8] R. A. Cooper, T. A. Corfman, S. G. Fitzgerald, M. L. Boninger, D. M. Spaeth, W. Ammer, and J. Arva, "Performance assessment of a pushrim-activated power-assisted wheelchair control system," *Ieee Trans. Control Syst. Technol.*, vol. 10, no. 1, pp. 121 –126, gener 2002.

[9] K. Abbruzzese, D. Lee, A. Swedberg, H. Talasan, and M. Paliwal, "An innovative design for an Assistive Arm Orthosis for stroke and muscle dystrophy," in *Bioengineering Conference (NEBEC), 2011 IEEE 37th Annual Northeast*, 2011, pp. 1 –2.

[10] M. Baklouti, P.-A. Guyot, E. Monacelli, and S. Couvet, "Force controlled upper-limb powered exoskeleton for rehabilitation," in *IEEE/RSJ International Conference on Intelligent Robots and Systems, 2008. IROS 2008*, 2008, p. 4202.

[11] W. Huo, J. Huang, Y. Wang, and J. Wu, "Control of a rehabilitation robotic exoskeleton based on intentional reaching direction," in *2010 International Symposium on Micro-NanoMechatronics and Human Science (MHS)*, 2010, pp. 357 –362.

[12] T. Rahman, R. Ramanathan, S. Stroud, W. Sample, R. Seliktar, W. Harwin, M. Alexander, and M. Scavina, "Towards the control of a powered orthosis for people with muscular dystrophy," *Proc. Inst. Mech. Eng. [H]*, vol. 215, no. 3, pp. 267–274, Mar. 2001.

[13] R. D. Lipschutz, B. Lock, J. Sensinger, A. E. Schultz, and T. A. Kuiken, "Use of two-axis joystick for control of externally powered shoulder disarticulation prostheses," *J. Rehabil. Res. Dev.*, vol. 48, no. 6, pp. 661–667, 2011.

[14] W. Yu, J. Rosen, and X. Li, "PID admittance control for an upper limb exoskeleton," in *American Control Conference (ACC), 2011*, 2011, pp. 1124–1129.

[15] B. E. Dicianno, R. A. Cooper, and J. Coltellaro, "Joystick Control for Powered Mobility: Current State of Technology and Future Directions," *Phys. Med. Rehabil. Clin. N. Am.*, vol. 21, no. 1, pp. 79–86, Feb. 2010.

[16] V. Maheu, J. Frappier, P. S. Archambault, and F. Routhier, "Evaluation of the JACO robotic arm: Clinico-economic study for powered wheelchair users with upper-extremity disabilities," in *2011 IEEE International Conference on Rehabilitation Robotics (ICORR)*, 2011, pp. 1–5.

[17] G. R. B. E. Romer, H. J. A. Stuyt, and A. Peters, "Cost-savings and economic benefits due to the assistive robotic manipulator (ARM)," in *9th International Conference on Rehabilitation Robotics, 2005. ICORR 2005*, 2005, pp. 201–204.

[18] Y. Losier, K. Englehart, and B. Hudgins, "Evaluation of shoulder complex motion-based input strategies for endpoint prosthetic-limb control using dual-task paradigm," *J. Rehabil. Res. Dev.*, vol. 48, no. 6, pp. 669–678, 2011.

[19] E. A. Corbett, E. J. Perreault, and T. A. Kuiken, "Comparison of electromyography and force as interfaces for prosthetic control," *J. Rehabil. Res. Dev.*, vol. 48, no. 6, p. 629, 2011.

[20] J.-Y. Guo, Y.-P. Zheng, L. P. J. Kenney, A. Bowen, D. Howard, and J. J. Canderle, "A Comparative Evaluation of Sonomyography, Electromyography, Force, and Wrist Angle in a Discrete Tracking Task," *Ultrasound Med. Biol.*, vol. 37, no. 6, pp. 884–891, Jun. 2011.

[21] D. T. Mcruer and H. R. Jex, "A Review of Quasi-Linear Pilot Models," *Ieee Trans. Hum. Factors Electron.*, vol. HFE-8, no. 3, pp. 231 – 249, Sep. 1967.

[22] H. J. Hermens, B. Freriks, R. Merletti, D. Stegeman, J. Blok, G. Rau, C. Disselhorst-Klug, and G. Hägg, *European recommendations for surface electromyography*. Roessingh Research and Development The Netherlands, 1999.

[23] D. T. Westwick and R. E. Kearney, *Identification of Nonlinear Physiological Systems*. Wiley, 2003.

[24] C. E. Shannon, "A mathematical theory of communication," *Sigmobile Mob Comput Commun Rev*, vol. 5, no. 1, pp. 3–55, gener 2001.

[25] R. B. Chan and D. S. Childress, "On information transmission in human-machine systems: channel capacity and optimal filtering," *Ieee Trans. Syst. Man Cybern.*, vol. 20, no. 5, pp. 1136 –1145, Oct. 1990.

[26] J. I. Elkind and L. T. Sprague, "Transmission of Information in Simple Manual Control Systems," *Ire Trans. Hum. Factors Electron.*, vol. HFE-2, no. 1, pp. 58–60, 1961.

[27] K. Søgaard, S. C. Gandevia, G. Todd, N. T. Petersen, and J. L. Taylor, "The effect of sustained low-intensity contractions on supraspinal fatigue in human elbow flexor muscles," *J. Physiol.*, vol. 573, no. 2, pp. 511–523, Jun. 2006.

[28] I. A. F. Stokes, "Relationships of EMG to effort in the trunk under isometric conditions: force-increasing and decreasing effects and temporal delays," *Clin. Biomech. Bristol Avon*, vol. 20, no. 1, pp. 9–15, Jan. 2005.

[29] J. A. Doubler and D. S. Childress, "An analysis of extended physiological proprioception as a prosthesis-control technique," *J. Rehabil. Res. Dev.*, vol. 21, no. 1, pp. 5–18, May 1984.

[30] P. M. Fitts, "The information capacity of the human motor system in controlling the amplitude of movement," *J. Exp. Psychol.*, vol. 47, no. 6, pp. 381–391, 1954.

APPENDIX A: LITERATURE STUDY

Existing Non-Invasive Interfaces for the Control of Active Movement-Assistive Devices

Joan Lobo-Prat[1-2]

[1] Dept. of Biomechanical Engineering, Delft University of Technology, Delft
[2] Laboratory of Biomechanical Engineering, University of Twente, Enschede

Abstract— **Active movement-assistive devices can increase the independence and quality of life for patients with severe neuromusculoskeletal disorders. This technology requires interaction between the user and the device for its control, which is mediated by a control interface. An essential function of the control interface is the detection of the user's movement intent. The selection of the control interface in response to specific user needs and capabilities -which may change over time- is a crucial determinant of the usability of the assistive device. Researchers have explored a wide variety of invasive and non-invasive methods to derive the movement intent of the user, and there remains considerable confusion on which strategy is the most suited to each specific type of impairment and task. With the goal of clarifying the suitability of the current range of strategies for the detection of motion intention, this article presents a critical and systematic review of non-invasive control interfaces used in active movement-assistive devices.**

Keywords— **control interface, active movement-assistive device, motion intention detection, biomechatronics, prosthesis, orthosis.**

Introduction

The ability to move in a controlled and stable manner is an essential trait of the human body. This quality enables the subject to interact with the environment during the activities of daily living. From the biomechatronics perspective, the Human Movement Control System (HMCS) has been modeled as a controlled dynamic system (**Fig. 1**) that consists of a mechanical structure (*the plant*), which represents the skeleton and passive tissues with possible external loads (i.e. the environment); the *actuators,* that represent the muscles; and a *controller,* that represents the central nervous system and receives sensory feedback from the physiological *sensors* (Veltink, 1999; Veltink et al., 2001). The HMCS might be impaired due to disease or trauma (some examples are shown in Fig. 1). Impairments can occur at various levels of the HMCS, affecting one or several components of the system. In the case of amputations the plant is affected, while in the case of muscular dystrophy (e.g. Duchenne muscular dystrophy) the affected components are the actuators, and in the case of blindness (e.g. retinitis pigmentosa) the sensory system is affected. Spinal cord injury (SCI) or myelitis affect the control of the spinal circuits, and stroke, Parkinson's or cerebral palsy (CP) directly affect the control function of the brain.

Movement-assistive devices play a crucial role in increasing the independence and quality of life for patients with severe neuromusculoskeletal disorders. Assistive devices have been classified by the International Organization for Standardization (ISO) in the standards catalogue ISO 9999:2011 according to their main function. In general, a device acting as a functional *replacement* of a part of the human body is classified as a *prosthesis,* while if the device *supports* a bodily function it is classified as an *orthosis*. Movement-assistive devices that are not directly connected to the missing or dysfunctional body part (e.g. wheelchairs, walkers, external robotic arms or crutches) are classified as *external* movement-assistive devices in this paper.

Advances in neuroscience, engineering and computer science have led to an acceleration in the development of biomechatronic systems that are capable of *actively* assisting the impaired motor functions of patients affected by severe neuromusculoskeletal disorders (Dollar and Herr, 2008; Pons, 2008; Veltink et al., 2001).

From the biomechatronics perspective, the Assistive Movement Control System (AMCS) consists (as in the HMCS) of a plant representing the mechanical structure and the passive elements (e.g. springs or dampers), actuators that represent the motors, and an artificial controller that receives the measured data from the sensors and generates control signals to operate the actuators (**Fig. 2**). Note that an AMCS functions in parallel to the impaired HMCS.

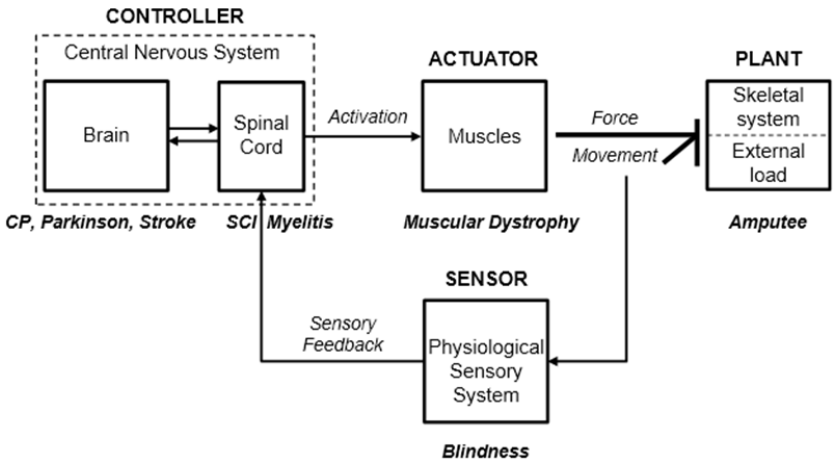

Figure 1. Schematic block diagram of the Human Movement Control System. Note that the interaction between the actuators and the plant is pictured with a bond graph which represents the energy exchange between them (i.e. movement and force in this particular case). The reader is referred to Borutzky (2010) for further information on bond graphs. Modified from Veltink et al. (2001).

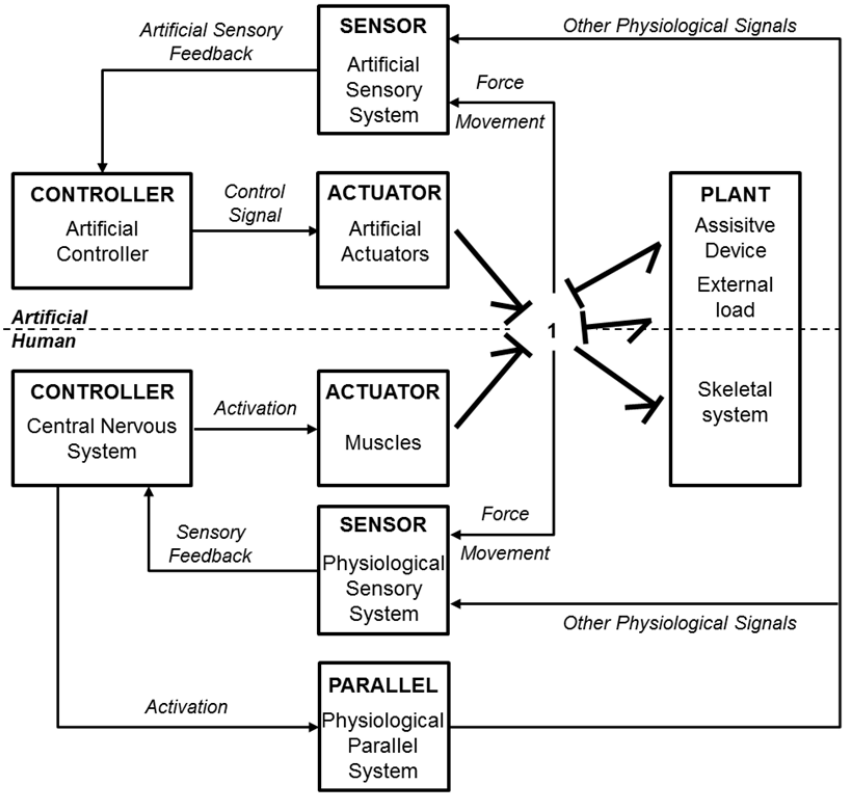

Figure 2. Schematic block diagram of the Human Movement Control System in parallel with the Artificial Movement Control System. Both the human and artificial systems are depicted as dynamic systems, in which both the human muscles and artificial actuators generate forces to transfer power and hence move the combined plant composed of the mechanical structure of the assistive device and the human musculoskeletal system. The power 1-junction states a common velocity of all components. The reader is referred to Borutzky (2010) for further information on bond graphs. Modified from Veltink (1999).

Three kinds of interactions between the human and the active movement-assistive device can be distinguished: (1) detection of the motion intention of the user; (2) provision of feedback to the user regarding the state of the AMCS or of the environment; and (3) exchange of mechanical power. Note that providing feedback to the user is especially relevant in those cases in which the user has lost proprioceptive feedback (e.g. amputates). This article focuses on the first type of the interaction defined above: *motion intention detection*.

Several physiological phenomena take place in every subsystem of the HMCS. Some of these phenomena can be measured and associated to the motion intention of the user, and therefore can be exploited for the effective control of the AMCS. Neural signals from the central nervous system [e.g. electroencephalography (EEG)], neural activation of the muscle [e.g. electromyography (EMG)], muscle interaction forces and body movements are some common examples of signals that are *implicitly* related to the motion intention. Motion intention can also be derived from the *explicit* commands of the user, for example by pressing command switches, through speech and through head or eye movement.

The high percentage (23%-33.7%) in published studies (Biddiss and Chau, 2007; Datta et al., 2004; Meurs et al., 2006) of arm amputees that abandon their prosthetic device is a clear indication that the design of intuitive control interfaces that meet the daily needs of the users remains challenging. The personalization of the control interface in response to specific user needs and capabilities, which may change over time, is a crucial determinant of the usability of the assistive device. Researchers have explored a wide variety of invasive and non-invasive methods to derive the movement intent of the user, and there remains considerable confusion on which strategy is the most suitable for each specific type of impairment and task.

With the goal of clarifying the suitability of the current range of strategies for the detection of motion intention, this article presents a critical and systematic review of non-invasive control interfaces used in active movement-assistive devices.

Existing Control Interfaces

Classification Method

The inventory of control interfaces for motion intention detection resulting from the literature search was stratified through a classification at four levels (see **Table 1**). The 1st level was defined according to the subsystems that are present in the HMCS (controller, actuators, plant and parallel systems), and the 2nd level was defined according to the physiological phenomena that takes place in every subsystem. The set of signals that can be measured for every physiological phenomenon defines a 3rd level of classification and the sensors used to measure these signals define a 4th level. For each sensor/signal its transduction principle, interface with the body, area of application and key references were indicated.

Interfacing with the Controller: Brain Computer Interfaces (BCIs)

Current noninvasive brain-computer interfaces (BCIs) derive the movement intention of the user from electrical and/or hemodynamic signals from the brain.

Electrical Brain Activity

Electroencephalography (EEG) and magnetoencephalography (MEG) are well established non-invasive methods that measure the average dendritic currents of a large proportion of cells from the scalp (Wolpaw et al., 2002). Several brain signals have been used for BCIs including slow cortical potentials, low frequency changes in filed potentials (such as P300) and α and β rhythms. Even though MEG provides a much higher signal quality than EEG and does not require the attachment of scalp electrodes, the latter is portable (i.e. does not require a shielded room) and is both less expensive and less cumbersome than MEG. Consequently, EEG-based BCIs are currently commercially available (e.g. intendiX®, g.tec medical engineering GmbH, Schiedlberg, Austria) for personal use to operate spelling and domestic devices.

While the majority of current research on EEG- and MEG-based BCIs focus on providing basic communication control to people suffering from severe motor impairments (Kübler and Birbaumer, 2008; Mellinger et al., 2007), researchers have been also exploring their capabilities for providing movement control of orthotic (**Fig. 3**; Buch et al., 2008; Pfurtscheller et al., 2000), prosthetic (Muller-Putz and Pfurtscheller, 2008) and external movement-assistive devices, such us robotic arms and wheelchairs (Galán et al., 2008; McFarland and Wolpaw, 2008). The main drawbacks of current EEG-based BCIs include the long training periods to learn to modulate specific brain potentials (generally in the order of several months), the need to attach multiple electrodes to the scalp –both a time and appearance issue–, and the low information transmission rate due to the filtering properties of the skull. In addition, control signals generated through EEG-based BCIs lack of speed, accuracy and reliability which limits their applicability as control interfaces of active movement-assistive devices (McFarland and Wolpaw, 2008).

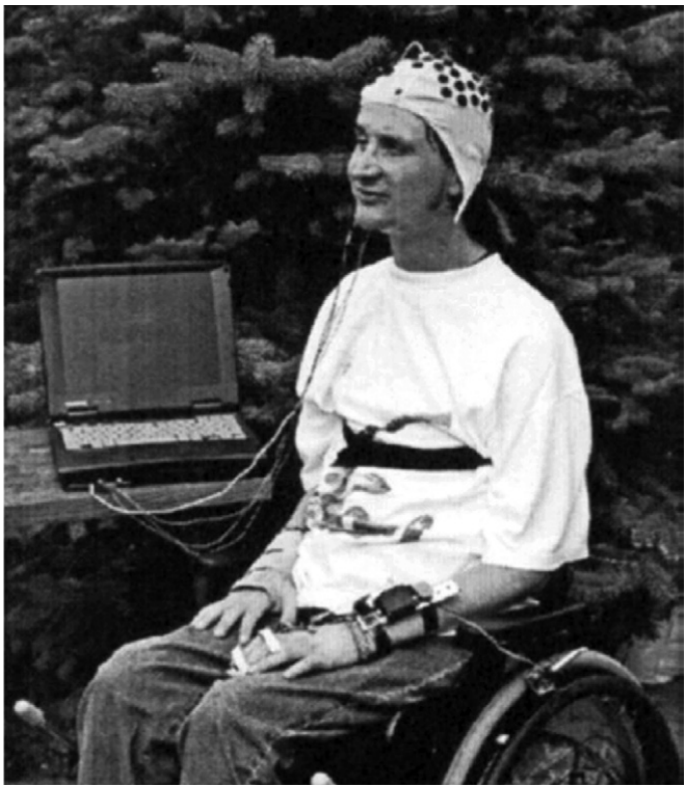

Figure 3. A SCI patient controlling a hand orthosis with an EEG-based BCI. Adapted from Pfurtscheller et al (2000).

Brain Hemodynamics

Beyond electric activity, hemodynamic signals from the brain are also used in BCI. These signals are measured by functional magnetic resonance imaging (fMRI) or near infrared spectroscopy (NIRS). Both methods rely on the measurement of the task-induced blood oxygen level-dependent (BOLD) response which has been proved to be strongly correlated to the electrical brain activity (Sitaram et al., 2009). Most studies using fMRI- and NIRS-based BCIs focused on their application to neurofeedback (Kanoh et al., 2009; Weiskopf, 2012; Weiskopf et al., 2003), and only a few studies have aimed to develop interfaces for communication (Naito et al., 2007; Sorger et al., 2009), cursor control (Yoo et al., 2004), environmental control (Ayaz et al., 2011; Sagara and Kido, 2012) and external robotic arm control (Lee et al., 2009; Misawa et al., 2012). As for EEG, NIRS is also portable and both less expensive and less cumbersome than fMRI. Furthermore, in contrast to fMRI, when using NIRS subjects can be examined under normal conditions (e.g. sitting or standing), without movement constraints. On the other hand, the depth of brain tissue that can be measured using NIRS is only 1 to 3 cm (i.e. cortical regions; Sitaram et al., 2009). While these functional imaging methods are promising for non-invasive recording of activity across the entire brain (or cortex in the case of NIRS) at high spatial resolution (i.e. millimeter range; Sitaram et al., 2009), fMRI- and NIRS-based BCIs are still in the early phases of research and development, and therefore their potential value as interface remains uncertain (Shih et al., 2012). Furthermore both fMRI and NIRS methods suffer from poor information transfer rate (Ward and Mazaheri, 2008; Power et al., 2011) which limits their functionality.

Interfacing with the Actuators: Muscle Activation Interfaces (MAIs)

The recording of the electrical signals from muscle activation is known as electromyography (EMG). From a biomechatronic perspective the muscle can be conceived as a biological signal amplifier of the low amplitude electric potential that comes from the efferent nerves. The large majority of active orthoses and prosthesis existing today, including commercially available devices (e.g. DynamicArm®, Otto Bock HealthCare GmbH, Duderstadt, Germany; HAL-5 Cyberdyne Inc., Tsukuba, Japan), are controlled using surface EMG signals (Asghari Oskoei and Hu, 2007; Fougner et al., 2012). Furthermore, EMG-based interfaces have also been used to control powered wheelchairs (Felzer and Freisleben, 2002; Han et al., 2003; Moon et al., 2005).

Myoelectric prostheses are generally controlled by measuring EMG from two independent residual muscles or by distinguishing different activation levels of one residual muscle. Switching techniques such as muscle co-contraction or the use of mechanical switches or force-sensitive resistors are commonly implemented for enabling the sequential operation of several degrees of freedom (DOF; Muzumdar, 2004). In the case of active orthoses, these are generally controlled trough proportional myoelectric control using the EMG signals from the muscles associated to the supported motion.

EMG-based control interfaces are widely used because of its easy access and generation, and its direct correlation to the motion intention. However, EMG-based interface presents several drawbacks: requires significant signal processing before it can be used as control signal due to its broad bandwidth and low voltage amplitude; the relation between EMG and force or torque is highly non-linear (Lenzi et al., 2012), which makes the control challenging for the users; many patients have difficulties generating isolated and repeatable contractions which are in most prosthesis required for their control (Schultz and Kuiken, 2011); and finally, the filtering properties of the limb tissue and the movement of the skin beneath the electrode notably affect the long term recordings (Muzumdar, 2004). In order to overcome some of these limitations, innovative pattern recognition algorithms and surgical procedures such as targeted muscle reinnervation (TMR) are being developed.

Pattern recognition techniques are based on the assumption that humans can generate different yet repeatable muscle activation patterns that are associated to specific movements such us different grasping configurations. This technique has the potential to eliminate the need for isolated muscle activation and allow for a more natural control of the assistive device (Schultz and Kuiken, 2011). The pattern recognition algorithms first extract features of the EMG signal from one or multiple adjacent muscles and then search for activation patterns which are subsequently assigned to a "class" of movement. Many different variations of each of these steps have been investigated trying to find a fair tradeoff between speed and performance (Asghari Oskoei and Hu, 2007; Fougner et al., 2012). Pattern recognition is currently not commercially available but considerable efforts, such as developing practical adaptive algorithms (Sensinger et al., 2009), are being made to bring this technology into clinical practice.

MTR was developed by Kuiken et al. (2007) and consists on rerouting the nerves that originally innervated the amputated limb to muscles on the chest wall (**Fig. 4**). TMR is a one-time invasive method that allows a more intuitive control of a larger number of DOF (Miller et al., 2008) than standard EMG methods, since the myoelectric prosthesis is controlled by the same nerves that previously controlled the amputated limb. Moreover, there is evidence that cutaneous sensory feedback of the amputated hand can be regained through stimulation of the reinnervated muscles (Kuiken et al., 2007). In contrast to pattern recognition techniques, TMR seems most suitable for high-level amputations (Bueno Jr et al., 2011). Current implementations still experience some difficulties separating the EMG signals from the different chest muscles. Therefore, recent studies try to combine MTR with pattern recognition techniques (Kuiken et al., 2009).

Interfacing with the Actuators: Muscle Contraction Interfaces (MCIs)

Several signals derived from the muscle contraction phenomena have been used to detect motion intention detection: muscle vibration, dimensional change, stiffness and force. Most of these methods have only been used for the control of prosthetic devices.

Muscle Vibration

The mechanical vibration that is generated when the muscles contracts can be measured with microphones (Barry et al., 1986; Posatskiy and Chau, 2012a), accelerometers (Antonelli et al., 2009) or a combination of both (Silva and Chau, 2003; Silva et al., 2005). This method is known as phonomyography (PMG), acoustic myography (AMG) or mechanomyography (MMG).

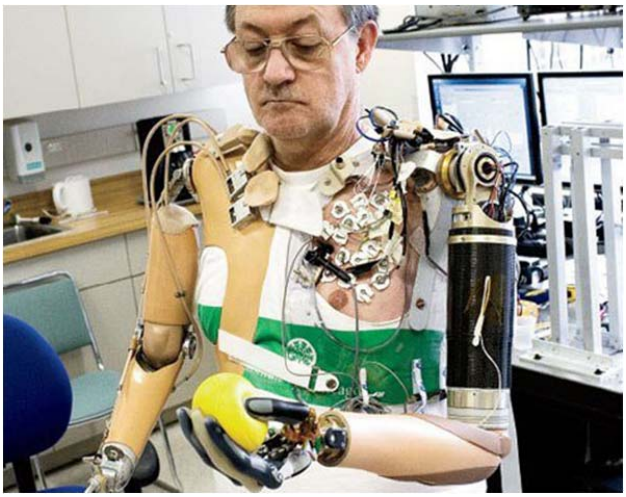

Figure 4. A targeted reinnervation patient performing a functional manipulation task with an active prosthetic arm. Adapted from Kuiken et al (2009).

Orizio et al. reported a linear relationship between the root-mean-square (RMS) values of MMG signals recorded from the biceps brachii and the force of the contraction between 20% to 80% of the maximum voluntary contraction (MVC; Orizio, 1993), which makes MMG potentially suitable for prosthesis control. MMG offers several advantages over conventional EMG, including no need of direct contact with the skin, robustness to changes on skin impedance, less specific sensor placement and reduced sensor cost (Barry et al., 1986; Silva et al., 2005). However, microphones and especially accelerometers are highly prone to dynamic noise (i.e. limb movement artifacts) which compromises signal detection and classification (Posatskiy and Chau, 2012a). To overcome this major problem, Silva and Chau (2003) developed a coupled microphone-accelerometer sensor (embedded in silicone) that fuses data from both transducers to reduce dynamic noise. In their design, the accelerometer is used as a dynamic reference sensor to determine the source of the measured vibration (muscle contraction or limb movement). Recently, Posatskiy and Chau (2012b) developed a novel microphone with cylindrical and conical acoustic chambers that prevents the recording of limb movement artifacts.

Muscle Dimensional change

When the muscle contracts, dimensional changes also occur: the muscle shortens and consequently its cross section area increases. The measured signals resulting from this phenomenon are known as myokinemetric (MK) signals.

Evidence from Heath (2003) and Kenney et al. (1999) suggests that MK signals are inherently low in noise and that its magnitude can be directly used for control avoiding any kind of

signal processing. MK signals have been measured with Hall-effect sensors (Heath, 2003; Kenney et al., 1999) or tendon activated pneumatic (TAP) foam sensors (Abboudi et al., 1999; Curcie et al., 2001). The study of Kenny et al. (1999) developed a Hall-effect sensor that measured radial displacements of the muscle bulge. They found that the MK signals of 6 upper-limb amputees could be generated with sufficient accuracy to perform a one-dimension tracking tasks with errors averaging 10%, and therefore had potential for the control of active upper limb prosthesis. However, it was also found that MK signals recorded with the Hall-effect sensor were susceptible to socket slippage with time, as well as socket re-donning. The study of Heath (2003) improved the Hall-effect sensor interface and proved the feasibility of using MK signal for the proportional position control prosthetic fingers.

The TAP sensors developed by Abboudi et al. (1999) measured pressure differential at the skin surface generated by tendon displacements when finger flexors or extensors muscles contracted. TAP sensors presented a linear relation to force, allowing proportional force control. Trials on 3 upper-limb amputees showed that the TAP sensors could provide effective control of voluntary flexions of individual fingers and grasping motions. Since the performance of the TAP control interface is highly dependent upon accurate sensor placement and specific movement resolution at each sensor location, Curcie et al. (2001) developed a pressure vector decoder (PVD) able to discriminate specific finger flexion commands in real-time. The PVD decreased the dependence upon sensor location offering a more robust and reliable controller of the TAP-based interface.

Recent studies propose the use of ultrasound scanners (Chen et al., 2010; Shi et al., 2010; Zheng et al., 2006) to measure changes in muscle thickness for the control of prosthetic devices. This method is known as sonomyography (SMG). SMG presents similar profiles of wrist angle for non-disabled subjects and amputees (Zheng et al., 2006), suggesting that simple proportional control could be implemented. Furthermore a recent study from Shi et al. (2010) shows that SMG can be implemented in real-time using a two-dimensional logarithmic search algorithm. While it has been demonstrated that SMG could be potentially used for the control of active prosthetic devices, the current system used for the SMG measurements (i.e. standard ultrasound scanner) is not suitable for its practical implementation because it is expensive and cumbersome (Chen et al., 2010).

Another signal derived from dimensional changes of the muscle was examined in the early 1970s by Kadefors and Olsson (1972). The study investigated electrical impedance as a measure of motion intent for the control of an artificial hand. The electrical impedance measured on the skin above a muscle varied (among other factors) when the dimensions of the muscle changed due to its contraction. To our knowledge this method has not been developed further since then without any specific reason.

Muscle Force

Direct muscle force control by muscle tunnel cineplasties (**Fig. 5**) was first performed in the early 1900s, becoming popular after the World War II (Childress, 2002; Weir et al., 2001). The major advantage of this one-time invasive method is that is capable of providing tactile and proprioceptive feedback from the terminal device back to the user complying with the concept of extended physiological proprioception (EPP; Simpson, 1974; Weir et al., 2001). However, such procedures lost favor in the 1970s due to the advent of clinically available myoelectric prostheses, which do not require any surgery, and lack of sufficient muscle force to power the prosthesis (Childress, 2002).

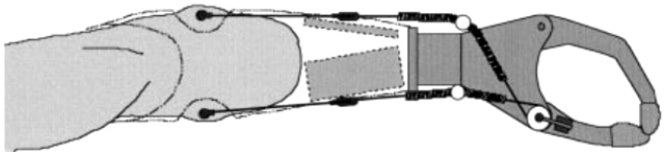

Figure 5. Schematic of the modified Otto Bock Hand that is controlled by two muscle tunnel cineplasties. Adapted from Wier et al. (2001).

While traditionally tunnel cineplasties provided simultaneously the control and the actuation of the prosthetic prehensor (Brava et al., 1957), recently, Wier et al. (2001) proposed a hybrid method where the tunnel cineplasty provides the control signal for the prosthetic prehensor but where the grasping force was supplied by an external power source. The authors of the study suggested that the implementation of multiple miniature forearm tunnel cineplasties could be potentially used as control signals for independent multi-finger control. However, to our knowledge no further advancements on this method have been made up to date.

Muscle Stiffness

The stiffness of muscle tissue increases when this contracts. The measured force signals resulting from this phenomenon are known as myotonic (MT; Heath, 2003) or myokinetic (MKT; Wininger et al., 2008) signals. These signals have been measured using arrays of force-sensitive resistors (FSRs; Wininger et al., 2008) or pressure sensors (Moromugi et al., 2004). MKT signals have been used for proportional force control using a simple summation of the recorded forces (Moromugi et al., 2004).

Recently, a study from Han et al. (2012) presented a novel muscle stiffness sensor –that could be worn over clothing– based on the measure of the muscle resonance frequency. This sensor measured muscle stiffness by generating and sensing resonance vibrations using piezoelectric transducers: as the muscle became stiffer, the resonance frequency became higher.

Muscle stiffness-based interfaces are still in the early phases of research and development, and therefore their potential value as control interfaces for active movement-assistive devices remains uncertain.

Interfacing with the Plant: Movement Interfaces (MIs)

The human body moves as a result of the interaction between the forces generated by the muscles and the configuration of the skeletal system. Measurements of angular displacement between two adjacent body segments and of translations of one body segment (linear displacement) have been used to detect motion intention. It is worth noting that the implementation of movement-based interfaces requires very light mechanical plants in order to not constrain the movement of the user.

Angular displacement

Angular displacement between two adjacent body segments is measured using electro-goniometers, which are attached to the two adjacent body segments and produce an electrical signal proportional to the angle. Several kinds of electro-goniometers have been used to measure angular displacements. Early goniometers used simple angular potentiometers. Doubler and Childress (1984) and Gibbons et al. (1987) used these sensors to implement the EPP concept in the control of active upper extremity prostheses. Although potentiometers can measure rotations about only one axis and the accuracy of the measurements depend on their alignment with the human joint, these sensors are still a common component in active movement-assistive devices (e.g. Blaya and Herr, 2004; Herr and Wilkenfeld, 2003). Currently, more advanced goniometers are being implemented for the control of active prosthetic and orthotic devices, which are able to measure rotations about two axes simultaneously based on optic sensors (Herle et al., 2010; Shah et al., 2011) or strain gauges (Orengo et al., 2009; Takagi et al., 2009). Another common solution for measuring angular displacement to control active prosthetic and orthotic devices is angular encoders (Font-Llagunes et al., 2011; Martinez-Villalpando et al., 2008; Yamada et al., 2001). It is worthy of note that there are no goniometers that can record three angles between two body segments, which naturally limits the applicability of this methods for control strategies that require information of three-dimensional joint rotations (Latash, 2012).

Body segment translation

Hall-effect sensors and potentiometers integrated in a joystick are the most common sensors used to measure body segment translations in movement interfaces. Joysticks are generally implemented for the control of powered wheelchairs (Dicianno et al., 2010) and external robotic arms (Maheu et al., 2011; Romer et al., 2005). However, recent studies also investigated the performance of controlling prosthetic arms with the residual shoulder motion measured with a two-DOFs joystick (**Fig. 6A**; Lipschutz et al., 2011; Losier et al., 2011). Additionally, the study from Johnson et al., 2001 developed a five-DOFs upper-extremity orthoses, in which the end point position was controlled with a joystick at the contralateral hand (**Fig. 6B**).

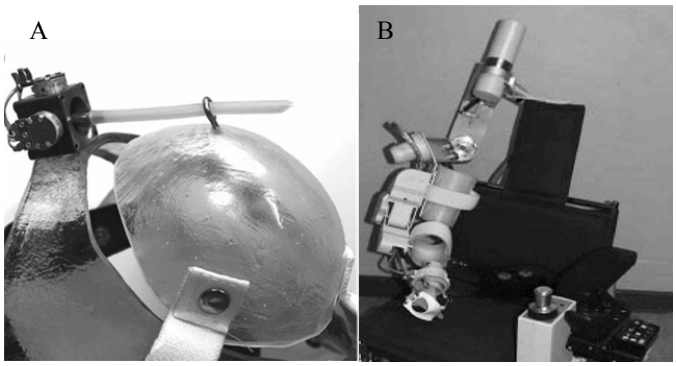

Figure 6. Joystick based interfaces. A) Two-DOF joystick for the control of a prosthetic arm with the residual shoulder motion. Adapted from Lipschutz et al. (2011). B) Five-DOF active upper-extremity orthosis controller with a hand 5-DOF joystick. Adapted from Johnson et al. (2001).

Joysticks are commonly controlled with the hand but in some cases the interface is adapted to be controlled with other body parts (i.e. parallel systems). Some joysticks contain built in damping and stiffness features or digital filters to eliminate some human unintentional movement such as tremor, or environmental vibrations (Dicianno et al., 2010).

Interfacing with the Plant: Force Interfaces (FI)

The human plant can exert forces to the environment that can provide information about the motion intention of the user. Force-based interfaces have been used in assisted-powered wheelchairs (Cooper et al., 2002) where the wheelchair detects and amplifies the force applied by the user. Additionally, recent studies implemented six-DOFs force-torque sensors or simple force sensor resistors for the control of active upper-extremity orthoses (Abbruzzese et al., 2011, 2011; M. Baklouti et al., 2008; Huo et al., 2010) and prosthesis (Lipschutz et al., 2011).

Force-based interfaces generally implement admittance control strategies where the input is force and the output is velocity or position (Yu et al., 2011). Recently, Ragonesi et al. (2011) published a study where they measured residual joint force and torques in patients with muscle weakness with the end goal of obtaining a robust model that could be used for the control of an active arm orthoses. The authors found that voluntary forces for weak individuals were very hard to measure since gravitational forces were much larger. Subject specific models were suggested to optimize the measurement of voluntary forces.

The main advantage of force-based interfaces is that force sensors can be embedded in the mechanical structure of the assistive device, avoiding any preparation for the placement of the sensors on the user. Furthermore, the implementation of force-based interfaces do not specially require a light mechanical plant as in the case of position-based interfaces.

Interfacing with Parallel systems

A part from deriving the motion intention from signals that come from the supported systems, several methods have been proposed which use signals from parallel systems such as the eyes, the mouth or the head. This section reviews four relevant interfaces that derive the intent of the user through signals generated by parallel systems.

Eye Movement Interface

Eye tracking systems are a common method for the control of spelling devices or computer cursors in patients with severe movement-impairments. Several eye-trackers have been developed including camera-based methods, which measure changes in corneal reflection while infrared light is projected to the eye (Betke et al., 2002), and electrical-based methods that measure the electrooculagrphic (EOG) potential from surface electrodes.

Duvinage et al., (2011) proposed an innovative system based on EOG and a programmable central pattern generator to control a lower limb prosthesis. The control method was composed of two steps: first, an EOG-based eye tracking system generated high-level control commands (such as faster, slower or stop), according to specific eye movement sequences executed by the user; and secondly, a pattern generator, following the high level commands derived from the user's eye motion, provided the low level commands for the control of the actuators.

In the study from Chen and Newman (2004), EOG was used to control two–dimensional movement of an external robotic arm that resembled the human arm configuration. Eye movement patterns such us saccades, fixation or blinks were detected from the raw eye gaze movement data by a pattern recognition algorithm and converted into control signals according to predefined protocols. The authors suggested that one option to extend the movement control to three-dimensional space was to switch between predefined action planes in which the EOG control would still be two-dimensional.

While eye movement interfaces proved to be very accurate in two-dimensional space, three-dimensional gaze tracking is more challenging (Morimoto and Mimica, 2005). The three-dimensional gaze tracking problem consists of mapping pupil coordinates for left and right eye to a three-dimensional point referenced to the user's head coordinated. Recently, a study from Onose et al., (2012) investigated the feasibility of using a combined eye-tracking and EEG-based interface in tetraplegic patients for the control of a robotic arm. Two pair of head-mounted cameras tracked the left and right pupil while a position and rotation of the head was measured using an optoelectronic system. The target point was calculated using the gaze-tracker while the different robot actions, such as grabbing the object and placing it on a drinking position, were controlled with the BCI. The authors conclude that the potential of the system was limited but real for self-assistance in tetraplegic patients.

Tongue Movement Interface

Tongue movement has been interfaced using electrical switches (Clayton et al., 1992), hall-effect sensors (Buchhold, 1995), pressure sensors (Masaki et al., 2005, commercially available) and by measuring changes in the inductance of an air-cored induction coil, by moving a ferro magnetic material attached to the tongue into the core of the coil (Huo et al., 2008; Struijk et al., 2009; Struijk, 2006). Tongue movement interfaces take advantage of high sensitivity and selectivity of the tongue. Furthermore, in most designs the interface is placed inside the mouth being very inconspicuous.

The tongue interface developed by Huo et al (2008) has the inductive coil mounted in front of the mouth and the user has to stick out the tongue to operate. This system was tested in 13 high-level SCI patients during a navigation task with a powered wheelchair. The study reported that the subjects were able to perform the experimental task with 82% accuracy (Huo and Ghovanloo, 2010).

The tongue interface developed by Struijk et al. (2009) integrated the induction coils under the palate where eighteen sensors allowed real-time proportional control of both speed and direction similar to a conventional joystick (**Fig. 7**). The system's functionality was demonstrated in a pilot experiment with one healthy subject, where a typing rate of up to 70 characters per minute was obtained with an error rate of 3%.

Recently, two alternative sensor designs based on the previously described system have been proposed in order to reduce the size of the sensor pad and increasing the easiness of wear of the oral interface (Lontis and Andreasen Struijk, 2012).

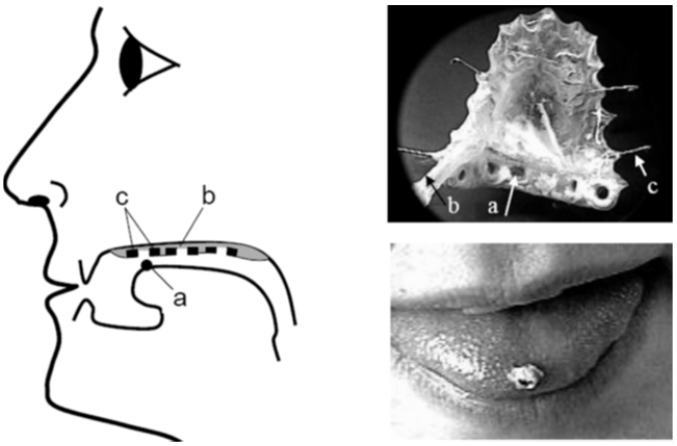

Figure 7. Tongue movement-based interfaces. Left: the inductive tongue control system. a: The activation unit, b: the palatal plate, c: the inductors. The tongue activates the sensors by placing the tongue-mounted activation unit at or inside a coil. Right, top: the palatal plate with 5 sensors. a: the lead wires, b: the coils, c: the clamps keeping the plate in place. Right, bottom: the activation unit glued to the tongue. Adapted from Struijk et al. (2009).

Head Movement Interface

Head movements are generally measured using accelerometers and used to control powered-wheelchairs (Craig and Nguyen, 2006; Fusco and Balbinot, 2011; Hinkel III, 2010; Joseph and Nguyen, 1998; Taylor and Nguyen, 2003). The direction of the inclination controls the wheelchair's direction and the velocity of the wheelchair is proportional to the inclination angle. Artificial neural networks are usually implemented in the control interface to detect with higher accuracy (i.e. 97%; Craig and Nguyen, 2006) the movement intention of the user. However, all the research studies found were tested with healthy subjects which does not provide truly evidence of its actual usability in patients with severe movement impairments.

Alternative sensors include ultrasonic sensors (Coyle, 1995) and camera-based interfaces (M. Baklouti et al., 2008; Malek Baklouti et al., 2008). An important disadvantage of the camera-based interfaces is that their functionality largely depends on the light conditions which results in the need of repetitive calibrations during the day (Bergasa et al., 2000).

Speech Interface

In speech-based interfaces the voice commands of the user are recorded using conventional microphones and translated into control signals through speech recognition algorithms. Generally speech recognition requires training which consists of the recording of the voice commands and their subsequent manual classification. It is worth noting that there is a tradeoff between the amount of trained voice commands and the recognition accuracy of the algorithm (Fan and Li, 2010).

Fan and Li, (2010) developed a speech-based interface for the control of an upper-extremity prosthesis which could recognize 15 different voice commands with an accuracy of 96% . Speech has been also used to control powered wheelchairs (Simpson and Levine, 2002) or external robotic arms (Rogalla et al., 2002). The main drawback of speech-based interfaces is its high sensitivity to ambient noise which compromises signal detection and classification. The recognition accuracy of the speech-based interface developed by Lv et al. (2008) for the control a robot was decreased by 30% when ambient noise was present.

Design Considerations

A proper design of the control interface is a prerequisite for the usability and acceptance of the active movement-assistive device. Good functional performance of the control interface is not sufficient to justify its clinical implementation and the following design considerations should be taken into account.

Intuitiveness

A control interface should be intuitive, enabling the user to operate their active movement-assistive device subconsciously (i.e. the way healthy people control their limbs) with a short training period and to think about other things while using the device. This kind of control may require proprioceptive feedback (i.e. EPP; Simpson, 1974) in cases where normal sensory feedback has been lost (e.g. amputees) to not only rely on visual feedback which requires considerable mental effort (Farrell et al., 2005). Another control strategy that can reduce the user's mental effort is the shared-control paradigm, which aims at combining the intelligence of the human and of the robot. Providing a certain degree of autonomy to the robot has been proved to increase task performance (Galán et al., 2008; Kim et al., 2006).

The reviewed literature shows that most control interfaces are tested in laboratory environments, in which users can concentrate on the experimental task with minimal distractions. However, users in the "real world" have to deal with much more complex situations, where mental effort cannot be entirely (or even primarily) dedicated to the control of the assistive device, as they have to interact with other people or the environment. Therefore, considering that many processes run simultaneously in the brain, it is plausible to conjecture that noninvasive-BCIs

would require a considerable effort of concentration to generate those specific brain signals required for the control of an active movement-assistive device. On the other hand, peripheral signals such as force, EMG or ENG are more closely linked to the control of movement. Consequently, one could reasonably speculate that control interfaces using these signals would appear to be more natural and intuitive for the user than noninvasive-BCIs. An obvious exception is the case of paralyzed patients, for whom peripheral signals are not available.

It is worth noting that research using invasive BCIs shows potential to provide a faster and more intuitive interface for the control of active movement-assistive devices since the measured signals present higher signal-to-noise ratio and are more selective that EEG-based BCIs (Hochberg et al., 2006; Schalk and Leuthardt, 2011; Yanagisawa et al., 2011). However, invasive BCIs face substantial clinical risk due to the need for the implantation of the electrode arrays in or on the cortex and therefore research in humans has been limited. Furthermore the electrodes require long-term stability and consistent performance which still remains a challenge (McFarland and Wolpaw, 2008).

Information source for the control interface

A second consideration in the design of a control interface required to gain both user and clinical acceptance of active movement-assistive devices, is that the control interface should avoid the sacrifice of a "useful" body function from parallel systems (e.g. eye, head or tongue movement) for deriving the motion intention of the user. Nevertheless, signals from parallel systems can be used for "supplementary control" such as tuning control settings or switching on and off control modalities. Note that supplementary control is used on occasional basis and therefore, does not require continuous attention of the user and never implies the sacrifice of the parallel system functionality.

Response Time

Another essential feature of the control interface that has a determinative effect on the performance of the assistive device is the response time or delay (Farrell and Weir, 2007). A tradeoff between speed and accuracy exists regarding the control delay. Large delays increase accuracy of the motion intention detection, but at the same time, decreases responsiveness (and therefore performance) of the active assistive device. Farrell and Weir (2007) concluded that control delays should be kept below 100 ms for proper control of myoelectric prosthesis.

Coordination of the DOF

From a functional point of view, a control interface for active movement-assistive devices should be able to coordinate multiple DOF simultaneously in an effective way. Coordinated movements would give a more natural appearance than if every DOF was controlled separately. Nevertheless, it is worth noting that the user may also need to control an individual DOF when performing a precision task.

Independence

Ideally, an active movement-assistive device should be completely controlled by its user and should not require assistance from other people (e.g. caretakers or family). Unfortunately, most of the reviewed devices present control interfaces that require considerable assistance for the preparation of the equipment, such as placing the sensors in the correct location or sensor calibration. Therefore, control interfaces that use implantable sensors or sensors integrated on the artificial plant (e.g. force sensors) inherently offer a clear advantage in terms of user friendliness.

Adaptability

In cases where active movement-assistive devices are designed for patients suffering from degenerative diseases (e.g. DMD), the control interface (and the rest of the device) should be able to adapt to the varying needs and capabilities of the user. Note that changes can occur over the short term (during a day) as well as over long term (years) periods. The monitoring of specific biomechanical descriptors could give an indication of the changing needs of the user and adapt the control interface to the new situation. Moreover this information could be used by clinicians to evaluate a disease's progression.

Even if this might not be an exhaustive list of design requirements for the development of control interfaces, these recommendations do capture the fundamental aspects that are clearly worth analyzing when designing control interfaces for active movement-assistive devices.

Discussion and Conclusions

Despite the fact that many innovative control interfaces for active movement-assistive devices are rapidly being developed, passive systems, which are usually limited in functionality but highly effective and easy to use, still prevail in clinical practice. Active movement-assistive devices have the potential of offering a more flexible solution adapting their performance to the patient's needs and capabilities, but it is clear from literature that the clinical application of these devices continues to lag behind initial expectations.

All the reviewed control interfaces are still far below the performance of the physiological movement control which hinders their acceptance. Each of the methods described

previously present unique advantages and limitations and may eventually find a specific application for a specific patient's group. However, the rate at which these technologies are advancing should provide hope for the development of better control interfaces for active movement-assistive devices.

It is worth noting that while there is a large variety of control interfaces under development and a considerable confusion as to which one is the most suitable for each type of impairment and task, only a few studies have focused on their performance evaluation and comparison. Currently, there is no standard method to evaluated the performance of control interfaces which prevents their objective evaluation and comparison.

We believe that a better understanding of the limitations and capabilities of the different control interfaces, through objective and quantitative evaluations during functional tasks, can provide relevant information for the selection of the most suited control interface for a specific application. One example of this approach is the study from Corbett et al. (2011) which evaluates the performance of EMG-, force- and position-based control interfaces in terms of tracking error, information transmission rate and human-operator bandwidth during a one-dimensional screen-based position-tracking task. Additionally, the study from Guo et al. (2011) compares SMG-, EMG-, force- and wrist angle-based interfaces during a series of screen-based discrete tracking tasks with and without a simultaneous auditory attention task. Even though these two studies do not evaluate the interface performance during functional movement-tasks, they can provide a first insight of their potential value as control interfaces for active movement-assistive devices.

Acknowledgements

This research was supported by the Flextension project through the Dutch Technology Foundation (STW), the Duchenne Parent Project, Spieren voor Spieren, Prinses Beatrix Fonds, Johanna Kinderfonds and Rotterdams Kinderrevalidatie Fonds Adriaanstichting, Focal Meditech, OIM Orthopedie and Ambroise.

References

Abboudi, R.L., Glass, C.A., Newby, N.A., Flint, J.A., Craelius, W., 1999. A biomimetic controller for a multifinger prosthesis. IEEE Transactions on Rehabilitation Engineering 7, 121 –129.

Abbruzzese, K., Lee, D., Swedberg, A., Talasan, H., Paliwal, M., 2011. An innovative design for an Assistive Arm Orthosis for stroke and muscle dystrophy, in: Bioengineering Conference (NEBEC), 2011 IEEE 37th Annual Northeast. Presented at the Bioengineering Conference (NEBEC), 2011 IEEE 37th Annual Northeast, pp. 1 –2.

Antonelli, M.G., Beomonte Zobel, P., Giacomin, J., 2009. Use of MMG Signals for the Control of Powered Orthotic Devices: Development of a Rectus Femoris Measurement Protocol. Assistive Technology 21, 1–12.

Asghari Oskoei, M., Hu, H., 2007. Myoelectric control systems—A survey. Biomedical Signal Processing and Control 2, 275–294.

Ayaz, H., Shewokis, P.A., Bunce, S., Onaral, B., 2011. An optical brain computer interface for environmental control, in: Engineering in Medicine and Biology Society,EMBC, 2011 Annual International Conference of the IEEE. pp. 6327 –6330.

Baklouti, M., Guyot, P.-A., Monacelli, E., Couvet, S., 2008. Force controlled upper-limb powered exoskeleton for rehabilitation, in: IEEE/RSJ International Conference on Intelligent Robots and Systems, 2008. IROS 2008. Presented at the IEEE/RSJ International Conference on Intelligent Robots and Systems, 2008. IROS 2008, p. 4202.

Baklouti, M., Monacelli, E., Guitteny, V., Couvet, S., 2008. Intelligent Assistive Exoskeleton with Vision Based Interface, in: Helal, S., Mitra, S., Wong, J., Chang, C.K., Mokhtari, M. (Eds.), Smart Homes and Health Telematics, Lecture Notes in Computer Science. Springer Berlin Heidelberg, pp. 123–135.

Barry, D.T., Leonard, J.A., Jr, Gitter, A.J., Ball, R.D., 1986. Acoustic myography as a control signal for an externally powered prosthesis. Arch Phys Med Rehabil 67, 267–269.

Bergasa, L.M., Mazo, M., Gardel, A., Barea, R., Boquete, L., 2000. Commands generation by face movements applied to the guidance of a wheelchair for handicapped people, in: 15th International Conference on Pattern Recognition, 2000. Proceedings. Presented at the 15th International Conference on Pattern Recognition, 2000. Proceedings, pp. 660–663 vol.4.

Bertos, Y.A., Heckathorne, C.W., Weiss, R.F., Childress, D.S., 1997. Microprocessor based E.P.P. position controller for electric-powered upper-limb prostheses, in: Proceedings of the 19th Annual International Conference of the IEEE Engineering in Medicine and Biology Society, 1997. Presented at the Proceedings of the 19th Annual International Conference of the IEEE Engineering in Medicine and Biology Society, 1997, pp. 2311 –2314 vol.5.

Betke, M., Gips, J., Fleming, P., 2002. The Camera Mouse: visual tracking of body features to provide computer access for people with severe disabilities. IEEE Transactions on Neural Systems and Rehabilitation Engineering 10, 1–10.

Biddiss, E.A., Chau, T.T., 2007. Upper limb prosthesis use and abandonment: A survey of the last 25 years. Prosthetics and Orthotics International 31, 236–257.

Blaya, J.A., Herr, H., 2004. Adaptive control of a variable-impedance ankle-foot orthosis to assist drop-foot gait.

IEEE Transactions on Neural Systems and Rehabilitation Engineering 12, 24 –31.

Borutzky, W., 2010. Bond Graph Methodology: Development and Analysis of Multidisciplinary Dynamic System Models. Springer.

BRAV, E.A., SPITTLER, A.W., LUSOMBE, H.B., KUITERT, J.H., MACDONALD, W.F., VULTEEJR., F.E., WOODARD, G.H., FLETCHER, M.J., LEONARD, F., 1957. Cineplasty An End-Result Study. J Bone Joint Surg Am 39, 59–76.

Buch, E., Weber, C., Cohen, L.G., Braun, C., Dimyan, M.A., Ard, T., Mellinger, J., Caria, A., Soekadar, S., Fourkas, A., Birbaumer, N., 2008. Think to move: a neuromagnetic brain-computer interface (BCI) system for chronic stroke. Stroke 39, 910–917.

Buchhold, N., 1995. Apparatus for controlling peripheral devices through tongue movement, and method of processing control signals.

Bueno Jr, R.A., French, B., Cooney, D., Neumeister, M.W., 2011. Targeted Muscle Reinnervation of a Muscle-Free Flap for Improved Prosthetic Control in a Shoulder Amputee: Case Report. The Journal of Hand Surgery 36, 890–893.

Chen, X., Zheng, Y.-P., Guo, J.-Y., Shi, J., 2010. Sonomyography (smg) control for powered prosthetic hand: A Study with normal subjects. Ultrasound in Medicine and Biology 36, 1076–1088.

Chen, Y., Newman, W.S., 2004. A human-robot interface based on electrooculography, in: 2004 IEEE International Conference on Robotics and Automation, 2004. Proceedings. ICRA '04. Presented at the 2004 IEEE International Conference on Robotics and Automation, 2004. Proceedings. ICRA '04, pp. 243–248 Vol.1.

Childress, D.S., 2002. Presentation highlights: Tunnel cineplasty. Journal of Rehabilitation Research and Development 39, 9–10.

Cipriani, C., Zaccone, F., Micera, S., Carrozza, M.C., 2008. On the shared control of an EMG-controlled prosthetic hand: Analysis of user-prosthesis interaction. IEEE Transactions on Robotics 24, 170–184.

Clayton, C., Platts, R.G.S., Steinberg, M., Hennequin, J.R., 1992. Palatal tongue controller. Journal of Microcomputer Applications 15, 9–12.

Cooper, R.A., Corfman, T.A., Fitzgerald, S.G., Boninger, M.L., Spaeth, D.M., Ammer, W., Arva, J., 2002. Performance assessment of a pushrim-activated power-assisted wheelchair control system. IEEE Transactions on Control Systems Technology 10, 121 –126.

Corbett, E.A., Perreault, E.J., Kuiken, T.A., 2011. Comparison of electromyography and force as interfaces for prosthetic control. The Journal of Rehabilitation Research and Development 48, 629.

Coyle, E.D., 1995. Electronic wheelchair controller designed for operation by hand-operated joystick, ultrasonic noncontact head control and utterance from a small word-command vocabulary, in: IEE Colloquium on New Developments in Electric Vehicles for Disabled Persons. Presented at the IEE Colloquium on New Developments in Electric Vehicles for Disabled Persons, pp. 3/1–3/4.

Craig, D.A., Nguyen, H.T., 2006. Wireless real-time head movement system using a personal digital assistant (PDA) for control of a power wheelchair, in: Engineering in Medicine and Biology Society, 2005. IEEE-EMBS 2005. 27th Annual International Conference of The. pp. 772–775.

Curcie, D.J., Flint, J.A., Craelius, W., 2001. Biomimetic finger control by filtering of distributed forelimb pressures. IEEE Transactions on Neural Systems and Rehabilitation Engineering 9, 69 –75.

Datta, D., Selvarajah, K., Davey, N., 2004. Functional outcome of patients with proximal upper limb deficiency--acquired and congenital. Clin Rehabil 18, 172–177.

Dicianno, B.E., Cooper, R.A., Coltellaro, J., 2010. Joystick Control for Powered Mobility: Current State of Technology and Future Directions. Phys Med Rehabil Clin N Am 21, 79–86.

Dollar, A.M., Herr, H., 2008. Lower Extremity Exoskeletons and Active Orthoses: Challenges and State-of-the-Art. IEEE Transactions on Robotics 24, 144 –158.

Doubler, J.A., Childress, D.S., 1984. An analysis of extended physiological proprioception as a prosthesis-control technique. J Rehabil Res Dev 21, 5–18.

Duvinage, M., Castermans, T., Dutoit, T., 2011. Control of a lower limb active prosthesis with eye movement sequences, in: 2011 IEEE Symposium on Computational Intelligence, Cognitive Algorithms, Mind, and Brain (CCMB). Presented at the 2011 IEEE Symposium on Computational Intelligence, Cognitive Algorithms, Mind, and Brain (CCMB), pp. 1 –7.

Fan, B.H., Li, K.Y., 2010. The speech control system of intelligent robot prosthesis, in: Proceedings - 2010 2nd WRI Global Congress on Intelligent Systems, GCIS 2010. pp. 407–409.

Farrell, T.R., Weir, R.F., 2007. The Optimal Controller Delay for Myoelectric Prostheses. IEEE Transactions on Neural Systems and Rehabilitation Engineering 15, 111 –118.

Farrell, T.R., Weir, R.F., Heckathorne, C.W., Childress, D.S., 2005. The effects of static friction and backlash on extended physiological proprioception control of a powered prosthesis. J Rehabil Res Dev 42, 327–341.

Felzer, T., Freisleben, B., 2002. HaWCoS: The "Hands-free" Wheelchair Control System, in: In Proc. ASSETS 2002. ACM Press, pp. 127–134.

Fleischer, C., Hommel, G., 2008. A human-exoskeleton interface utilizing electromyography. IEEE Transactions on Robotics 24, 872–882.

Font-Llagunes, J.M., Arroyo, G., Serrancolí, G., Romero, F., 2011. A powered lower limb orthosis for gait assistance in incomplete spinal cord injured subjects, in: ACM International Conference Proceeding Series.

Fougner, A., Stavdahl, O., Kyberd, P.J., Losier, Y.G., Parker, P.A., 2012. Control of Upper Limb Prostheses:

Terminology and Proportional Myoelectric Control #x2014;A Review. IEEE Transactions on Neural Systems and Rehabilitation Engineering 20, 663 –677.

Fusco, D.A., Balbinot, A., 2011. Prototype for managing the wheelchair movements by accelerometry. Sensors and Transducers 126, 31–41.

Galán, F., Nuttin, M., Lew, E., Ferrez, P.W., Vanacker, G., Philips, J., Millán, J. del R., 2008. A brain-actuated wheelchair: Asynchronous and non-invasive Brain–computer interfaces for continuous control of robots. Clinical Neurophysiology 119, 2159–2169.

Gibbons, D.T., O'riain, M.D., Philippe-Auguste, S., 1987. An Above-Elbow Prosthesis Employing Programmed Linkages. IEEE Transactions on Biomedical Engineering BME-34, 493 –498.

Gopura, R.A.R.C., Kiguchi, K., 2009. Electromyography (EMG)-signal based fuzzy-neuro control of a 3 degrees of freedom (3DOF) exoskeleton robot for human upper-limb motion assist. Journal of the National Science Foundation of Sri Lanka 37.

Guo, J.-Y., Zheng, Y.-P., Kenney, L.P.J., Bowen, A., Howard, D., Canderle, J.J., 2011. A Comparative Evaluation of Sonomyography, Electromyography, Force, and Wrist Angle in a Discrete Tracking Task. Ultrasound in Medicine & Biology 37, 884–891.

Han, Hyonyoung, Han, Heeseop, Kim, J., 2012. Development of real-time muscle stiffness sensor based on resonance frequency for physical Human Robot Interactions, in: 2012 Annual International Conference of the IEEE Engineering in Medicine and Biology Society (EMBC). Presented at the 2012 Annual International Conference of the IEEE Engineering in Medicine and Biology Society (EMBC), pp. 2367 –2370.

Han, J.-S., Zenn Bien, Z., Kim, D.-J., Lee, H.-E., Kim, J.-S., 2003. Human-machine interface for wheelchair control with EMG and its evaluation, in: Proceedings of the 25th Annual International Conference of the IEEE Engineering in Medicine and Biology Society, 2003. Presented at the Proceedings of the 25th Annual International Conference of the IEEE Engineering in Medicine and Biology Society, 2003, pp. 1602 – 1605 Vol.2.

Heath, G.H., 2003. Control of proportional grasping using a myokinemetric signal. Technology and Disability 15, 73–83.

Herle, S., Man, S., Lazea, G., Marcu, C., Raica, P., Robotin, R., 2010. Hierarchical myoelectric control of a human upper limb prosthesis, in: 2010 IEEE 19th International Workshop on Robotics in Alpe-Adria-Danube Region (RAAD). Presented at the 2010 IEEE 19th International Workshop on Robotics in Alpe-Adria-Danube Region (RAAD), pp. 55 –60.

Herr, H., Wilkenfeld, A., 2003. User-adaptive control of a magnetorheological prosthetic knee. Industrial Robot: An International Journal 30, 42–55.

Hinkel III, J.B., 2010. Head-guided wheelchair control system, in: ASSETS'10 - Proceedings of the 12th International ACM SIGACCESS Conference on Computers and Accessibility. pp. 313–314.

Hochberg, L.R., Serruya, M.D., Friehs, G.M., Mukand, J.A., Saleh, M., Caplan, A.H., Branner, A., Chen, D., Penn, R.D., Donoghue, J.P., 2006. Neuronal ensemble control of prosthetic devices by a human with tetraplegia. Nature 442, 164–171.

Huo, W., Huang, J., Wang, Y., Wu, J., 2010. Control of a rehabilitation robotic exoskeleton based on intentional reaching direction, in: 2010 International Symposium on Micro-NanoMechatronics and Human Science (MHS). Presented at the 2010 International Symposium on Micro-NanoMechatronics and Human Science (MHS), pp. 357 –362.

Huo, X., Ghovanloo, M., 2010. Evaluation of a wireless wearable tongue–computer interface by individuals with high-level spinal cord injuries. J. Neural Eng. 7, 026008.

Huo, X., Wang, J., Ghovanloo, M., 2008. A Magneto-Inductive Sensor Based Wireless Tongue-Computer Interface. IEEE Transactions on Neural Systems and Rehabilitation Engineering 16, 497–504.

Johnson, G.R., Carus, D.A., Parrini, G., Scattareggia Marchese, S., Valeggi, R., 2001. The design of a five-degree-of-freedom powered orthosis for the upper limb. Proceedings of the Institution of Mechanical Engineers, Part H: Journal of Engineering in Medicine 215, 275–284.

Joseph, T., Nguyen, H., 1998. Neural network control of wheelchairs using telemetric head movement, in: Engineering in Medicine and Biology Society, 1998. Proceedings of the 20th Annual International Conference of the IEEE. pp. 2731–2733.

Kadefors, R., Olsson, T., 1972. Electrical impedance as a source of information in man-machine systems. Proceedings of the IEEE 60, 724 – 725.

Kanoh, S., Murayama, Y.M., Miyamoto, K., Yoshinobu, T., Kawashima, R., 2009. A NIRS-based brain-computer interface system during motor imagery: system development and online feedback training. Conference proceedings : ... Annual International Conference of the IEEE Engineering in Medicine and Biology Society. IEEE Engineering in Medicine and Biology Society. Conference 2009, 594–597.

Kenney, L.P.., Lisitsa, I., Bowker, P., Heath, G.., Howard, D., 1999. Dimensional change in muscle as a control signal for powered upper limb prostheses: a pilot study. Medical Engineering & Physics 21, 589–597.

Kim, H.K., Biggs, S.J., Schloerb, D.W., Carmena, J.M., Lebedev, M.A., Nicolelis, M.A.L., Srinivasan, M.A., 2006. Continuous shared control for stabilizing reaching and grasping with brain-machine interfaces. IEEE Trans Biomed Eng 53, 1164–1173.

Kübler, A., Birbaumer, N., 2008. Brain–computer interfaces and communication in paralysis: Extinction of goal directed thinking in completely paralysed patients? Clinical Neurophysiology 119, 2658–2666.

Kuiken, T.A., Li, G., Lock, B.A., Lipschutz, R.D., Miller, L.A., Stubblefield, K.A., Englehart, K., 2009. Targeted Muscle Reinnervation for Real-Time Myoelectric Control of Multifunction Artificial Arms. JAMA 301, 619–628.

Kuiken, T.A., Miller, L.A., Lipschutz, R.D., Lock, B.A., Stubblefield, K., Marasco, P.D., Zhou, P., Dumanian, G.A., 2007. Targeted reinnervation for enhanced prosthetic arm function in a woman with a proximal amputation: a case study. Lancet 369, 371–380.

Latash, M.L., 2012. Fundamentals of Motor Control. Academic Press.

Lee, J.-H., Ryu, J., Jolesz, F.A., Cho, Z.-H., Yoo, S.-S., 2009. Brain-machine interface via real-time fMRI: preliminary study on thought-controlled robotic arm. Neurosci. Lett. 450, 1–6.

Lenzi, T., De Rossi, S.M.M., Vitiello, N., Carrozza, M.C., 2012. Intention-based EMG control for powered exoskeletons. IEEE Trans Biomed Eng 59, 2180–2190.

Lipschutz, R.D., Lock, B., Sensinger, J., Schultz, A.E., Kuiken, T.A., 2011. Use of two-axis joystick for control of externally powered shoulder disarticulation prostheses. J Rehabil Res Dev 48, 661–667.

Lontis, E.R., Andreasen Struijk, L.N.S., 2012. Alternative design of inductive pointing device for oral interface for computers and wheelchairs, in: 2012 Annual International Conference of the IEEE Engineering in Medicine and Biology Society (EMBC). Presented at the 2012 Annual International Conference of the IEEE Engineering in Medicine and Biology Society (EMBC), pp. 3328–3331.

Losier, Y., Englehart, K., Hudgins, B., 2011. Evaluation of shoulder complex motion-based input strategies for endpoint prosthetic-limb control using dual-task paradigm. Journal of Rehabilitation Research and Development 48, 669–678.

Lv, X., Zhang, M., Li, H., 2008. Robot control based on voice command, in: IEEE International Conference on Automation and Logistics, 2008. ICAL 2008. Presented at the IEEE International Conference on Automation and Logistics, 2008. ICAL 2008, pp. 2490–2494.

Maheu, V., Frappier, J., Archambault, P.S., Routhier, F., 2011. Evaluation of the JACO robotic arm: Clinico-economic study for powered wheelchair users with upper-extremity disabilities, in: 2011 IEEE International Conference on Rehabilitation Robotics (ICORR). Presented at the 2011 IEEE International Conference on Rehabilitation Robotics (ICORR), pp. 1–5.

Martinez-Villalpando, E.C., Weber, J., Elliott, G., Herr, H., 2008. Design of an agonist-antagonist active knee prosthesis, in: 2nd IEEE RAS EMBS International Conference on Biomedical Robotics and Biomechatronics, 2008. BioRob 2008. Presented at the 2nd IEEE RAS EMBS International Conference on Biomedical Robotics and Biomechatronics, 2008. BioRob 2008, pp. 529 –534.

Masaki, A.H.I.P.R.L.S., Ooue, T., WAKUMOTO, A.H.I.P.R.L.M., 2005. System for measuring tongue pressure.

McFarland, D.J., Wolpaw, J.R., 2008. Brain-Computer Interface Operation of Robotic and Prosthetic Devices. Computer 41, 52 –56.

Mellinger, J., Schalk, G., Braun, C., Preissl, H., Rosenstiel, W., Birbaumer, N., Kübler, A., 2007. An MEG-based brain-computer interface (BCI). Neuroimage 36, 581–593.

Meurs, M., Maathuis, C.G.B., Lucas, C., Hadders-Algra, M., van der Sluis, C.K., 2006. Prescription of the first prosthesis and later use in children with congenital unilateral upper limb deficiency: A systematic review. Prosthet Orthot Int 30, 165–173.

Miller, L.A., Lipschutz, R.D., Stubblefield, K.A., Lock, B.A., Huang, H., Williams III, T.W., Weir, R.F., Kuiken, T.A., 2008. Control of a Six Degree of Freedom Prosthetic Arm After Targeted Muscle Reinnervation Surgery. Archives of Physical Medicine and Rehabilitation 89, 2057–2065.

Misawa, T., Goto, K., Takano, S., Hirobayashi, S., 2012. A development of NIRS-based brain-computer interface for robot control. IEEJ Transactions on Sensors and Micromachines 132, 355–361.

Moon, I., Lee, M., Chu, J., Mun, M., 2005. Wearable EMG-based HCI for Electric-Powered Wheelchair Users with Motor Disabilities, in: Proceedings of the 2005 IEEE International Conference on Robotics and Automation, 2005. ICRA 2005. Presented at the Proceedings of the 2005 IEEE International Conference on Robotics and Automation, 2005. ICRA 2005, pp. 2649 – 2654.

Morimoto, C.H., Mimica, M.R.M., 2005. Eye gaze tracking techniques for interactive applications. Computer Vision and Image Understanding 98, 4–24.

Moromugi, S., Koujina, Y., Ariki, S., Okamoto, A., Tanaka, T., Feng, M.Q., Ishimatsu, T., 2004. Muscle stiffness sensor to control an assistance device for the disabled. Artif Life Robotics 8, 42–45.

Muller-Putz, G.R., Pfurtscheller, G., 2008. Control of an Electrical Prosthesis With an SSVEP-Based BCI. IEEE Transactions on Biomedical Engineering 55, 361 –364.

Muzumdar, A. (Ed.), 2004. Powered Upper Limb Prostheses: Control, Implementation and Clinical Application, 1st ed. Springer.

Naito, M., Michioka, Y., Ozawa, K., Ito, Y., Kiguchi, M., Kanazawa, T., 2007. A Communication Means for Totally Locked-in ALS Patients Based on Changes in Cerebral Blood Volume Measured with Near-Infrared Light. IEICE - Trans. Inf. Syst. E90-D, 1028–1037.

Onose, G., Grozea, C., Anghelescu, A., Daia, C., Sinescu, C.J., Ciurea, A.V., Spircu, T., Mirea, A., Andone, I., Spânu, A., Popescu, C., Mihăescu, A.-S., Fazli, S., Danóczy, M., Popescu, F., 2012. On the feasibility of using motor imagery EEG-based brain–computer interface in chronic tetraplegics for assistive robotic arm control: a

clinical test and long-term post-trial follow-up. Spinal Cord 50, 599–608.

Orengo, G., Giovannini, L., Latessa, G., Saggio, G., Giannini, F., 2009. Characterization of piezoresistive sensors for goniometric glove in hand prostheses, in: 1st International Conference on Wireless Communication, Vehicular Technology, Information Theory and Aerospace Electronic Systems Technology, 2009. Wireless VITAE 2009. Presented at the 1st International Conference on Wireless Communication, Vehicular Technology, Information Theory and Aerospace Electronic Systems Technology, 2009. Wireless VITAE 2009, pp. 684 –687.

Orizio, C., 1993. Muscle sound: bases for the introduction of a mechanomyographic signal in muscle studies. Crit Rev Biomed Eng 21, 201–243.

Parker, P., Englehart, K., Hudgins, B., 2006. Myoelectric signal processing for control of powered limb prostheses. Journal of Electromyography and Kinesiology 16, 541–548.

Pfurtscheller, G., Guger, C., Müller, G., Krausz, G., Neuper, C., 2000. Brain oscillations control hand orthosis in a tetraplegic. Neurosci. Lett. 292, 211–214.

Pons, J.L., 2008. Wearable Robots: Biomechatronic Exoskeletons, 1st ed. Wiley.

Posatskiy, A.O., Chau, T., 2012a. The effects of motion artifact on mechanomyography: A comparative study of microphones and accelerometers. Journal of Electromyography and Kinesiology 22, 320–324.

Posatskiy, A.O., Chau, T., 2012b. Design and evaluation of a novel microphone-based mechanomyography sensor with cylindrical and conical acoustic chambers. Medical Engineering & Physics 34, 1184–1190.

Power, S.D., Kushki, A., Chau, T., 2011. Towards a system-paced near-infrared spectroscopy brain-computer interface: differentiating prefrontal activity due to mental arithmetic and mental singing from the no-control state. J Neural Eng 8, 066004.

Rogalla, O., Ehrenmann, M., Zollner, R., Becher, R., Dillmann, R., 2002. Using gesture and speech control for commanding a robot assistant, in: 11th IEEE International Workshop on Robot and Human Interactive Communication, 2002. Proceedings. Presented at the 11th IEEE International Workshop on Robot and Human Interactive Communication, 2002. Proceedings, pp. 454–459.

Romer, G.R.B.E., Stuyt, H.J.A., Peters, A., 2005. Cost-savings and economic benefits due to the assistive robotic manipulator (ARM), in: 9th International Conference on Rehabilitation Robotics, 2005. ICORR 2005. Presented at the 9th International Conference on Rehabilitation Robotics, 2005. ICORR 2005, pp. 201–204.

Rosen, J., Brand, M., Fuchs, M.B., Arcan, M., 2001. A myosignal-based powered exoskeleton system. IEEE Transactions on Systems, Man, and Cybernetics Part A:Systems and Humans. 31, 210–222.

Sagara, K., Kido, K., 2012. Evaluation of a 2-channel NIRS-based optical brain switch for motor disabilities' communication tools. IEICE Transactions on Information and Systems E95-D, 829–834.

Schalk, G., Leuthardt, E.C., 2011. Brain-Computer Interfaces Using Electrocorticographic Signals. Biomedical Engineering, IEEE Reviews in 4, 140 –154.

Schultz, A.E., Kuiken, T.A., 2011. Neural Interfaces for Control of Upper Limb Prostheses: The State of the Art and Future Possibilities. PM&R 3, 55–67.

Sensinger, J.W., Lock, B.A., Kuiken, T.A., 2009. Adaptive pattern recognition of myoelectric signals: exploration of conceptual framework and practical algorithms. IEEE Trans Neural Syst Rehabil Eng 17, 270–278.

Shah, B., McNally, D., Patel, K., Frone, S., Sutaria, S., 2011. Design and fabrication of an intuitive leg assist device to address lower extremity weakness, in: 2011 IEEE 37th Annual Northeast Bioengineering Conference, NEBEC 2011.

Shi, J., Chang, Q., Zheng, Y.-P., 2010. Feasibility of controlling prosthetic hand using sonomyography signal in real time: preliminary study. J Rehabil Res Dev 47, 87–98.

Shih, J.J., Krusienski, D.J., Wolpaw, J.R., 2012. Brain-computer interfaces in medicine. Mayo Clinic Proceedings 87, 268–279.

Silva, J., Chau, T., 2003. Coupled microphone-accelerometer sensor pair for dynamic noise reduction in MMG signal recording. Electronics Letters 39, 1496 – 1498.

Silva, J., Heim, W., Chau, T., 2005. A Self-Contained, Mechanomyography-Driven Externally Powered Prosthesis. Archives of Physical Medicine and Rehabilitation 86, 2066–2070.

Simpson, D.C., 1974. The choice of control system for the multimovement prosthesis: extended physiological proprioception (epp). The control of upper-extremity prostheses and orthoses 146–150.

Simpson, R.C., Levine, S.P., 2002. Voice control of a powered wheelchair. IEEE Transactions on Neural Systems and Rehabilitation Engineering 10, 122–125.

Sitaram, R., Caria, A., Birbaumer, N., 2009. Hemodynamic brain–computer interfaces for communication and rehabilitation. Neural Networks 22, 1320–1328.

Sorger, B., Dahmen, B., Reithler, J., Gosseries, O., Maudoux, A., Laureys, S., Goebel, R., 2009. Another kind of "BOLD Response": answering multiple-choice questions via online decoded single-trial brain signals, in: Steven Laureys, N.D.S. and A.M.O. (Ed.), Progress in Brain Research. Elsevier, pp. 275–292.

Sorger, B., Reithler, J., Dahmen, B., Goebel, R., 2012. A Real-Time fMRI-Based Spelling Device Immediately Enabling Robust Motor-Independent Communication. Current Biology 22, 1333–1338.

Struijk, J.J., Lontis, E.R., Bentsen, B., Christensen, H.V., Caltenco, H.A., Lund, M.E., 2009. Fully integrated wireless inductive tongue computer interface for disabled people, in: Annual International Conference of the IEEE Engineering in Medicine and Biology

Society, 2009. EMBC 2009. Presented at the Annual International Conference of the IEEE Engineering in Medicine and Biology Society, 2009. EMBC 2009, pp. 547–550.

Struijk, L.N.S.., 2006. An Inductive Tongue Computer Interface for Control of Computers and Assistive Devices. IEEE Transactions on Biomedical Engineering 53, 2594–2597.

Takagi, M., Iwata, K., Takahashi, Y., Yamamoto, S.-I., Koyama, H., Komeda, T., 2009. Development of a grip aid system using air cylinders, in: IEEE International Conference on Robotics and Automation, 2009. ICRA '09. Presented at the IEEE International Conference on Robotics and Automation, 2009. ICRA '09, pp. 2312 – 2317.

Taylor, P.B., Nguyen, H.T., 2003. Performance of a head-movement interface for wheelchair control, in: Proceedings of the 25th Annual International Conference of the IEEE Engineering in Medicine and Biology Society, 2003. Presented at the Proceedings of the 25th Annual International Conference of the IEEE Engineering in Medicine and Biology Society, 2003, pp. 1590–1593 Vol.2.

Veltink, P.H., 1999. Sensory feedback in artificial control of human mobility. Technology and Health Care 7, 383–391.

Veltink, P.H., Koopman, H.F.J.M., van der Helm, F.C.T., Nene, A.V., 2001. Biomechatronics – Assisting the Impaired Motor System. Archives Of Physiology And Biochemistry 109, 1–9.

Ward, B.D., Mazaheri, Y., 2008. Information transfer rate in fMRI experiments measured using mutual information theory. J. Neurosci. Methods 167, 22–30.

Weir, R.F., Heckathorne, C.W., Childress, D.S., 2001. Cineplasty as a control input for externally powered prosthetic components. J Rehabil Res Dev 38, 357–363.

Weiskopf, N., 2012. Real-time fMRI and its application to neurofeedback. NeuroImage 62, 682–692.

Weiskopf, N., Veit, R., Erb, M., Mathiak, K., Grodd, W., Goebel, R., Birbaumer, N., 2003. Physiological self-regulation of regional brain activity using real-time functional magnetic resonance imaging (fMRI): methodology and exemplary data. Neuroimage 19, 577–586.

Wininger, M., Kim, N.-H., Craelius, W., 2008. Pressure signature of forearm as predictor of grip force. Journal of Rehabilitation Research and Development 45, 883–892.

Wolpaw, J.R., Birbaumer, N., McFarland, D.J., Pfurtscheller, G., Vaughan, T.M., 2002. Brain–computer interfaces for communication and control. Clinical Neurophysiology 113, 767–791.

Yamada, Y., Morizono, T., Sato, S., Shimohira, T., Umetani, Y., Yoshida, T., Aoki, S., 2001. Proposal of a SkilMate finger for EVA gloves, in: IEEE International Conference on Robotics and Automation, 2001. Proceedings 2001 ICRA. Presented at the IEEE International Conference on Robotics and Automation, 2001. Proceedings 2001 ICRA, pp. 1406 – 1412 vol.2.

Yanagisawa, T., Hirata, M., Saitoh, Y., Goto, T., Kishima, H., Fukuma, R., Yokoi, H., Kamitani, Y., Yoshimine, T., 2011. Real-time control of a prosthetic hand using human electrocorticography signals. J. Neurosurg. 114, 1715–1722.

Yoo, S.-S., Fairneny, T., Chen, N.-K., Choo, S.-E., Panych, L.P., Park, H., Lee, S.-Y., Jolesz, F.A., 2004. Brain-computer interface using fMRI: Spatial navigation by thoughts. NeuroReport 15, 1591–1595.

Yu, W., Rosen, J., Li, X., 2011. PID admittance control for an upper limb exoskeleton, in: American Control Conference (ACC), 2011. Presented at the American Control Conference (ACC), 2011, pp. 1124–1129.

Zecca, M., Micera, S., Carrozza, M.C., Dario, P., 2002. Control of multifunctional prosthetic hands by processing the electromyographic signal. Critical Reviews in Biomedical Engineering 30, 459–485.

Zheng, Y.P., Chan, M.M.F., Shi, J., Chen, X., Huang, Q.H., 2006. Sonomyography: Monitoring morphological changes of forearm muscles in actions with the feasibility for the control of powered prosthesis. Medical Engineering & Physics 28, 405–415.

Table 1. Stratified inventory of control interfaces used for motion intention detection in active movement-assistive devices.
C: communication; P: prosthesis; O: orthosis; E: external devices; * indicates one-time invasive method.

HUMAN SYSTEM		PHYSIOLOGICAL PHENOMENA (INTERFACE)		SIGNAL	SENSOR		TRANS. PRIN.	INTERFACE WITH BODY	APPLICATION	REFERENCE
CONTROLLER		Brain Activity (BCI)	Electric current	EEG	Electrode		-	Skin contact	C/P/O/E	Kübler and Birbaumer (2008) Muller-Putz and Pfurtscheller (2008) Galán et al. (2008) Pfurtscheller et al. (2000)
				MEG	MEG machine		Induction	No contact	C/O	Mellinger et al. (2007) Buch et al. (2008)
			Hemodynamics	fMRI	MRI machine		Induction	No contact	C/E	Sorger et al. (2012) Lee et al. (2009)
				NIRS	Spectrometer		Photoelectric	Near-infrared illumination of the brain	C/E	Misawa et al. (2012) Sagara and Kido (2012)
ACTUATORS		Muscle Activation (MAI)	Electric current	EMG	Electrode		-	Skin contact	O/P/E	Rosen et al. (2001) Gopura and Kiguchi (2009) Fleischer and Hommel (2008) Zecca et al. (2002) Cipriani et al. (2008) Parker et al. (2006) Han et al. (2003)
								Muscle Targeted Reinnervation*	P	Kuiken et al. (2007) Kuiken et al. (2009)
		Muscle Contraction (MCI)	Vibration	MMG (PMG or AMG)	Microphone		Induction Piezoelectric	Skin contact	P	Barry et al. (1986) Posatskiy and Chau (2012b) Silva et al. (2005) Silva and Chau (2003)
					Accelerometer		Piezoelectric	Skin contact	P	Antonelli et al. (2009)
			Dimensional change	MK	Hall-effect sensor		Induction	Magnet on the skin	P	Kenny et al. (1999) Heath (2003)
					Pneumatic sensor		Resistive Capacitive	Skin contact	P	Abboudi et al. (1999) Curcie et al. (2001)
				SMG	Ultrasound scanner		Piezoelectric	Skin contact	P	Zheng et al. (2006) Chen et al. (2010)
				Electric Impedance	Electrode		-	Electric current to skin	P	Kadefors and Olsson (1972)
			Stiffness	MT/MK	Pressure Senor (force sensor resistor)		Piezoresistive	Skin contact	O/P	Wininger et al., (2008) Moromugi et al., (2004)
					Piezoelectric transducer		Piezoelectric			Han et al. (2012)
			Force	Force	Strain gauges		Piezoresistive	Tunnel cineplasty / Tendon exteriorized cineplasty*	P	Weir et al. (2001) Bertos et al. (1997)
PLANT		Movement (MI)		Body Segment Translation	Joystick (potentiometer/Hal- effect sensor)		-	Skin contact	P/E/O	Lipschutz et al. (2011) Losier et al. (2011) Johnson et al. (2001) Dicianno et al. (2010) Maheu et al. (2011)
				Angular Displacement (Joint Angle)	Goniometer	Potentiometer	-	Skin contact	P/O	Doubler and Childress (1984) Gibbons et al. (1987)
						Optic	Photoelectric		P/O	Shah et al. (2011) Herle et al. (2010)
						Strain gauge	Piezoresisitive	Skin contact	P/O	Orengo et al. (2009) Takagi et al. (2009)
						Angular Encoder	Photoelectric	Skin contact /No contact	P/O	Martinez-Villalpando et al. (2008) Font-Llagunes et al. (2011) Yamada et al. (2001)
		Force / Pressure (FI)		Deformation	6 DOF Force/Torque sensor (strain gauges)		Piezoresisitive	No comtact	P/O/E	Abbruzzese et al. (2011) Ragonesi et al. (2011)
					Pressure Sensor (force sensor resistor)			Skin Contact		M. Baklouti et al. (2008) Huo et al. (2010) Lipschutz et al. (2011)
PARALLEL SYSTEMS	Eye	Movement		Corneal reflection	Video Camera		Photoelectric	Near-infrared illumination of the cornea	P/E	Onose et al., (2012)
				EOG	Electrode		-	Skin contact		Duvinage et al. (2011) Chen and Newman (2004)
	Head	Movement		Inclination	Accelerometer		Piezoelectric	Skin contact	E	Hinkel III (2010) Craig and Nguyen, (2006) Fusco and Balbinot, (2011)
					Video camera		Photoelectric	No contact		M. Baklouti et al. (2008) Malek Baklouti et al. (2008)
					Ultrasonic sensor		Piezoelectric	Skin contact		Coyle (1995)
	Mouth	Tongue Movement		Contact with palate	Induction coil		Induction	Ferromagnetic material at the tip of the tongue	E/C	Huo et al. (2008) Struijk et al. (2009)
				Movement						
		Speech		Sound	Microphone		Induction Piezoelectric	No contact	P/E	Fan and Li (2010) Simpson and Levine (2002) Rogalla et al. (2002)

APPENDIX B: CONSENT FORM AND INFORMATION LETTER

UNIVERSITY OF TWENTE.

FLEXTENSION
ORTHOTICS AND INNOVATION

INFORMATION LETTER

Research Title: Evaluation of Electromyography, Force and Hand Joystick as Control Interface for Active Orthoses

---

Dear Madam/Sir,
We are hereby sending you this letter to ask for your participation in a study that aims at *Evaluating the Performance of Electromyography, Force and Hand Joystick as Control Interface for Active Orthoses*. This letter provides elaborate information about the research on which you can base you consent or refusal to participate in this experiment. This research study is part of the FLEXTENSION project. More information about the project can be found at the website: www.flextension.nl

Background and research purpose
Duchenne Muscular Dystrophy (DMD) is a genetic neuromuscular disease characterized by progressive muscle degeneration and loss of muscle strength. Duchenne patients are eventually unable to move their arms and become dependent one others for many activities of daily living. The development of an active orthosis, with a suitable control mechanism, would greatly increase the quality of life of these patients. Many options may be considered for the control of the orthosis, and at this point we pretend to evaluate the performance of electromyography (EMG), force and hand joystick as control interfaces for the active orthosis.

What does the participation in the research entail?
If you decide to participate in this study you will be asked to come once at HUMAN PERFORMANCE VIRTUAL REALITY LAB located on the second floor of the 'Horstring West building at the University of Twente. You will be seated in a chair in front of a computer screen in which we will display the experimental task. Muscle activity of your biceps and triceps and the resulting forces will be recorded using surface electrodes while you perform isometric contractions. You will not notice that EMG, force and position of the joystick are being recorded. To assure that contractions are isometric, we will immobilize your forearm, using two supports, one close to the elbow and the other one close to the wrist. On the screen a target will be displayed that moves unpredictably up and down (vertically) and a cursor that you can control by contracting biceps and triceps or by moving the joystick with your hand. You will be asked to track the target with the cursor keeping the cursor as close to the target as possible. The experiment consists of 10 training of 30 seconds each and 3 testing trials of 3 minutes for each interface (i.e. EMG, force or hand joystick). Breaks of 1 minute are planned after each trial. The total duration of the experiment will be approximately of 1.5 hours. You can choose to terminate your participation at any time and for whatever reason. If this is the case, further participation in this experiment is excluded. Before the start of the experiment, all necessary information will be given and a written informed consent will be obtained.

Are you eligible for participating in this experiment?
You are eligible for participating in this experiment if you are 18 years or older and have no history of neuromusculoskeletal disease/trauma affecting upper extremities.

Possible side effects/risks
The participation in this research isn't expected to result in any side effects or risks for the subjects. Resting periods will be granted liberally, as needed by each subject, to avoid muscle overwork and fatigue.

Possible benefits
The participation in this study will not bring you any personal benefit but it may contribute to choose the most suitable control interface for a powered upper extremity orthosis for Duchenne patients.

Confidentiality of information and data
The researchers will handle the participant's data collected during the experiment confidentially, and ensure that no unauthorized outsiders have access to this information.

Voluntary participation
Your cooperation in this study is completely voluntary. Even if you do consent to participate in this research, you are still able to terminate your participation at any time, including during the experiment, and without having to give any explanation. In case you decide to participate in this study, you and the researcher will sign a consent form on the day of the experiment.

Contacts for further information

Joan Lobo Prat, MSc
PhD Cand. Flextension project

Laboratory of Biomechanical Engineering
Faculty of Engineering Technology
University of Twente (Horstring W218)

PO Box 217
7500 AE Enschede, The Netherlands
Tel.: +31 (0)53 489 2720
Mob.: +31 (0)628 286 349
E-mail: j.loboprat@utwente.n

UNIVERSITY OF TWENTE.

FLEXTENSION
ORTHOTICS AND INNOVATION

CONSENT FORM

Research Title: *Evaluating the Performance of Electromyography, Force and Hand Joystick as Control Interface for Active Orthoses.*

I hereby confirm that I have the 'Information Letter' and have read and understood the information. I have had enough time to think about my participation and I had the opportunity to ask questions. These questions were satisfactorily answered.

I consent to participate in the above mentioned medical and scientific research.

I know that my participation is voluntary and that I may withdraw my consent at any time without providing any explanation.

I give permission for the data to be processed for the purposes described in the Information Letter.

Subject name: **Signature:**
Date:

Researcher name: **Signature:**
Date:

A copy of the signed Consent Form and of the Information Letter shall be given to the subject.

APPENDIX C: EXPERIMENT PROTOCOL

UNIVERSITY OF TWENTE.

FLEXTENSION
ORTHOTICS AND INNOVATION

EVALUATION OF ELECTROMYOGRAPHY, FORCE AND HAND JOYSTICK AS CONTROL INTERFACES FOR ACTIVE ORTHOSES

ABSTRACT

The design of an upper extremity orthosis that meets the growing needs of persons suffering with Duchenne Muscular Dystrophy would increase the independency and quality of life of these patients. At late stages of the disease a powered orthosis is necessary and the choice of the control interface for this device is of major importance as it will directly affect the user ability to control the orthosis and therefore the device performance. We pretend to evaluate the performance of EMG, force and hand joystick as control interface for active upper extremity orthosis for Duchenne patients. A first test was designed, consisting of a screen based one-dimensional tracking task, and will at this point be performed by healthy subjects. The evaluation of the control interface will be done in terms of tracking error, information transmission rate of the human-machine system and human-operator bandwidth. Additionally, we will be interested in examining the progression of the results of the training trials, as they may provide useful information concerning the intuitiveness of the control interfaces.

EXPERIMENT SETUP

A screen based one-dimensional tracking task was designed to evaluate the performance of electromyography, force and hand joystick as control interfaces for active orthoses. The tracking task is presented to the subjects on a computer screen by means of a MATLAB graphical user interface. The target (input signal) moves according to an unpredictable multi-sine signal composed of 10 sinusoidal signals between 0.1 and 3 Hz. Subjects are asked to keep the cursor (a pink dot) as close to the yellow square target as possible, as this latter moves vertically in the screen. The final purpose being to compare and select the most appropriate control system for a powered upper limb orthosis, it was assured that the dynamic properties of the cursor resemble the ones of the human arm.

Figure 1 shows the block diagram and the display of the experimental task. In the block diagram, w represents the target position, x the cursor position and u the myoelectric signal generated by the subject (by contracting biceps/triceps in the case of EMG and force or by controlling the joystick). Concerning the display, pink square and yellow dot are, correspondingly, target and cursor.

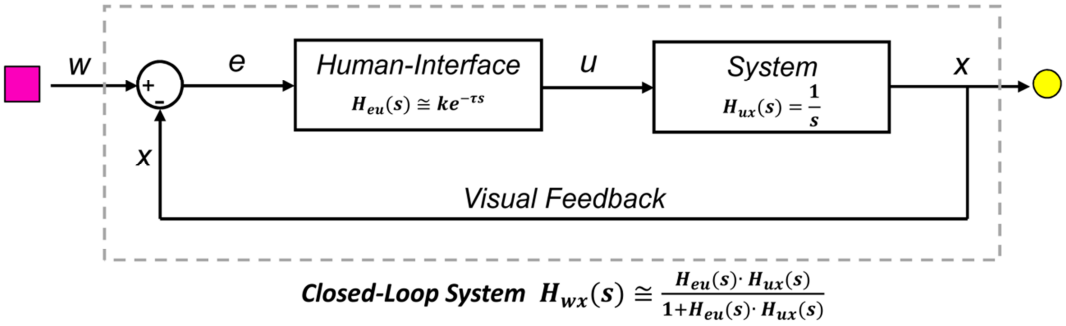

Figure 1 - Block diagram and display of the experimental task.

EXPERIMENT GOALS

- Evaluate the performance of EMG, force and hand joystick as control input signal for a screen based 1D tracking task. The tracking error (normalized mean square error between the target signal and the path followed by the cursor) will give a measure of the accuracy of the task performance. Further analysis includes the calculation of the bandwidths and the information transmission rates of the human-machine system.
- Examining the progression of the results of the training trials – look further into the learning phase of each interface.

DATA TO BE MEASURED

- Time (s).
- EMG, including MVC (V).
- Target's position
- Cursor's position
-

VARIABLES OF THE EXPERIMENT

- Interfaces (EMG, Force and Joystick)

SUBJECTS

- Eight able-bodied subjects will participate in this study.

INFORMATION TO TRANSMIT TO THE SUBJECTS

We designed a one-dimensional tracking test in which the target, a pink square, moves up and down in the screen in an unpredictable way. The goal is to keep the cursor, the smaller yellow dot, as close to the center of the target as possible.

We will use three different interfaces that will allow you to control the cursor. In two of them, EMG and force, you will be able to move the cursor up and down by contracting determined muscles. As for the hand joystick, only one degree of freedom will be available, allowing just vertical movements of the cursor.

The cursor position can be controlled by contracting determined muscles. We will ask you to sit in a chair and will immobilize your forearm in such a way that the elbow is flexed at 90 degrees. One support is used to fix the arm and this will guarantee isometric contractions; no movement will result from the contractions. The EMG electrodes will be placed in your biceps and triceps. Contracting the biceps, as if trying to flex the arm, (bringing it up in the direction of the forearm) will result in upwards displacement of the cursor. To move the cursor down you need to contract your triceps, as if trying to extend your arm. The cursor velocity is proportional to the force of the contraction: a stronger contraction will result in a faster movement of the cursor.

In order to implement this velocity-controlled system, we will ask you to perform what is called a maximum voluntary contraction for both biceps and triceps before starting the trials. That is, we are going to measure the electrical activity of your muscles and the resulting force exercised while you contract as hard as you can. Three 3 s contractions will be asked for both biceps and triceps.

Before the test trials there is a preparation and training phase. You will perform 10 training trials similar to the test trials but shorter, each one will have a duration of 30 s. This will happen for each control interface. Finally, the test trials will begin. You will first perform three evaluation trials, each one with duration of 3 minutes.

ARM POSITION

The subject will be sited on a chair with the forearm immobilized in such a way that the elbow is flexed at 90 degrees. One support is used to fix the arm to the setup, in contact with the styloid processes.

EXPERIMENT PROCEDURE

1. **Beforehand preparation**
   - Open Simulink model
   - Run initialization form
   - Built Model
   - Connect xPC target
   - Run UDPshow.exe
   - Run 3Dmouse.exe

2. **Administration**
   - Explanation of the objective and method of the experiment
   - Consent form

3. **Equipment and subject preparation**
   - Adjust setup for the subject (assure that the elbow is flexed at 90 degrees – a pillow may be used if necessary). Attach the forearm to the support, it must be positioned in the styloid processes.
   - Set the gains of channels 1 and 2 of the Delsys amplifier to 1k and all others to 0. Channel 1 corresponds to biceps, channel 2 to triceps.
   - Application of the Adhesive Sensor Interface.
   - Sensor placement:
     - Preparation of the skin.
     - Positioning the patient in a starting posture.
     - Determination of the sensor location. (see Figure 1).
     - Placement and fixation of the sensor:
       - inter electrode distance (if applicable);
       - orientation of electrodes;
       - fixation on the skin;
       - location of the reference electrode.

     - Testing of the connection.

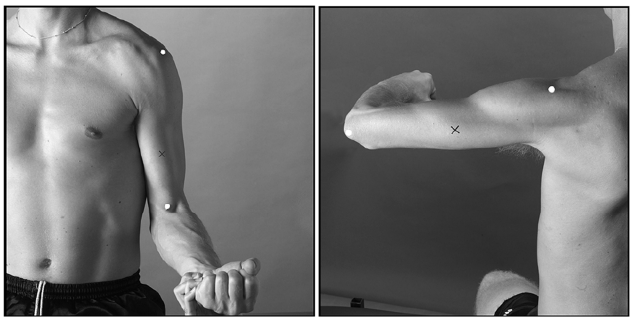

Figure 2 - Electrode location on the biceps brachii and on the long head of the triceps brachii.

UNIVERSITY OF TWENTE.

FLEXTENSION
ORTHOTICS AND INNOVATION

DATA COLLECTION DURING THE EXPERIMENT

Subject name/number:			**Date:**	
Task		Duration	Saved file	Comments (Calculated values: MVC, tracking error)
We start by asking you to perform what is called a MVC for both biceps and triceps. That is, we are going to measure the EMG of the muscle while you contract it as hard as you can for three seconds.				
Calibration	EMG offset	-		
	Force offset			
MVC	3 Biceps	30 s		
	3 Triceps	30 s		
Interface 1	Training trials	30 s		
		30 s		
		30 s		
		30 s		
		30 s		
		30 s		
		30 s		
		30 s		
		30 s		
		30 s		
	Evaluation trials	3 min		
		3 min		
		3 min		

UNIVERSITY OF TWENTE.

FLEXTENSION
ORTHOTICS AND INNOVATION

Interface 2	**Training trials**	**30 s**		
		30 s		
		30 s		
		30 s		
		30 s		
		30 s		
		30 s		
		30 s		
		30 s		
		30 s		
	Evaluation trials	3 min		
		3 min		
		3 min		
Interface 3	Training trials	30 s		
		30 s		
		30 s		
		30 s		
		30 s		
		30 s		
		30 s		
		30 s		
		30 s		
		30 s		
	Evaluation trials	3 min		
		3 min		
		3 min		

Order of preference: **1)** **2)** **3)**

APPENDIX D: MATLAB FUNCTIONS

DIAGRAM OF THE MATLAB FUNCTIONS

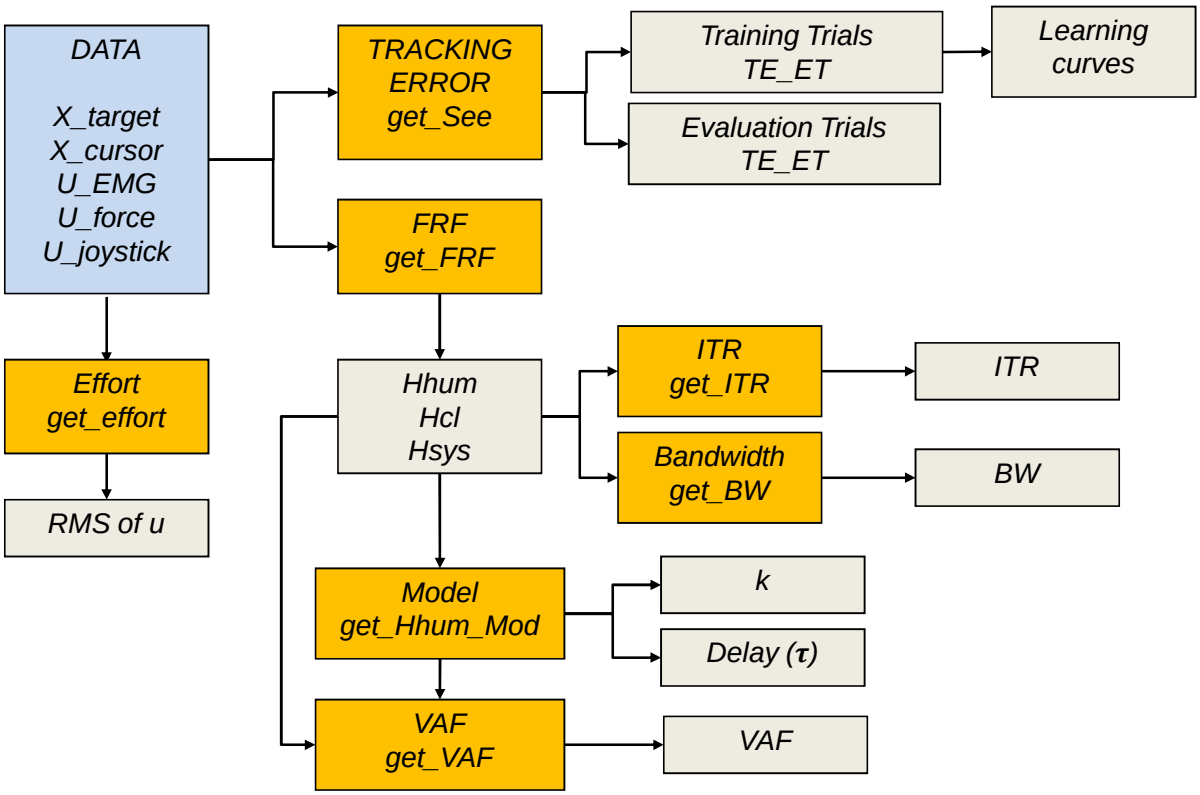

TRACKING ERROR

```
clc; clear all; close all;
%% Compute See for TRAINING TRIALS
%EMG and Force
Fc=3;
n=1;
for s=1:14
    if s~=2 && s~=6 && s~=9 && s~=10 && s~=11 && s~=12    %Exclude↙
subjects
        [EMGmSee_T(:,n)]=get_See_TT(s,'EMG_T',Fc);
        [FORmSee_T(:,n)]=get_See_TT(s,'F_T',Fc);
        n=n+1
    end
end

%Joystick
n=1;
for s=10:16
        [JOYmSee_T(:,n)]=get_See_TT(s,'J_T',Fc);
        n=n+1
end


%% Compute See for EVALUATION TRIALS
n=1;
for s=1:14
    if s~=2 && s~=6 && s~=9 && s~=10 && s~=11 && s~=12    %Exclude↙
subjects
        [EMGmSee_E(:,n),EMGmSee2_E(:,:,n)]=get_See_ET(s,'EMG_E',Fc);
        [FORmSee_E(:,n),FORmSee2_E(:,:,n)]=get_See_ET(s,'F_E',Fc);
        n=n+1
    end
end

%Joystick
n=1;
for s=10:16
        [JOYmSee_E(:,n),JOYmSee2_E(:,:,n)]=get_See_ET(s,'J_E',Fc);
        n=n+1
end
```

```
%% Data arrangement
%EMG
EMGmSee_T_E = [EMGmSee_T ; EMGmSee_E];
for s=1:8
  EMGmSee2_EE(:,s)=[EMGmSee2_E(:,1,s);EMGmSee2_E(:,2,s);EMGmSee2_E(:,3,↙
s)];
end

%FOR
FORmSee_T_E = [FORmSee_T ; FORmSee_E];
for s=1:8
  FORmSee2_EE(:,s)=[FORmSee2_E(:,1,s);FORmSee2_E(:,2,s);FORmSee2_E(:,3,↙
s)];
end

%JOY
JOYmSee_T_E = [JOYmSee_T ; JOYmSee_E];
for s=1:7
  JOYmSee2_EE(:,s)=[JOYmSee2_E(:,1,s);JOYmSee2_E(:,2,s);JOYmSee2_E(:,3,↙
s)];
end

%% delete outliers Evaluation
[outEMG_all]=deleteoutliers(reshape(EMGmSee2_EE,15*8,1),0.05);
[outFOR_all]=deleteoutliers(reshape(FORmSee2_EE,15*8,1),0.05);
[outJOY_all]=deleteoutliers(reshape(JOYmSee2_EE,15*7,1),0.05);

[outEMG]=deleteoutliers(reshape(EMGmSee_E,3*8,1),0.1);
[outFOR]=deleteoutliers(reshape(FORmSee_E,3*8,1),0.1);
[outJOY]=deleteoutliers(reshape(JOYmSee_E,3*7,1),0.1);

disp('DONE!')
break
%% BOXPLOTS EVALUATION See
hFig =figure()
x1 = reshape(EMGmSee2_EE,15*8,1);
x2 = reshape(FORmSee2_EE,15*8,1);
x3 = [reshape(JOYmSee2_EE,15*7,1);nan(15,1)];
b=boxplot([x1,x2,x3],'notch','on','labels',{'EMG','Force','Joystick'})
set(b,'LineWidth',1.5)
```

```
h = findobj(gca)
children = get(h(2),'children');%In my case boxplot happens to be the↙
second object of the plot.
for i = 1:3
set(children(i), 'FontSize', 11,↙
'FontName','Arial','FontWeight','Bold');%To change label properties
end
h = findobj(gca,'Tag','Box');
 for j=1
    patch(get(h(j),'XData'),get(h(j),'YData'),'c','FaceAlpha',.5);
 end
 for j=2
    patch(get(h(j),'XData'),get(h(j),'YData'),'g','FaceAlpha',.5);
 end
 for j=3
    patch(get(h(j),'XData'),get(h(j),'YData'),'y','FaceAlpha',.5);
 end
% ylabel('Tracking Error [m^2/Hz^2]','FontSize', 11,↙
'FontName','Arial','FontWeight','Bold')
% set(gca,'FontSize', 11, 'FontName','Arial','FontWeight','Bold')
% set(gca,'box','off');
% axis([0.5 3.5 1.5e4 6.1e4])


ylabel('Tracking Error [m^2/Hz]','FontSize', 11,↙
'FontName','Arial','FontWeight','Bold')
axis([0.5 3.5 1.5e4 6.1e4])
hAx1 = gca;   %# get a handle to first axis
set(hAx1,'FontSize', 11, 'FontName','Arial','FontWeight','Bold')
set(hAx1,'box','off');


%# create a second transparent axis, as a copy of the first
hAx2 = copyobj(hAx1,hFig);
delete( get(hAx2,'Children') )
set(hAx2, 'Color','none')

%# show grid-lines of first axis, give them desired color, but hide text↙
labels
ylabel('','FontSize', 11, 'FontName','Arial','FontWeight','Bold')
```

```
set(hAx1, 'XColor','r', 'YColor',[0.7 0.7 0.7], ...
    'XMinorGrid','off', 'YMinorGrid','on', ...
    'FontSize', 11, 'FontName','Arial','FontWeight','Bold',...
    'XTickLabel',[], 'YTickLabel',[]);

set(gcf, 'Units','centimeters', 'Position',[0 0 14.8 10])
set(gcf, 'PaperPositionMode','auto')
% saveas(hFig, 'TE.tiff', 'Resolution', 600);
print -dtiff -f1 -r600 TE
%%
figure()
m1 = mean(outEMG);
s1 = std(outEMG);
m2 = mean(outFOR);
s2 = std(outFOR);
m3 = mean(outJOY);
s3 = std(outJOY);
barvalues=[m1,m2,m3];
errors=[s1,s2,s3];
barweb(barvalues, errors, 0.5, [], [], [], [], [], [], [], [],↙
[])

%%
figure()
x1 = reshape(EMGmSee_E,3*8,1);
x2 = reshape(FORmSee_E,3*8,1);
x3 = [reshape(JOYmSee_E,3*7,1);nan(3,1)];
boxplot([x1,x2,x3],'boxstyle','outline','notch','on','labels',↙
{'EMG','Force','Joystick'})
ylabel('Tracking Error [cm^2/Hz]')
%%
figure()
x1 = [outEMG;nan(2,1)];
x2 = outFOR;
x3 = [outJOY;nan(3,1)];
boxplot([x1,x2,x3],'notch','off','labels',{'EMG','Force','Joystick'})
ylabel('Tracking Error [cm^2/Hz]')
%%
figure()
x1 = [outEMG_all;nan(5,1)];
x2 = [outFOR_all;nan(2,1)];
```

```
x3 = [outJOY_all;nan(18,1)];
boxplot([x1,x2,x3],'notch','on','labels',{'EMG','Force','Joystick'})
ylabel('Tracking Error [cm^2/Hz]')

%% Export EVALUATION
csvwrite('EMG_TE_E.dat',EMGmSee_E)
csvwrite('FOR_TE_E.dat',FORmSee_E)
csvwrite('JOY_TE_E.dat',JOYmSee_E)
%% Export TRAINING
csvwrite('EMG_TE_T.dat',EMGmSee_T)
csvwrite('FOR_TE_T.dat',FORmSee_T)
csvwrite('JOY_TE_T.dat',JOYmSee_T)


%% PLOT E

plot(JOYmSee_E)
```

```
function [mSee,mSee2]=get_See_ET(subjectnumber,interface,F)

snumber=int2str(subjectnumber);
datapath = strcat('D:↙
\Dropbox\INTERFACE_EXPERIMENT\Analysis\Data\Subject',snumber);
allfiles = dir(fullfile(datapath,'*.mat'));
ind = 0;
aux=char.empty(1,length(allfiles),0);
for k=1:length(allfiles)
    t=strcat('D:\Dropbox\INTERFACE_EXPERIMENT\Analysis\Data\Subject',↙
snumber,'\',allfiles(k,1).name);
    if strcmp(allfiles(k,1).name,'workspace.mat')==1
        aux{k}='workspace';
    elseif strcmp(allfiles(k,1).name,'matlab.mat')==1
        aux{k}='matlab.mat';
    else
    load(t);
    aux{k}=xpcdata2.description;
    tmpstring = strrep(aux{k}, '_', '');
    tmpinterface = strrep(interface, '_', '');
    res = strfind( tmpstring,tmpinterface);
    if ~isempty(res)
        ind = ind+1;
        finalaux{ind} = aux{k};
%         disp(finalaux{ind})
        finalnames{ind} = allfiles(k,1).name;
%         disp(finalnames{ind})
%         disp(' ')
    end
    end

end

files = finalnames;
N = 180000;                 %Total number of samples in 3 min trial
M = 6;                      %Number of cycles in 3 min trial
Fs= 1000;                   %Sample Freq. (Hz)
dt= 1/Fs;                   %Sample time 0.001s
T = dt * N;                 %Time 180 s
Tc = N/M/Fs;                %Time of cycle 30s
f= (0:N-1)' / T;            %Frequency vector
```

```
fa = (0:N/M-1)'/Tc;          %Frequency after averaging
df =1/30;                    %Frequency period

%First cycle excluded -> only 5 cycles, decrease in the total number of↙
samples
N2=N-30000;
M2=M-1;
N3=30000;

Fc=find(fa==F);              %Sum will be until 20 Hz

for expNr = 1:3

load(fullfile(datapath, files{expNr}));

target=xpcdata2.x_TAR/3800;
cursor=xpcdata2.x_CUR/3800;

aux =find(target,1)+N3;
e = target(aux:aux+N2-1,1)-cursor(aux:aux+N2-1,1);
e2 = reshape(e,N2/M2,M2);
me = mean(e2,2);
% mme (:,expNr)= mean(abs(me));

E = fft(me);
E2 = fft(e2);

See = 1/N3 * abs(E).^2;
See2 = 1/N3 * abs(E2).^2;

mSee(:,expNr) = mean(See(1:Fc));
mSee2(:,expNr) = mean(See2(1:Fc,:),1);
end
```

```
%% CO-CONTRACTION COMPARISON

function [mSee]=get_See_TT(subjectnumber,interface,F)

snumber=int2str(subjectnumber);
datapath = strcat('D:↙
\Dropbox\INTERFACE_EXPERIMENT\Analysis\Data\Subject',snumber);
allfiles = dir(fullfile(datapath,'*.mat'));
ind = 0;
aux=char.empty(1,length(allfiles),0);
for k=1:length(allfiles)
    t=strcat('D:\Dropbox\INTERFACE_EXPERIMENT\Analysis\Data\Subject',↙
snumber,'\',allfiles(k,1).name);
    if strcmp(allfiles(k,1).name,'workspace.mat')==1
        aux{k}='workspace';
    elseif strcmp(allfiles(k,1).name,'matlab.mat')==1
        aux{k}='matlab.mat';
    else
    load(t);
    aux{k}=xpcdata2.description;
    tmpstring = strrep(aux{k}, '_', '');
    tmpinterface = strrep(interface, '_', '');
    res = strfind( tmpstring,tmpinterface);
    if ~isempty(res)
        ind = ind+1;
        finalaux{ind} = aux{k};
%         disp(finalaux{ind})
        finalnames{ind} = allfiles(k,1).name;
%         disp(finalnames{ind})
%         disp(' ')
    end
    end

end

files = finalnames;
N = 35000;                  %Total number of samples in 3 min trial
M = 1;                       %Number of cycles in 3 min trial
Fs= 1000;                    %Sample Freq. (Hz)
dt= 1/Fs;                    %Sample time 0.001s
T = dt * N;                  %Time 180 s
```

```
Tc = N/Fs;                  %Time of cycle 30s
f= (0:N-1)' / T;              %Frequency vector
fa = (0:N/M-1)'/Tc;           %Frequency after averaging
df =1/30;                     %Frequency period
N2=N-5000;                    %Number of samples after 5 s
Fc=find(fa==F);               %Sum will be until 20 Hz

for expNr = 1:10

load(fullfile(datapath, files{expNr}));

target=xpcdata2.x_TAR/3800;
cursor=xpcdata2.x_CUR/3800;

aux=find(target,1)+5000;
e=target(aux:aux+N2-1,1)-cursor(aux:aux+N2-1,1);
% me(:,expNr)=mean(abs(e));
E =fft(e);
See = 1/N2 * abs(E).^2;
mSee(:,expNr) = mean(See(1:Fc));
end
```

FREQUENCY RESPONSE FUNCTIONS

```
%% CO-CONTRACTION COMPARISON

function [Hhm,Hsys,Hcl,Coh]=get_FRF_ET(subjectnumber,interface)

snumber=int2str(subjectnumber);
datapath = strcat('D:↙
\Dropbox\INTERFACE_EXPERIMENT\Analysis\Data\Subject',snumber);
allfiles = dir(fullfile(datapath,'*.mat'));
ind = 0;
aux=char.empty(1,length(allfiles),0);
for k=1:length(allfiles)
    t=strcat('D:\Dropbox\INTERFACE_EXPERIMENT\Analysis\Data\Subject',↙
snumber,'\',allfiles(k,1).name);
    if strcmp(allfiles(k,1).name,'workspace.mat')==1
        aux{k}='workspace';
    elseif strcmp(allfiles(k,1).name,'matlab.mat')==1
        aux{k}='matlab.mat';
    else
    load(t);
    aux{k}=xpcdata2.description;
    tmpstring = strrep(aux{k}, '_', '');
    tmpinterface = strrep(interface, '_', '');
    res = strfind( tmpstring,tmpinterface);
    if ~isempty(res)
        ind = ind+1;
        finalaux{ind} = aux{k};
%         disp(finalaux{ind})
        finalnames{ind} = allfiles(k,1).name;
%         disp(finalnames{ind})
%         disp(' ')
    end
    end

end

files = finalnames;
N = 180000;                 %Total number of samples in 3 min trial
M = 6;                      %Number of cycles in 3 min trial
Fs= 1000;                   %Sample Freq. (Hz)
dt= 1/Fs;                   %Sample time 0.001s
T = dt * N;                 %Time 180 s
```

```
Tc = N/M/Fs;                %Time of cycle 30s
f= (0:N-1)' / T;            %Frequency vector
fa = (0:N/M-1)'/Tc;         %Frequency after averaging
df =1/30;                   %Frequency period


%First cycle excluded -> only 5 cycles, decrease in the total number of↙
samples
N2=N-30000;
M2=M-1;
N3=30000;

for expNr = 1:3

load(fullfile(datapath, files{expNr}));

aux =find(xpcdata2.x_TAR,1);
w=xpcdata2.x_TAR(aux+N3:aux+N,1);
x=xpcdata2.x_CUR(aux+N3:aux+N,1);
e=w-x;

if strcmp(interface,'EMG_E')
    u = (diff(xpcdata2.x_CUR(aux+N3:aux+N,1)))*100;

elseif strcmp(interface,'F_E')
    u = (diff(xpcdata2.x_CUR(aux+N3:aux+N,1)))*100;

elseif strcmp(interface,'J_E')
    u = (diff(xpcdata2.x_CUR(aux+N3:aux+N,1)))*100;
end


wm = reshape(w(1:N2),N2/M2,M2);
xm = reshape(x(1:N2),N2/M2,M2);
em = reshape(e(1:N2),N2/M2,M2);
um = reshape(u(1:N2),N2/M2,M2);

W =fft(wm);
X =fft(xm);
E =fft(em);
U =fft(um);
```

```
Sxx = M2/N2 * abs(X).^2;
Sww = M2/N2 * abs(W).^2;
Swx = M2/N2 * conj(W).*X;
Swe = M2/N2 * conj(W).*E;
Swu = M2/N2 * conj(W).*U;

mSww = mean(Sww,2);      %Average over cycles
mSxx = mean(Sxx,2);
mSwx = mean(Swx,2);
mSwe = mean(Swe,2);
mSwu = mean(Swu,2);

Hhm(:,expNr) = mSwu./mSwe;
Hsys(:,expNr) = mSwx./mSwu;
Hcl(:,expNr) = mSwx./mSww;

Coh(:,expNr) = (abs(mSwx).^2) ./ (mSww .* mSxx);

% Swx(:,expNr) = Swx
% Sww(:,expNr) = Sww
% Sxx(:,expNr) = Sxx
%
% mSwx = mean(Swx,2)
% mSww = mean(Sww,2)
% mSxx = mean(Sxx,2)
%
% end
% mCoh =(abs(mSwx).^2) ./ (mSww .* mSxx)
end
```

INFORMATION TRANSMISSION RATE

```
clc; clear all; close all;

N = 180000;                 %Total number of samples in 3 min trial
M = 6;                      %Number of cycles in 3 min trial
Fs= 1000;                   %Sample Freq. (Hz)
dt= 1/Fs;                   %Sample time 0.001s
T = dt * N;                 %Time 180 s
Tc = N/M/Fs;                %Time of cycle 30s
f= (0:N-1)' / T;            %Frequency vector
fa = (0:N/M-1)'/Tc;         %Frequency after averaging
df =1/30;                   %Frequency period
fselect=[4 5 7 10 15 21 30 43 63 91];
F=3;
Fc=find(fa==F);             %Sum will be until 20 Hz

%% Compute See for EVALUATION TRIALS
n=1;

for s=1:14
    if s~=2 && s~=6 && s~=9 && s~=10 && s~=11 && s~=12    %Exclude↙
subjects
        [EMG_ITR(:,:,n),EMG_sumITR(:,n)]=get_ITR_ET(s,'EMG_E',F);
        [FOR_ITR(:,:,n),FOR_sumITR(:,n)]=get_ITR_ET(s,'F_E',F);
        n=n+1
    end
end

%Joystick
n=1;
for s=10:16
    [JOY_ITR(:,:,n),JOY_sumITR(:,n)]=get_ITR_ET(s,'J_E',F);
    n=n+1
end

%% Data arrangement sumITR
mEMG_sumITR = reshape(EMG_sumITR,3*8,1);
mFOR_sumITR = reshape(FOR_sumITR,3*8,1);
mJOY_sumITR = reshape(JOY_sumITR,3*7,1);


[outEMG_sumITR]=deleteoutliers(mEMG_sumITR,0.05,1);
```

```
[outFOR_sumITR]=deleteoutliers(mFOR_sumITR,0.05,1);
[outJOY_sumITR]=deleteoutliers(mJOY_sumITR,0.05,1);
break
%% BOXPLOT sumITR
figure()
x1 = mEMG_sumITR;
x2 = mFOR_sumITR;
x3 = [mJOY_sumITR;nan(3,1)];
boxplot([x1,x2,x3],'notch','on','labels',{'EMG','Force','Joystick'})
ylabel('ITR [b/s]')

%%
hFig =figure(1)
x1 = mEMG_sumITR;
x2 = mFOR_sumITR;
x3 = [mJOY_sumITR;nan(3,1)];
b=boxplot([x1,x2,x3],'notch','on','labels',{'EMG','Force','Joystick'})
set(b,'LineWidth',1.5)


h = findobj(gca)
children = get(h(2),'children');%In my case boxplot happens to be the↙
second object of the plot.
for i = 1:3
set(children(i), 'FontSize', 11,↙
'FontName','Arial','FontWeight','Bold');%To change label properties
end
h = findobj(gca,'Tag','Box');
 for j=1
    patch(get(h(j),'XData'),get(h(j),'YData'),'c','FaceAlpha',.5);
 end
 for j=2
    patch(get(h(j),'XData'),get(h(j),'YData'),'g','FaceAlpha',.5);
 end
 for j=3
    patch(get(h(j),'XData'),get(h(j),'YData'),'y','FaceAlpha',.5);
 end
% ylabel('Tracking Error [m^2/Hz^2]','FontSize', 11,↙
'FontName','Arial','FontWeight','Bold')
% set(gca,'FontSize', 11, 'FontName','Arial','FontWeight','Bold')
% set(gca,'box','off');
```

```
% axis([0.5 3.5 1.5e4 6.1e4])


ylabel('Information Transmission Rate [b/s]','FontSize', 11,↙
'FontName','Arial','FontWeight','Bold')
axis([0.5 3.5 2.5 4])
hAx1 = gca;   %# get a handle to first axis
set(hAx1,'FontSize', 11, 'FontName','Arial','FontWeight','Bold')
set(hAx1,'box','off');


%# create a second transparent axis, as a copy of the first
hAx2 = copyobj(hAx1,hFig);
delete( get(hAx2,'Children') )
set(hAx2, 'Color','none')

%# show grid-lines of first axis, give them desired color, but hide text↙
labels
ylabel('','FontSize', 11, 'FontName','Arial','FontWeight','Bold')
set(hAx1, 'XColor','r', 'YColor',[0.7 0.7 0.7], ...
    'XMinorGrid','off', 'YMinorGrid','on', ...
    'FontSize', 11, 'FontName','Arial','FontWeight','Bold',...
    'XTickLabel',[], 'YTickLabel',[]);

set(gcf, 'Units','centimeters', 'Position',[0 0 14.8 10])
set(gcf, 'PaperPositionMode','auto')
% saveas(hFig, 'TE.tiff', 'Resolution', 600);
print -dtiff -f1 -r600 BW

%% Data arrangement ITR

F=3
Fc=find(fa==F);              %Sum will be until 20 Hz

for i=1:8
Fc_EMG_ITR =reshape(sum(EMG_ITR(fselect,:,:)),1,3*8);
Fc_FOR_ITR =reshape(sum(FOR_ITR(fselect,:,:)),1,3*8);
Fc_JOY_ITR =reshape(sum(JOY_ITR(fselect,:,:)),1,3*7);
end

[outFc_EMG_ITR]=deleteoutliers(Fc_EMG_ITR,0.05,1)';
```

```
[outFc_FOR_ITR]=deleteoutliers(Fc_FOR_ITR,0.05,1)';
[outFc_JOY_ITR]=deleteoutliers(Fc_JOY_ITR,0.05,1)';

%BOXPLOT Fc_ITR
figure()
x1 = outFc_EMG_ITR;
x2 = outFc_FOR_ITR;
x3 = [outFc_JOY_ITR;nan(3,1)];

boxplot([x1,x2,x3],'notch','on','labels',{'EMG','Force','Joystick'})
ylabel('ITR [b/s]')
break
%% Export EVALUATION
csvwrite('EMG_ITR.dat',EMG_sumITR)
csvwrite('FOR_ITR.dat',FOR_sumITR)
csvwrite('JOY_ITR.dat',JOY_sumITR)
```

```
%% CO-CONTRACTION COMPARISON

function [ITR,sumITR]=get_ITR_ET(subjectnumber,interface,F)

snumber=int2str(subjectnumber);
datapath = strcat('D:↙
\Dropbox\INTERFACE_EXPERIMENT\Analysis\Data\Subject',snumber);
allfiles = dir(fullfile(datapath,'*.mat'));
ind = 0;
aux=char.empty(1,length(allfiles),0);
for k=1:length(allfiles)
    t=strcat('D:\Dropbox\INTERFACE_EXPERIMENT\Analysis\Data\Subject',↙
snumber,'\',allfiles(k,1).name);
    if strcmp(allfiles(k,1).name,'workspace.mat')==1
        aux{k}='workspace';
    elseif strcmp(allfiles(k,1).name,'matlab.mat')==1
        aux{k}='matlab.mat';
    else
    load(t);
    aux{k}=xpcdata2.description;
    tmpstring = strrep(aux{k}, '_', '');
    tmpinterface = strrep(interface, '_', '');
    res = strfind( tmpstring,tmpinterface);
    if ~isempty(res)
        ind = ind+1;
        finalaux{ind} = aux{k};
%         disp(finalaux{ind})
        finalnames{ind} = allfiles(k,1).name;
%         disp(finalnames{ind})
%         disp(' ')
    end
    end

end

files = finalnames;
N = 180000;                 %Total number of samples in 3 min trial
M = 6;                      %Number of cycles in 3 min trial
Fs= 1000;                   %Sample Freq. (Hz)
dt= 1/Fs;                   %Sample time 0.001s
T = dt * N;                 %Time 180 s
```

```
Tc = N/M/Fs;                    %Time of cycle 30s
f= (0:N-1)' / T;                %Frequency vector
fa = (0:N/M-1)'/Tc;             %Frequency after averaging
df =1/30;                       %Frequency period
fselect=[4 5 7 10 15 21 30 43 63 91];
Fc=find(fa==F);                 %Sum will be until 20 Hz

%First cycle excluded -> only 5 cycles, decrease in the total number of↙
samples
N2=N-30000;
M2=M-1;
N3=30000;

for expNr = 1:3

load(fullfile(datapath, files{expNr}));

aux =find(xpcdata2.x_TAR,1);
w=xpcdata2.x_TAR(aux+N3:aux+N,1);
x=xpcdata2.x_CUR(aux+N3:aux+N,1);

w = reshape(w(1:N2),N2/M2,M2);
x = reshape(x(1:N2),N2/M2,M2);

W =fft(w);
X =fft(x);

Sxx = M2/N2 * abs(X).^2;
Sww = M2/N2 * abs(W).^2;
Swx = M2/N2 * conj(W).*X;

mSxx = mean(Sxx,2);      %Average over cycles
mSww = mean(Sww,2);
mSwx = mean(Swx,2);


mH=mSwx./mSww;
aux2=mSxx./(mSxx-(abs(mH).^2.*mSww));
sumITR(expNr)=1/(N2/M2*dt)*sum(log2((aux2(1:Fc))));
ITR(:,expNr)=1/(N2/M2*dt).*log2((aux2));
```

```
% for K=1:1
% H=Swx(:,K)./Sww(:,K);
% aux2=Sxx(:,K)./(Sxx(:,K)-(abs(H).^2.*Sww(:,K)));
% sumITR(K,expNr)=1/(N2/M2*dt)*sum(log2((aux2(fselect))));
% ITR(:,K,expNr)=1/(N2/M2*dt)*log2((aux2(fselect)));
% end
end
```

BANDWIDTH

```
clc; clear all; close all;

N = 180000;                 %Total number of samples in 3 min trial
M = 6;                      %Number of cycles in 3 min trial
Fs= 1000;                   %Sample Freq. (Hz)
dt= 1/Fs;                   %Sample time 0.001s
T = dt * N;                 %Time 180 s
Tc = N/M/Fs;                %Time of cycle 30s
f= (0:N-1)' / T;            %Frequency vector
fa = (0:N/M-1)'/Tc;         %Frequency after averaging
df =1/30;                   %Frequency period
fselect=[4 5 7 10 15 21 30 43 63 91];
F=1.5;
Fc=find(fa==F);             %Sum will be until 20 Hz

%% Compute See for EVALUATION TRIALS
n=1;

for s=1:14
    if s~=2 && s~=6 && s~=9 && s~=10 && s~=11 && s~=12    %Exclude↙
subjects
        [EMG_bw(:,n)]=get_BW_ET(s,'EMG_E',F);
        [FOR_bw(:,n)]=get_BW_ET(s,'F_E',F);
        n=n+1
    end
end

%Joystick
n=1;
for s=10:16
        [JOY_bw(:,n)]=get_BW_ET(s,'J_E',F);
    n=n+1
end

disp('Done!')
break
%% Data arrangement sumITR
EMG_BW = reshape(EMG_bw,3*8,1);
FOR_BW = reshape(FOR_bw,3*8,1);
JOY_BW = reshape(JOY_bw,3*7,1);
```

```
[outEMG_BW]=deleteoutliers(EMG_BW,0.05);
[outFOR_BW]=deleteoutliers(FOR_BW,0.05);
[outJOY_BW]=deleteoutliers(JOY_BW,0.05);

%% BOXPLOT sumITR
figure()
x1 = EMG_BW;
x2 = FOR_BW;
x3 = [JOY_BW;nan(3,1)];
boxplot([x1,x2,x3],'notch','on','labels',{'EMG','Force','Joystick'})
ylabel('Bandwidth [Hz]')

%%
hFig =figure(1)
x1 = EMG_BW;
x2 = FOR_BW;
x3 = [JOY_BW;nan(3,1)];
b=boxplot([x1,x2,x3],'notch','on','labels',{'EMG','Force','Joystick'})
set(b,'LineWidth',1.5)


h = findobj(gca)
children = get(h(2),'children');%In my case boxplot happens to be the↙
second object of the plot.
for i = 1:3
set(children(i), 'FontSize', 11,↙
'FontName','Arial','FontWeight','Bold');%To change label properties
end
h = findobj(gca,'Tag','Box');
 for j=1
    patch(get(h(j),'XData'),get(h(j),'YData'),'c','FaceAlpha',.5);
 end
 for j=2
    patch(get(h(j),'XData'),get(h(j),'YData'),'g','FaceAlpha',.5);
 end
 for j=3
    patch(get(h(j),'XData'),get(h(j),'YData'),'y','FaceAlpha',.5);
 end
% ylabel('Tracking Error [m^2/Hz^2]','FontSize', 11,↙
'FontName','Arial','FontWeight','Bold')
```

```
% set(gca,'FontSize', 11, 'FontName','Arial','FontWeight','Bold')
% set(gca,'box','off');
% axis([0.5 3.5 1.5e4 6.1e4])


ylabel('Bandwidth [Hz]','FontSize', 11,↙
'FontName','Arial','FontWeight','Bold')
axis([0.5 3.5 1.6 3])
hAx1 = gca;   %# get a handle to first axis
set(hAx1,'FontSize', 11, 'FontName','Arial','FontWeight','Bold')
set(hAx1,'box','off');


%# create a second transparent axis, as a copy of the first
hAx2 = copyobj(hAx1,hFig);
delete( get(hAx2,'Children') )
set(hAx2, 'Color','none')

%# show grid-lines of first axis, give them desired color, but hide text↙
labels
ylabel('','FontSize', 11, 'FontName','Arial','FontWeight','Bold')
set(hAx1, 'XColor','r', 'YColor',[0.7 0.7 0.7], ...
    'XMinorGrid','off', 'YMinorGrid','on', ...
    'FontSize', 11, 'FontName','Arial','FontWeight','Bold',...
    'XTickLabel',[], 'YTickLabel',[]);

set(gcf, 'Units','centimeters', 'Position',[0 0 14.8 10])
set(gcf, 'PaperPositionMode','auto')
% saveas(hFig, 'TE.tiff', 'Resolution', 600);
print -dtiff -f1 -r600 BW
%%
% csvwrite('EMG_BW.dat',EMG_BW)
% csvwrite('FOR_BW.dat',FOR_BW)
% csvwrite('JOY_BW.dat',JOY_BW)
```

```
%% CO-CONTRACTION COMPARISON

function [bw]=get_BW_ET(subjectnumber,interface,F)

snumber=int2str(subjectnumber);
datapath = strcat('D:↙
\Dropbox\INTERFACE_EXPERIMENT\Analysis\Data\Subject',snumber);
allfiles = dir(fullfile(datapath,'*.mat'));
ind = 0;
aux=char.empty(1,length(allfiles),0);
for k=1:length(allfiles)
    t=strcat('D:\Dropbox\INTERFACE_EXPERIMENT\Analysis\Data\Subject',↙
snumber,'\',allfiles(k,1).name);
    if strcmp(allfiles(k,1).name,'workspace.mat')==1
        aux{k}='workspace';
    elseif strcmp(allfiles(k,1).name,'matlab.mat')==1
        aux{k}='matlab.mat';
    else
    load(t);
    aux{k}=xpcdata2.description;
    tmpstring = strrep(aux{k}, '_', '');
    tmpinterface = strrep(interface, '_', '');
    res = strfind( tmpstring,tmpinterface);
    if ~isempty(res)
        ind = ind+1;
        finalaux{ind} = aux{k};
%         disp(finalaux{ind})
        finalnames{ind} = allfiles(k,1).name;
%         disp(finalnames{ind})
%         disp(' ')
    end
    end

end

files = finalnames;
N = 180000;                 %Total number of samples in 3 min trial
M = 6;                      %Number of cycles in 3 min trial
Fs= 1000;                   %Sample Freq. (Hz)
dt= 1/Fs;                   %Sample time 0.001s
T = dt * N;                 %Time 180 s
```

```
Tc = N/M/Fs;                    %Time of cycle 30s
f= (0:N-1)' / T;                %Frequency vector
fa = (0:N/M-1)'/Tc;             %Frequency after averaging
df =1/30;                       %Frequency period
fselect=[4 5 7 10 15 21 30 43 63 91];
Fc=find(fa==F);                 %Sum will be until 20 Hz

%First cycle excluded -> only 5 cycles, decrease in the total number of↙
samples
N2=N-30000;
M2=M-1;
N3=30000;

for expNr = 1:3

load(fullfile(datapath, files{expNr}));

aux =find(xpcdata2.x_TAR,1);
w=xpcdata2.x_TAR(aux+N3:aux+N,1);
x=xpcdata2.x_CUR(aux+N3:aux+N,1);

w = reshape(w(1:N2),N2/M2,M2);
x = reshape(x(1:N2),N2/M2,M2);

W =fft(w);
X =fft(x);

Sww = M2/N2 * abs(W).^2;
Swx = M2/N2 * conj(W).*X;

mmSww = mean(Sww,2);
mmSwx = mean(Swx,2);

mH=abs(mmSwx./mmSww);
x=fa([4 5 7 10 15 21 30 43 63 91]);     %10 excited frequencies
y=mH([4 5 7 10 15 21 30 43 63 91]);     %Values of Hcs at the 10↙
frequencies

x2=0.1:df:3;
y2=interp1(x,y,x2);
max=mean(y2(1:Fc-4));
```

```
% max2=mH(4);

yw=max/sqrt(2);
% xb2=max2/sqrt(2)

i=Fc-4;
k=0;
while i<=87 && k~=1
    tmp = y2(i);
    if tmp<=yw
        xw=x2(i);
        k=1;
    elseif i==87
        xw=nan;
    end
    i=i+1;
end
bw(:,expNr)=xw;
end
```

EFFORT MEASURE

```
%% COMPARISON OF EMG AND FORCE
function [mNEMG,mNFOR,mNJOY,mNEMG2]=get_EMGvsFORCE(subjectnumber,↙
interface)

snumber=int2str(subjectnumber);
datapath = strcat('D:↙
\Dropbox\INTERFACE_EXPERIMENT\Analysis\Data\Subject',snumber);
allfiles = dir(fullfile(datapath,'*.mat'));
ind = 0;
aux=char.empty(1,length(allfiles),0);
for k=1:length(allfiles)
    t=strcat('D:\Dropbox\INTERFACE_EXPERIMENT\Analysis\Data\Subject',↙
snumber,'\',allfiles(k,1).name);
    if strcmp(allfiles(k,1).name,'workspace.mat')==1
        aux{k}='workspace';
    elseif strcmp(allfiles(k,1).name,'matlab.mat')==1
        aux{k}='matlab.mat';
    else
    load(t);
    aux{k}=xpcdata2.description;
    tmpstring = strrep(aux{k}, '_', '');
    tmpinterface = strrep(interface, '_', '');
    res = strfind( tmpstring,tmpinterface);
    if ~isempty(res)
        ind = ind+1;
        finalaux{ind} = aux{k};
%         disp(finalaux{ind})
        finalnames{ind} = allfiles(k,1).name;
%         disp(finalnames{ind})
%         disp(' ')
    end
    end

end

files = finalnames;
N = 180000;                 %Total number of samples in 3 min trial
M = 6;                      %Number of cycles in 3 min trial
Fs= 1000;                   %Sample Freq. (Hz)
dt= 1/Fs;                   %Sample time 0.001s
T = dt * N;                 %Time 180 s
```

```
Tc = N/M/Fs;                %Time of cycle 30s
f= (0:N-1)' / T;            %Frequency vector
fa = (0:N/M-1)'/Tc;         %Frequency after averaging
df =1/30;                   %Frequency period

%First cycle excluded -> only 5 cycles, decrease in the total number of samples
N2=N-30000;
M2=M-1;
N3=30000;

% Fc=find(fa==F);             %Sum will be until 20 Hz
n=0;
for expNr = 1:3

load(fullfile(datapath, files{expNr}));
aux =find(xpcdata2.x_TAR,1);

% if strcmp(interface,'F_E')
%     for j=1:N-N3
%         if xpcdata2.N_T_EMG_B(aux+N3+j-1,1)>xpcdata2.N_T_EMG_T(aux+N3+j-1,1)
%             NEMG2(j)=xpcdata2.N_T_EMG_B(aux+N3+j-1,1)*-1;
%         else
%             NEMG2(j)=xpcdata2.N_T_EMG_T(aux+N3+j-1,1);
%         end
%     end
% end
    NEMG=(xpcdata2.N_T_EMG_B(aux+N3:aux+N,1)+xpcdata2.N_T_EMG_T(aux+N3:aux+N,1));
    NFOR=(xpcdata2.x_FOR(aux+N3:aux+N,1));
    NJOY=(diff(xpcdata2.x_CUR(aux+N3:aux+N,1)))*50;
    NEMG2=(diff(xpcdata2.x_CUR(aux+N3:aux+N,1)))*50;
% elseif strcmp(interface,'EMG_E')
%     NEMG= diff(xpcdata2.x_CUR(aux+N3:aux+N,1));
%     NFOR=(xpcdata2.x_FOR(aux+N3:aux+N,1));
% end


% ANEMG=abs(NEMG);
% ANFOR=abs(NFOR);
```

```
ANEMG=(NEMG);
ANFOR=(NFOR);

%MEAN
mNEMG(:,expNr)=rms(ANEMG);
mNEMG2(:,expNr)=rms(NEMG2);
mNFOR(:,expNr)=rms(ANFOR);
mNJOY(:,expNr)=rms(NJOY);
% mNEMG(:,expNr)=mean(ANEMG);
% mNFOR(:,expNr)=mean(ANFOR);

%AREA under curve
% A_NEMG(:,expNr) =dt* trapz(s,NEMG);
% A_NFOR(:,expNr) =dt* trapz(s,NFOR);
end

% %MEAN
% mmNEMG=mean(mNEMG,2);
% mmNFOR=mean(mNFOR,2);
%
% mA_NEMG=mean(A_NEMG,2);
% mA_NFOR=mean(A_NFOR,2);
```

HUMAN-INTERFACE MODELING

```
function [e, Hmod] = fitfun2(p, f, H,coh)
% Error function used by 'bmelab_analysis_demo.m'
% This function is used to fit a McRuer model on the spectral estimators
% of the human controller.

% Extract parameter from parameter vector
K = p(1);
delay = p(2);

% Vector of Laplace operators
s = (2*pi*f*1j);

% Model estimate
Hmod = K * exp(-delay*s);

% Error between model and spectral estimators
e =coh.^2.*(abs(log(H./ Hmod)));
end
```

```
function [VAF_x]=get_VAF(subjectnumber,interface,p)

snumber=int2str(subjectnumber);
datapath = strcat('D:↙
\Dropbox\INTERFACE_EXPERIMENT\Analysis\Data\Subject',snumber);
allfiles = dir(fullfile(datapath,'*.mat'));
ind = 0;
aux=char.empty(1,length(allfiles),0);
for k=1:length(allfiles)
    t=strcat('D:\Dropbox\INTERFACE_EXPERIMENT\Analysis\Data\Subject',↙
snumber,'\',allfiles(k,1).name);
    if strcmp(allfiles(k,1).name,'workspace.mat')==1
        aux{k}='workspace';
    elseif strcmp(allfiles(k,1).name,'matlab.mat')==1
        aux{k}='matlab.mat';
    else
    load(t);
    aux{k}=xpcdata2.description;
    tmpstring = strrep(aux{k}, '_', '');
    tmpinterface = strrep(interface, '_', '');
    res = strfind( tmpstring,tmpinterface);
    if ~isempty(res)
        ind = ind+1;
        finalaux{ind} = aux{k};
%         disp(finalaux{ind})
        finalnames{ind} = allfiles(k,1).name;
%         disp(finalnames{ind})
%         disp(' ')
    end
    end

end
n=1;
N = 180000;                 %Total number of samples in 3 min trial
M = 6;                      %Number of cycles in 3 min trial
Fs= 1000;                   %Sample Freq. (Hz)
dt= 1/Fs;                   %Sample time 0.001s
T = dt * N;                 %Time 180 s
Tc = N/M/Fs;                %Time of cycle 30s
f= (0:N-1)' / T;            %Frequency vector
fa = (0:N/M-1)'/Tc;         %Frequency after averaging
```

```
df =1/30;                       %Frequency period
fselect = [4 5 7 10 15 21 30 43 63 91];
N2=N-30000;
M2=M-1;
N3=30000;

files = finalnames;
%% Simulation of Human response with fitted model
% Transfer function
% p = [K, tau_lead, tau_lag, delay]'
k = p(1,subjectnumber);
delay = p(2,subjectnumber);
% tau_lead = p(2,subjectnumber);
% tau_lag = p(3,subjectnumber);



s = tf('s');
% Hhuman = k * (tau_lead*s+1) / (tau_lag*s+1) * exp(-delay*s);
Hhm = k * exp(-delay*s);
Hsys = 1/s;
Hl = Hhm * Hsys;
Hcl = Hl/(1+Hl);
% figure,bode(Hcs)
% figure,step(Hcs)


%% Simulation
for expNr = 1:3
load(fullfile(datapath, files{expNr}));
aux =find(xpcdata2.x_TAR,1);
t = 0:dt:150;
x = xpcdata2.x_CUR(aux+N3:aux+N,1);            % cursor position
w = xpcdata2.x_TAR(aux+N3:aux+N,1);            % target position

%Mean of cycles

% mx=mean(reshape(x(1:N2),N2/M2,M2),2);
% mw=mean(reshape(w(1:N2),N2/M2,M2),2);
% me=mean(reshape(e(1:N2),N2/M2,M2),2);
%
```

```
% mx_hat = lsim(Hcl,mw,mt);                % simulated cursor position
x_hat = lsim(Hcl,w,t);                    % simulated cursor position
%% VAF
VAF_x(:,expNr) = vaf(x,x_hat);
end
end
```

APPENDIX E: PILOT STUDY RESULTS

Evaluation of EMG, Force and Joystick as control interfaces for active upper-extremity orthoses

Report of Preliminary Results from the Pilot Sudy

By Joan Lobo and Diana Batista

INDEX

1. Introduction

Active orthoses can increase the independence of and quality of life for patients with severe neuromusculoskeletal disorders. The operation of these active assistive devices is mediated by a control interface. The selection of the interface strategy to control the device according to each user's needs and capabilities – which may change over time – is crucial for the usability and proper functioning of the active movement-assistive device. Currently, many control interfaces exist and it remains unclear which strategy is most suited to each type of impairment and task.

A better understanding of the limitations and capabilities of the different control interfaces, through objective and quantitative evaluations, can provide the relevant information for the selection of the most suited control interface for an specific application.

The goal of this study was to quantitatively evaluate the performance and the learning characteristics of force-, EMG- and hand joystick-based interfaces. The human operator abilities were tested using a screen-based one-dimensional position-tracking task, where the interface signal (u) is mapped to the velocity of the cursor. The target (w) was moving according to a multi-sine signal with a flat velocity spectrum.

The performance of the control interface was evaluated in terms of tracking error, human-operator bandwidth and information transmission rate. The learning characteristics were evaluated by analyzing the tracking error along a series of training trials. Furthermore, the subjects were asked to list the control interfaces in order of preference.

Preliminary results from 6 subjects show that force-, EMG- and joystick-based interfaces present very similar results in terms of tracking error. However, force- and joystick-based interfaces show considerably higher information transmission rate but lower bandwidth than EMG-based interface. Five of the six subjects stated that force-based interface was the most preferred interface followed by EMG- and joystick-based interface.

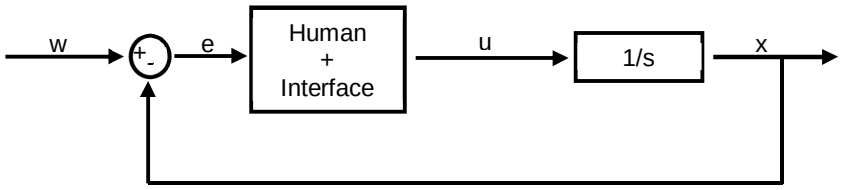

2. Time Domain Analysis

2.1. Learning Curves

Tracking Error Comparison

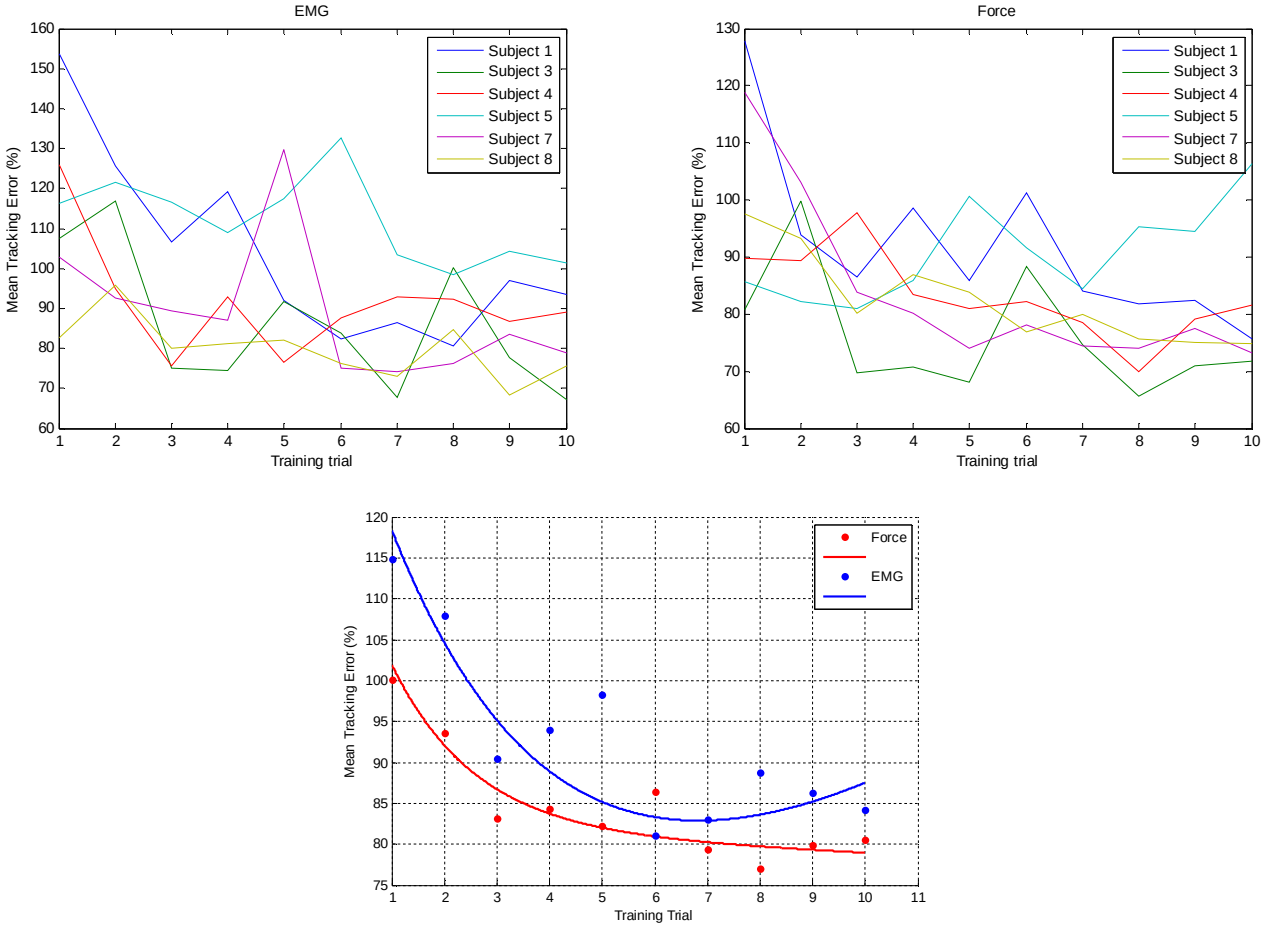

Notes: One outlier was detected and excluded for the 6th EMG training trial of one subject. Weights given by 1/variance were used. Mean (fitted model: f(x) = a*exp(b*x) + c*exp(d*x))

Observations: Curve fitting of the EMG learning curve is not realistic. If the curve fitting does not take into account the variance the fitting is realistic. Learning is clearly observed for both interfaces.

First results with the new joystick (3 subjects)

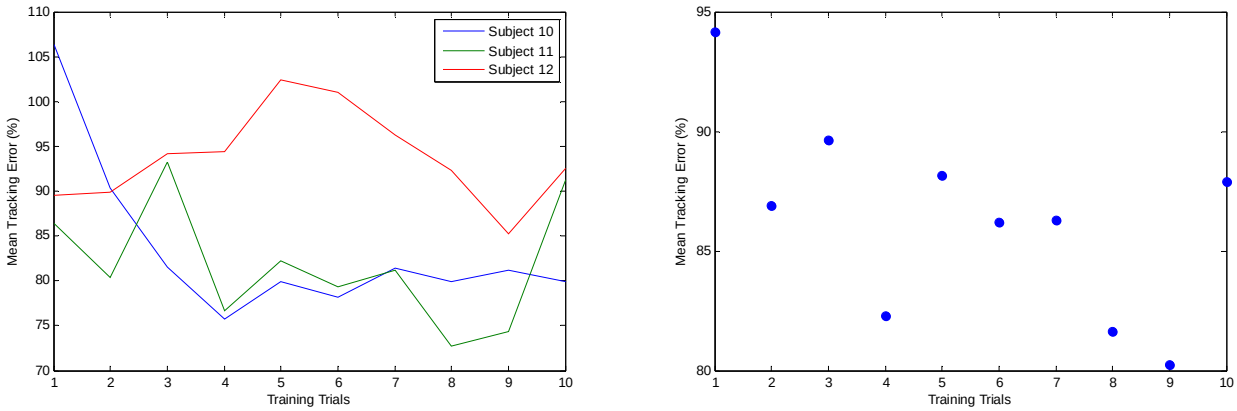

Observations: Although these results refer only to 3 subjects, it seems that the joystick tracking error is slightly inferior to both EMG and Force. However, it is not clear whether or not learning can be observed for this interface.

2.2. Tracking Error

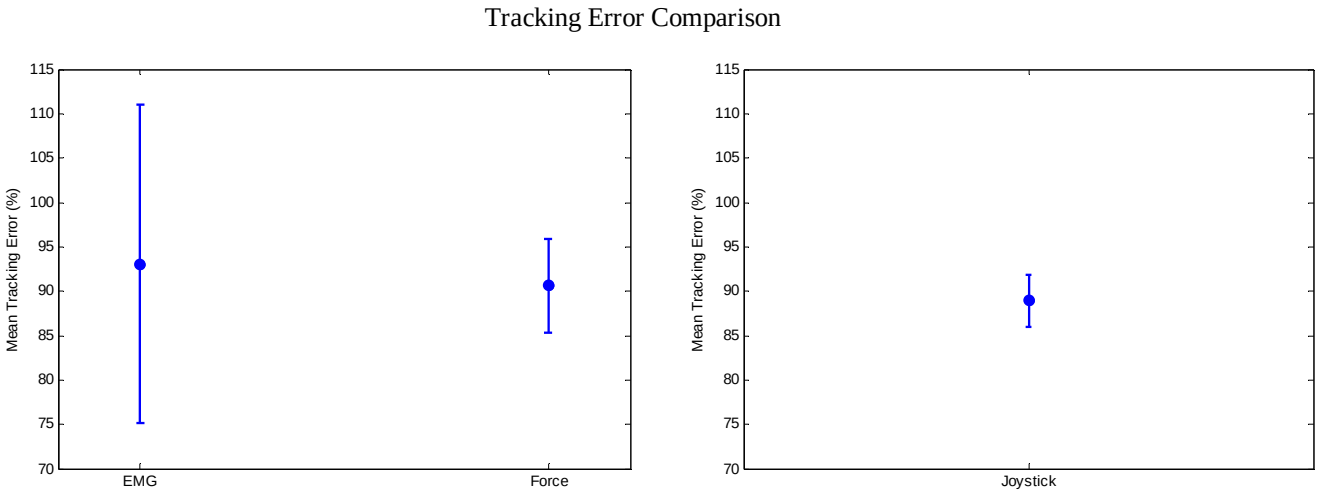

Note: First 5s are not taken into account. Joystick tracking error corresponds to only 3 subjects.

Observations: Mean tracking errors for all three interfaces are very similar.Force-based interface presents a considerably lower standard deviation of the tracking error than EMG-based interface.

Velocity – Tracking Error dependency

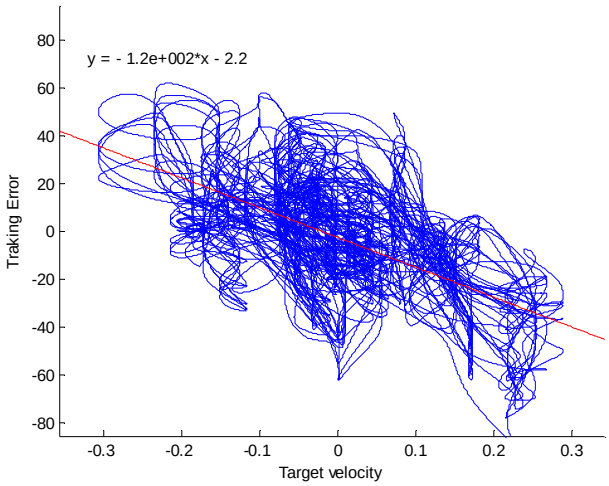

Learning curve using PSD of error signal (See)

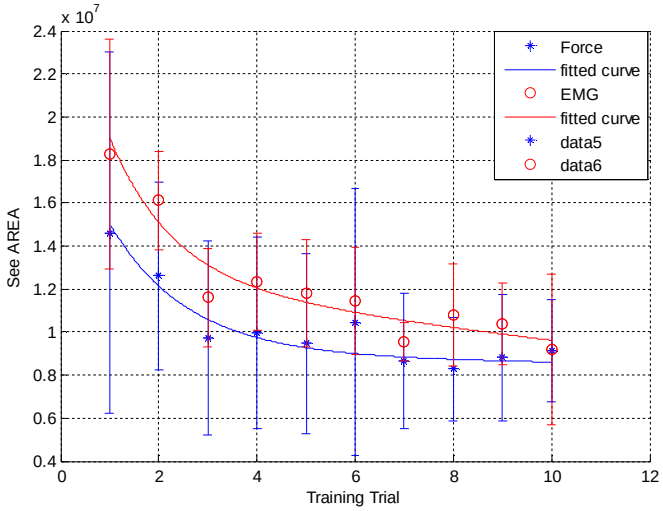

Observations: The tracking error is dependent to the target velocity. Because of the random phase of the multisine signal, the target does not have the same speed in all trials. This results in ~20% of uncertenty of the tracking error. This could be solved by using always the same multisine signal. Another approach would be to estimate the traking error for the frequency domain taking the integral of the PSD of the error signal (See).

2.3. Alternative to Tracking Error: Integral of See (form 0Hz to 20Hz)

Box plots of the See area for the 3 evaluation trials:

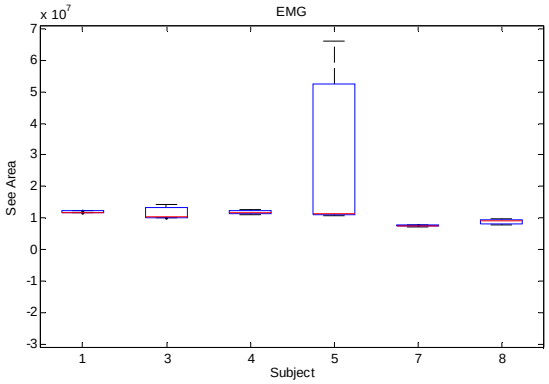

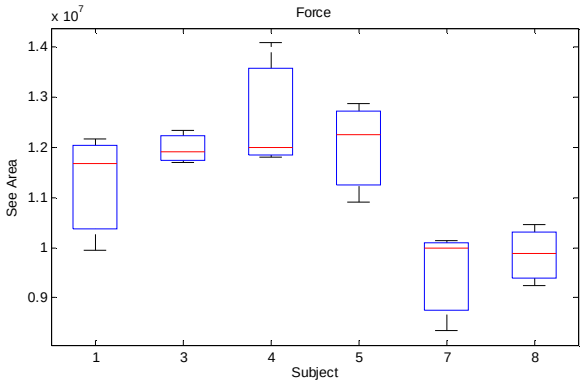

As can be seen from the EMG plot, subject 5 had an unexpectedly high tracking error for one of the trials and is therefore detected as an outlier when the box plot of the mean for all subjects is computed.

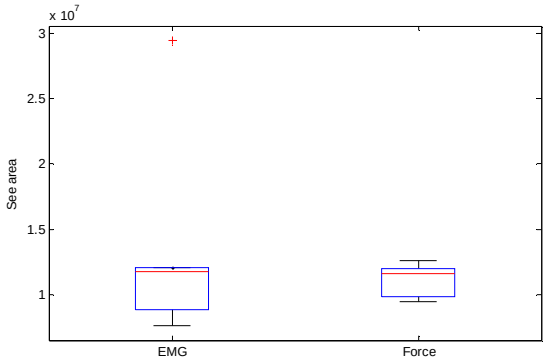

Tracking Error Comparison

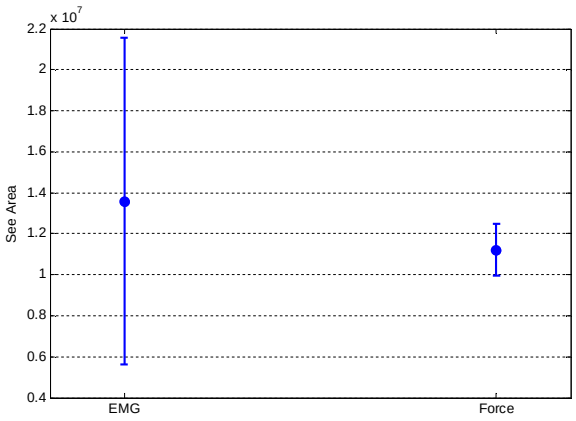

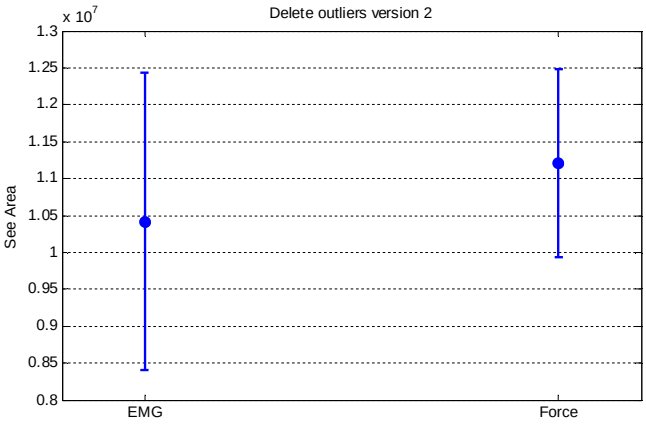

Notes: Delete outliers version 2 - Outlier detection is performed between subjects (after the See sum). This resulted in the exclusion of Subject 5 for EMG.
Observations: The area of the PSD of the error signal can give a more reliable measure of accuracy of the interface in the tracking task. The See area is very similar for EMG and Force; slightly inferior for Force when outliers aren't detected but slightly larger when they are.

2.4. Effort comparison (EMG vs Force)

Amount of Force comparison

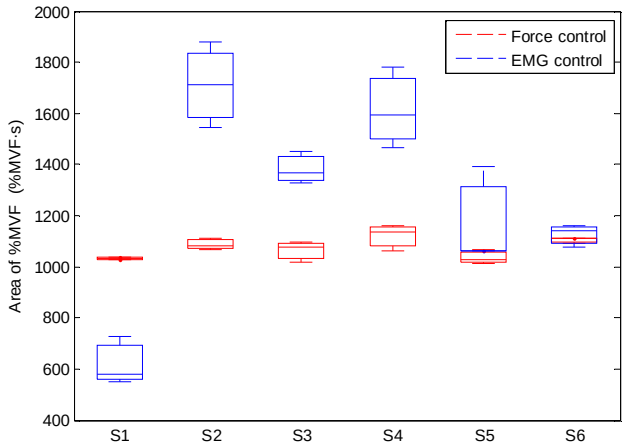

Amount of EMG comparison

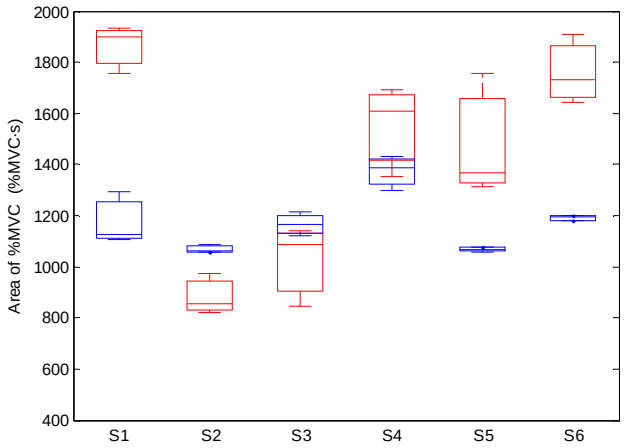

Observations: The amount of force (area of %MVF) is similar in all subjects when using the force-based interface. In contrast, the amount of EMG (area of %MVC) presents a higher intra-subject variability. This could be caused by the inherent differences in the control strategy between EMG and Force.

In the case of the EMG-based interface the direction of movement is determined depending on which muscle (biceps or triceps) is more active. In the Force-based interface the direction of movement is determined depending on the sign of the measured force. In both cases the velocity of the cursor is proportional to the amplitude of the signal.

Co-contraction comparison

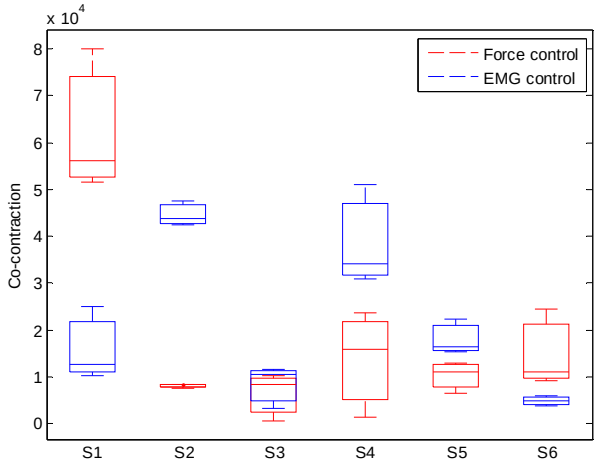

Observations: No considerable differences of co-contraction levels can be observed between Force-based interface and EMG-based interface.

3. Frequency Domain Analysis

Power spectral densities and cross-spectral densities were calculated using the fast-Fourier transform. For these calculations, the first cycle of 30 s was not taken into account. The remaining 5 cycles of the signals were averaged. Furthermore, for each subject, an average of spectral densities over the 3 evaluation trials was performed.

3.1. Power Spectral Densities

Input PSD

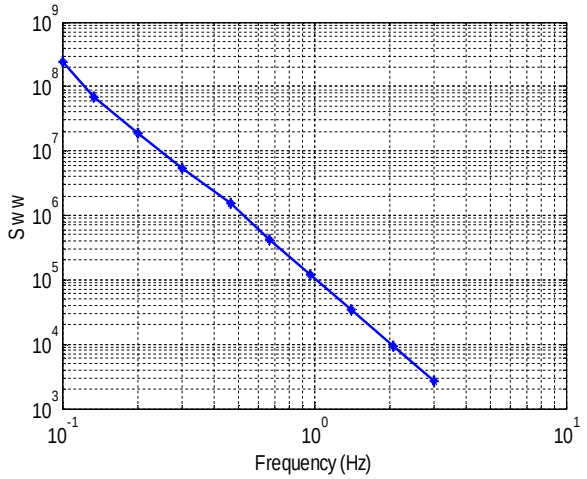

Human output PSD

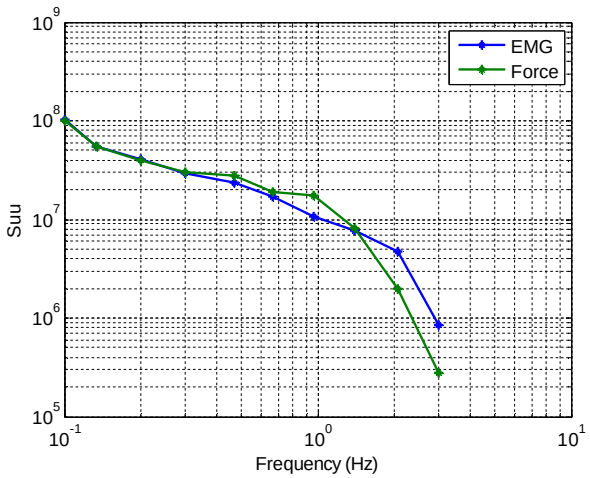

System Output PSD

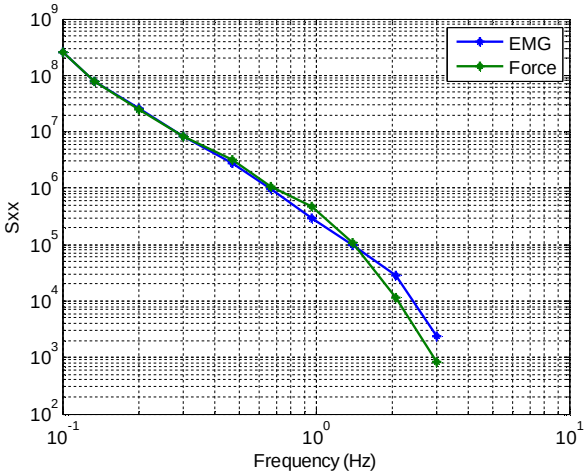

Error PSD

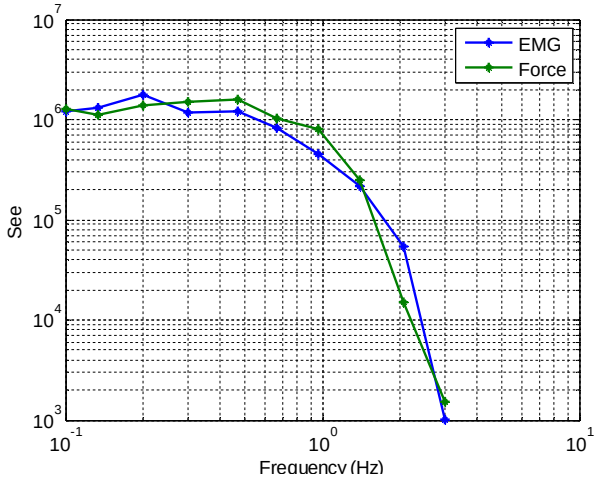

3.2. Frequency Response Functions

$$Hhuman = \frac{Swu}{Swe} \qquad Hsystem = \frac{Swx}{Swu} \qquad Hcs = \frac{Swx}{Sww}$$

3.2.1. EMG-based interface

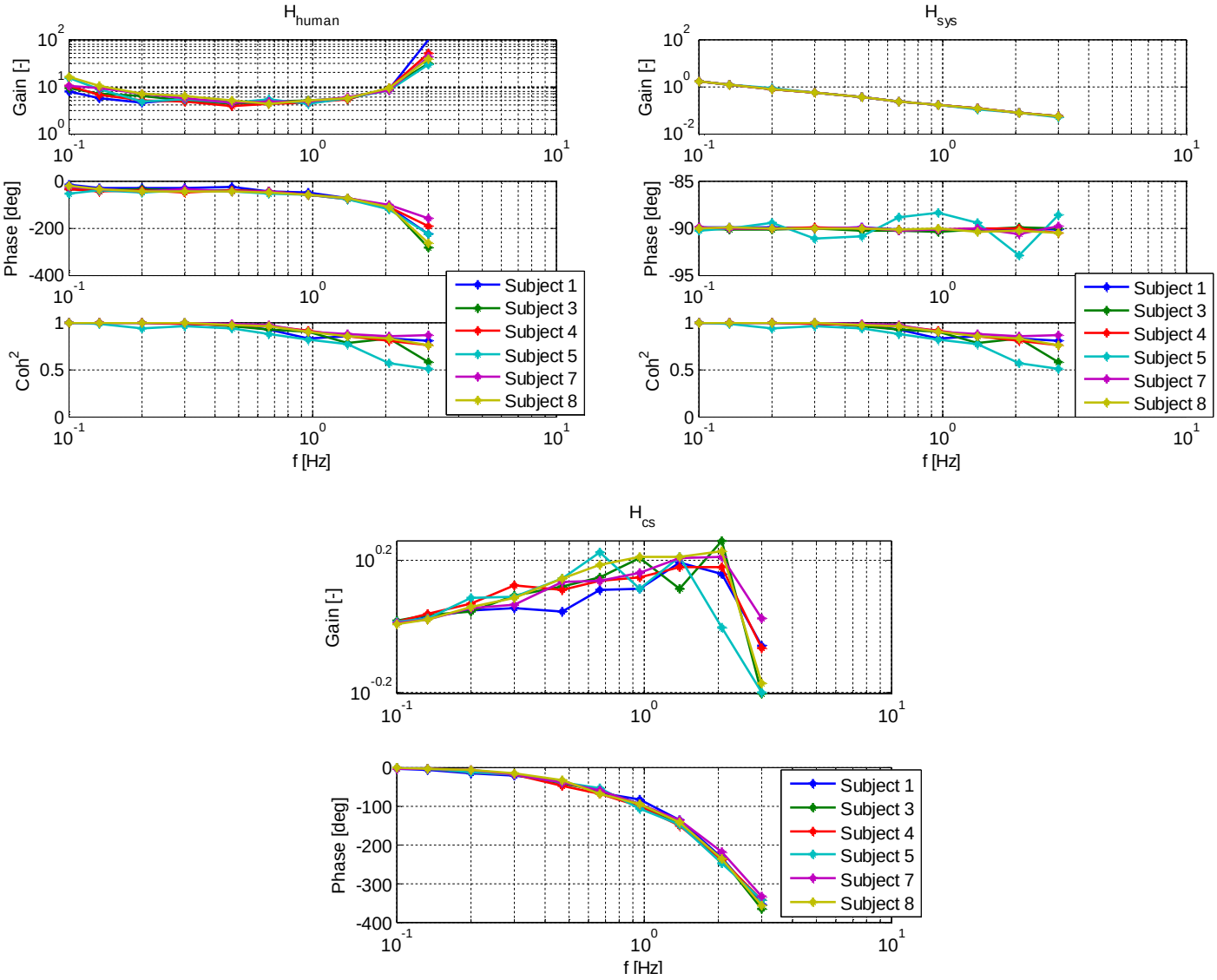

EMG FRF of subject 5

Problem with the phase is probably due to an abnormal error during the 1st evaluation trial (see figure). If we don't take into account this trial, Hsys is far closer to the obtained with the other subjects.

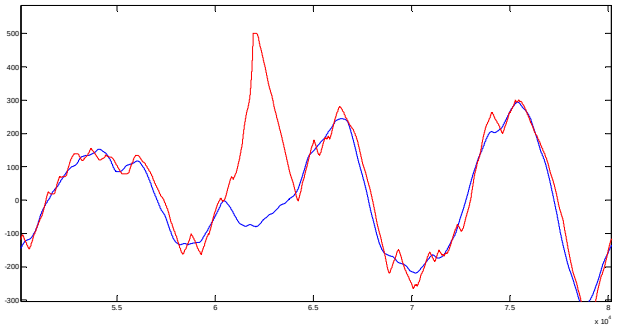

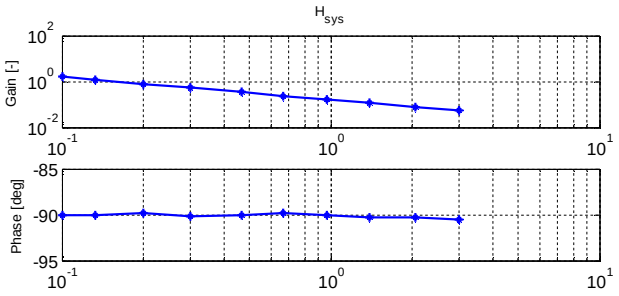

3.2.2. *FORCE-based interface*

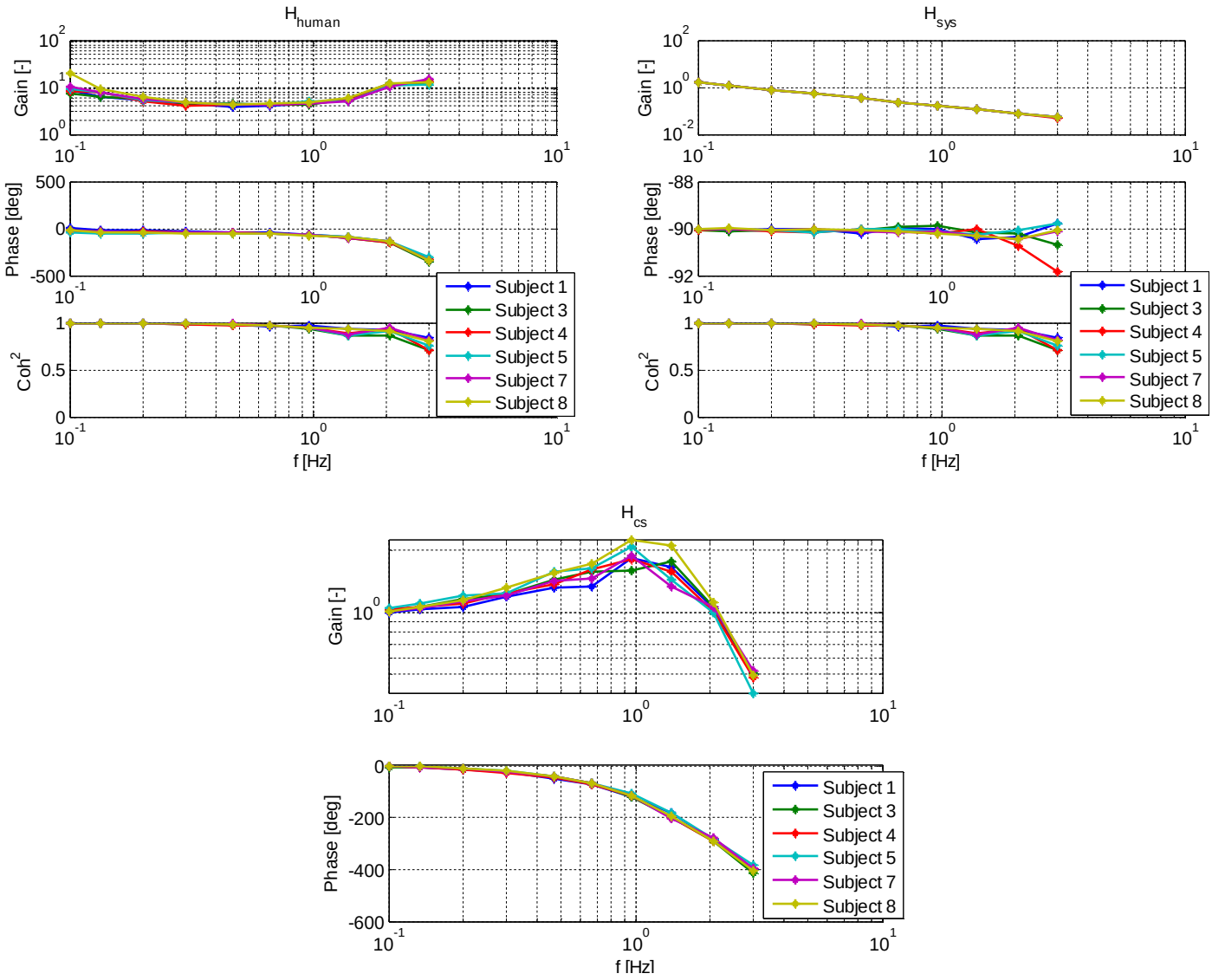

3.2.3. Average of all subjects

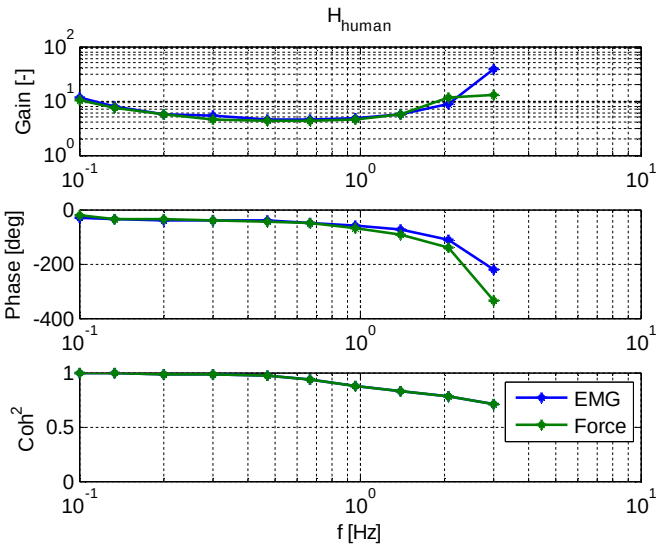

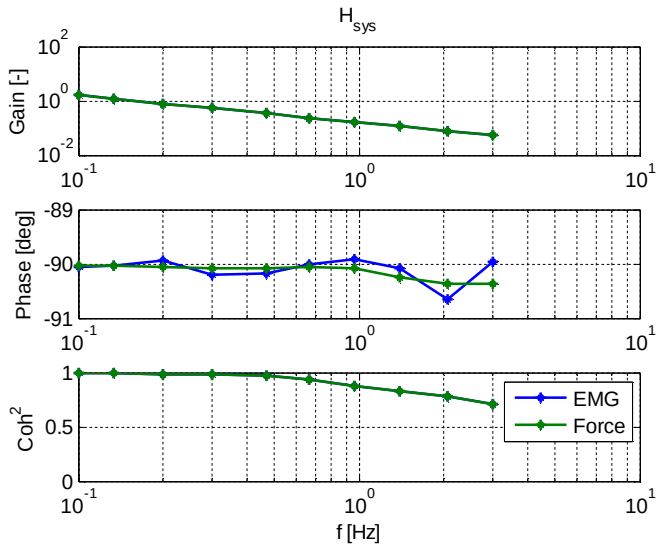

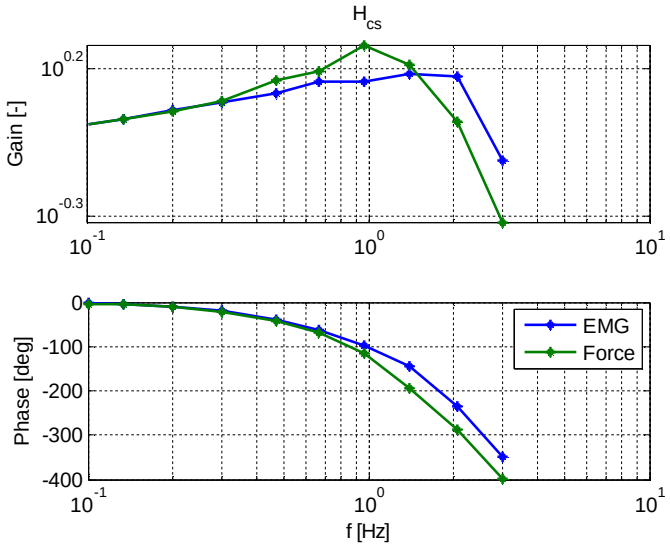

3.2.4. First results with the new joystick.

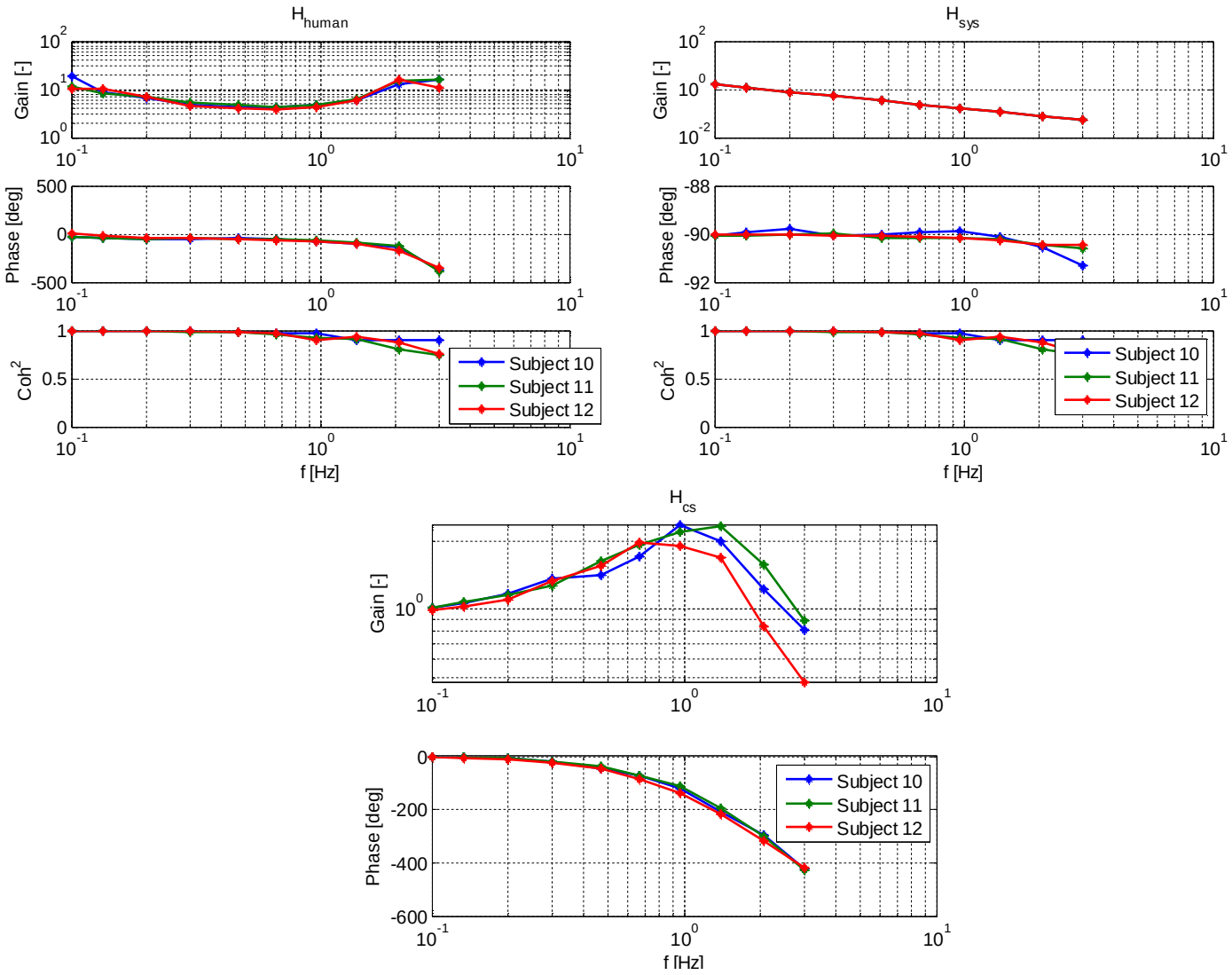

3.3. Information Transmission Rate

$$\dot{T} = \frac{1}{NT}\sum_{f_k \in K} \log_2\left[\frac{S_{xx}(f_k)}{S_{xx}(f_k) - |H(f_k)|^2 S_{ww}(f_k)}\right] \qquad H(f_k) = \frac{S_{wx}(f_k)}{S_{ww}(f_k)}$$

$$K = \{0.100, 0.133, 0.200, 0.300, 0.467, 0.667, 0.967, 1.400, 2.067, 3.000\}$$

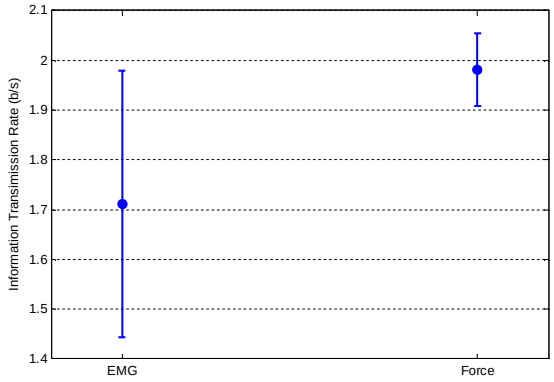

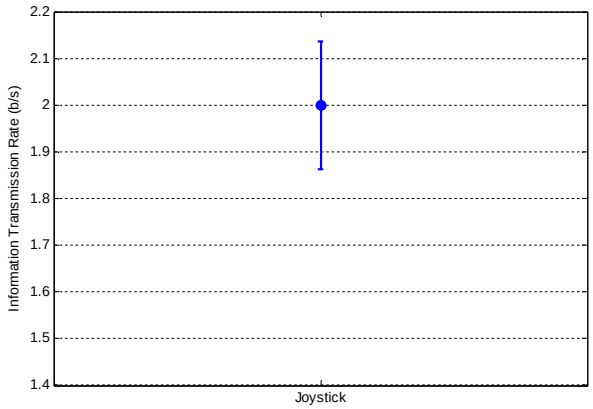

Note: Joystick – 3 subjects.

Observations: Force-based interface presents a higher information transmission rate and a considerably lower standard deviation than EMG-based interface.

3.4. Bandwidth

The human-operator bandwidth is obtained from Hcs. Since information is only available at the 10 excited frequencies, linear interpolation between these values was performed. The value at 0.1 Hz (1st frequency) is obtained and the bandwidth is defined as the frequency at which this value drops -3 dB (70%).

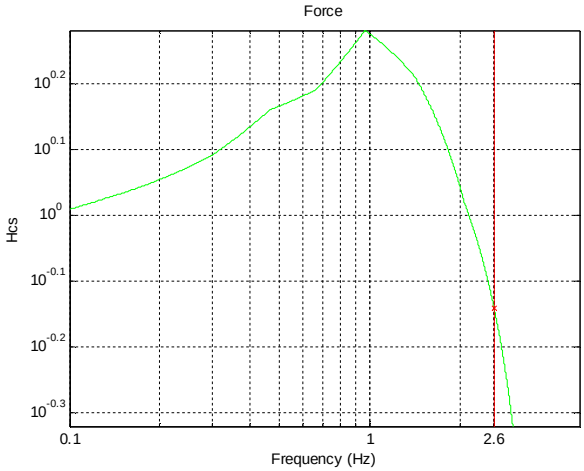

As for EMG, this 3 dB drop is not observed before 3 Hz (last frequency).

As we need a definition that holds for all interfaces, we defined the maximum as the mean value from 0.1 to 0.467 Hz. With this definition, we obtained a slightly larger bandwidth for EMG than for Force.

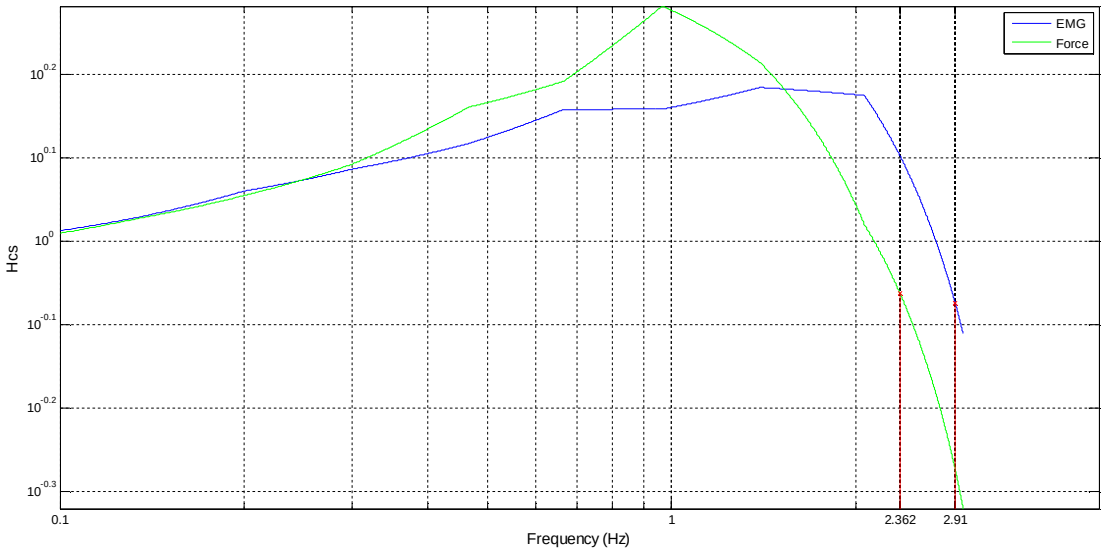

3.5. Parameter estimation

3.5.1. Training trials

The model $Hmod = K \times \exp(-delay \times s)$ was fitted to Hhuman for the 10 training trials (in the figure: subject 8, training trial number 4). Gain and delay parameters along training trials were computed.

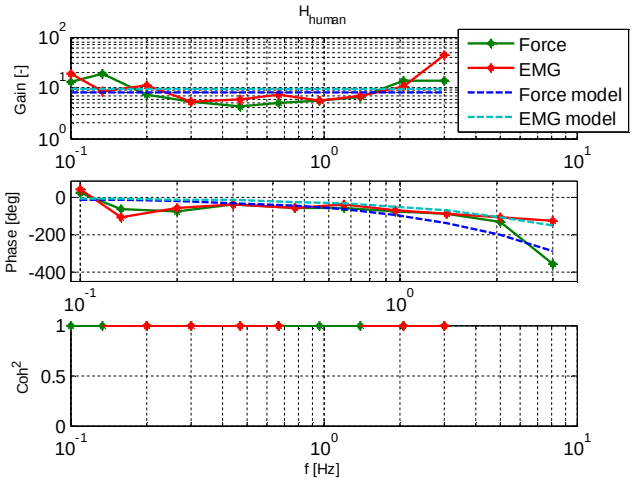

Subject 8

Force	K	8,69	8,24	9,82	8,22	9,19	9,80	10,09	9,33	9,41	8,69
	Delay	0,23	0,26	0,25	0,27	0,26	0,23	0,27	0,26	0,27	0,23
EMG	K	10,58	7,23	8,93	9,63	9,30	10,54	10,85	8,64	10,28	10,58
	Delay	0,10	0,17	0,10	0,14	0,25	0,13	0,12	0,10	0,12	0,10

Subject 7

Force	K	7,82	6,51	7,30	7,97	7,87	8,01	7,87	7,91	7,21	7,82
	Delay	0,25	0,27	0,27	0,27	0,25	0,23	0,24	0,24	0,24	0,25
EMG	K	7,59	5,74	6,58	6,53	6,02	7,46	8,00	7,95	7,11	7,59
	Delay	0,13	0,19	0,15	0,14	0,17	0,19	0,15	0,14	0,14	0,13

3.5.2. Evaluation trials

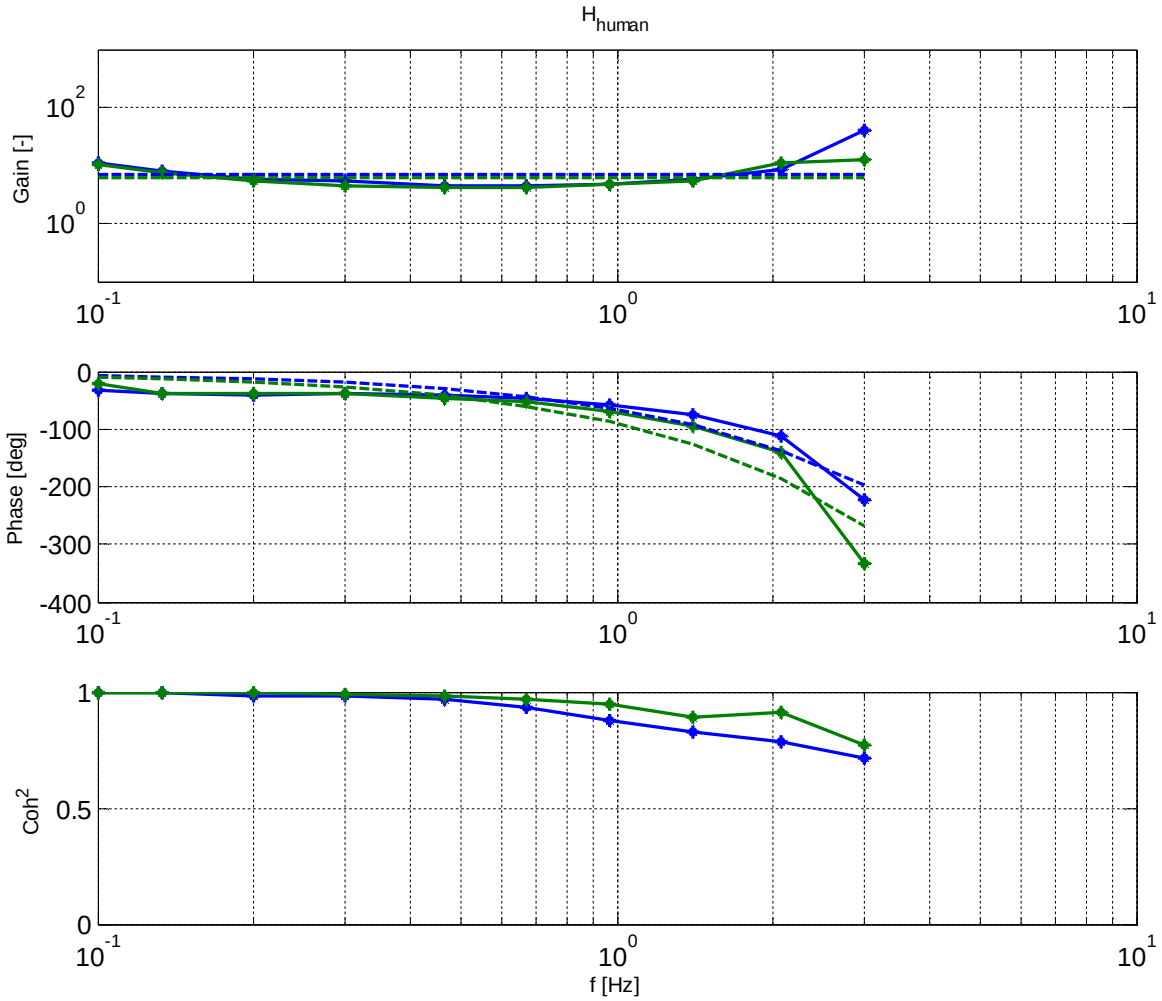

RESULTS OF PARAMETER FIT

Interface	K	delay
EMG	6.994	0.184
Force	6.280	0.249

APPENDIX F: OUTPUT FROM THE STATISTICAL ANALYSIS

BANDWIDTH

```
GLM EMG FOR JOY
  /WSFACTOR=Interface 3 Polynomial
  /METHOD=SSTYPE(3)
  /PLOT=PROFILE(Interface)
  /EMMEANS=TABLES(Interface) COMPARE ADJ(BONFERRONI)
  /PRINT=DESCRIPTIVE
  /CRITERIA=ALPHA(.05)
  /WSDESIGN=Interface.
```

General Linear Model

[DataSet0]

Within-Subjects Factors

Measure: MEASURE_1

Interface	Dependent Variable
1	EMG
2	FOR
3	JOY

Descriptive Statistics

	Mean	Std. Deviation	N
EMG	2,6048	,31429	14
FOR	2,0690	,19147	14
JOY	2,0071	,27524	14

Multivariate Tests[a]

Effect		Value	F	Hypothesis df	Error df	Sig.
Interface	Pillai's Trace	,817	26,715[b]	2,000	12,000	,000
	Wilks' Lambda	,183	26,715[b]	2,000	12,000	,000
	Hotelling's Trace	4,453	26,715[b]	2,000	12,000	,000
	Roy's Largest Root	4,453	26,715[b]	2,000	12,000	,000

a. Design: Intercept
Within Subjects Design: Interface

b. Exact statistic

Mauchly's Test of Sphericity[a]

Measure: MEASURE_1

Within Subjects Effect	Mauchly's W	Approx. Chi-Square	df	Sig.	Epsilon[b] Greenhouse-Geisser
Interface	,885	1,470	2	,479	,897

Mauchly's Test of Sphericity[a]

Measure: MEASURE_1

Within Subjects Effect	Epsilon[b] Huynh-Feldt	Lower-bound
Interface	1,000	,500

Tests the null hypothesis that the error covariance matrix of the orthonormalized transformed dependent variables is proportional to an identity matrix.

a. Design: Intercept
Within Subjects Design: Interface

b. May be used to adjust the degrees of freedom for the averaged tests of significance. Corrected tests are displayed in the Tests of Within-Subjects Effects table.

Tests of Within-Subjects Effects

Measure: MEASURE_1

Source		Type III Sum of Squares	df	Mean Square	F
Interface	Sphericity Assumed	3,024	2	1,512	29,162
	Greenhouse-Geisser	3,024	1,793	1,686	29,162
	Huynh-Feldt	3,024	2,000	1,512	29,162
	Lower-bound	3,024	1,000	3,024	29,162
Error(Interface)	Sphericity Assumed	1,348	26	,052	
	Greenhouse-Geisser	1,348	23,312	,058	
	Huynh-Feldt	1,348	26,000	,052	
	Lower-bound	1,348	13,000	,104	

Tests of Within-Subjects Effects

Measure: MEASURE_1

Source		Sig.
Interface	Sphericity Assumed	,000
	Greenhouse-Geisser	,000
	Huynh-Feldt	,000
	Lower-bound	,000
Error(Interface)	Sphericity Assumed	
	Greenhouse-Geisser	
	Huynh-Feldt	
	Lower-bound	

Tests of Within-Subjects Contrasts

Measure: MEASURE_1

Source	Interface	Type III Sum of Squares	df	Mean Square	F	Sig.
Interface	Linear	2,500	1	2,500	57,414	,000
	Quadratic	,524	1	,524	8,709	,011
Error(Interface)	Linear	,566	13	,044		
	Quadratic	,782	13	,060		

Tests of Between-Subjects Effects

Measure: MEASURE_1

Transformed Variable: Average

Source	Type III Sum of Squares	df	Mean Square	F	Sig.
Intercept	208,297	1	208,297	1937,557	,000
Error	1,398	13	,108		

Estimated Marginal Means

Interface

Estimates

Measure: MEASURE_1

Interface	Mean	Std. Error	95% Confidence Interval	
			Lower Bound	Upper Bound
1	2,605	,084	2,423	2,786
2	2,069	,051	1,958	2,180
3	2,007	,074	1,848	2,166

Pairwise Comparisons

Measure: MEASURE_1

(I) Interface	(J) Interface	Mean Difference (I-J)	Std. Error	Sig.[b]	95% Confidence Interval for Difference[b]	
					Lower Bound	Upper Bound
1	2	,536*	,100	,000	,262	,809
	3	,598*	,079	,000	,381	,814
2	1	-,536*	,100	,000	-,809	-,262
	3	,062	,078	1,000	-,152	,276
3	1	-,598*	,079	,000	-,814	-,381
	2	-,062	,078	1,000	-,276	,152

Based on estimated marginal means

*. The mean difference is significant at the ,05 level.

b. Adjustment for multiple comparisons: Bonferroni.

Multivariate Tests

	Value	F	Hypothesis df	Error df	Sig.
Pillai's trace	,817	26,715[a]	2,000	12,000	,000
Wilks' lambda	,183	26,715[a]	2,000	12,000	,000
Hotelling's trace	4,453	26,715[a]	2,000	12,000	,000
Roy's largest root	4,453	26,715[a]	2,000	12,000	,000

Each F tests the multivariate effect of Interface. These tests are based on the linearly independent pairwise comparisons among the estimated marginal means.

a. Exact statistic

Profile Plots

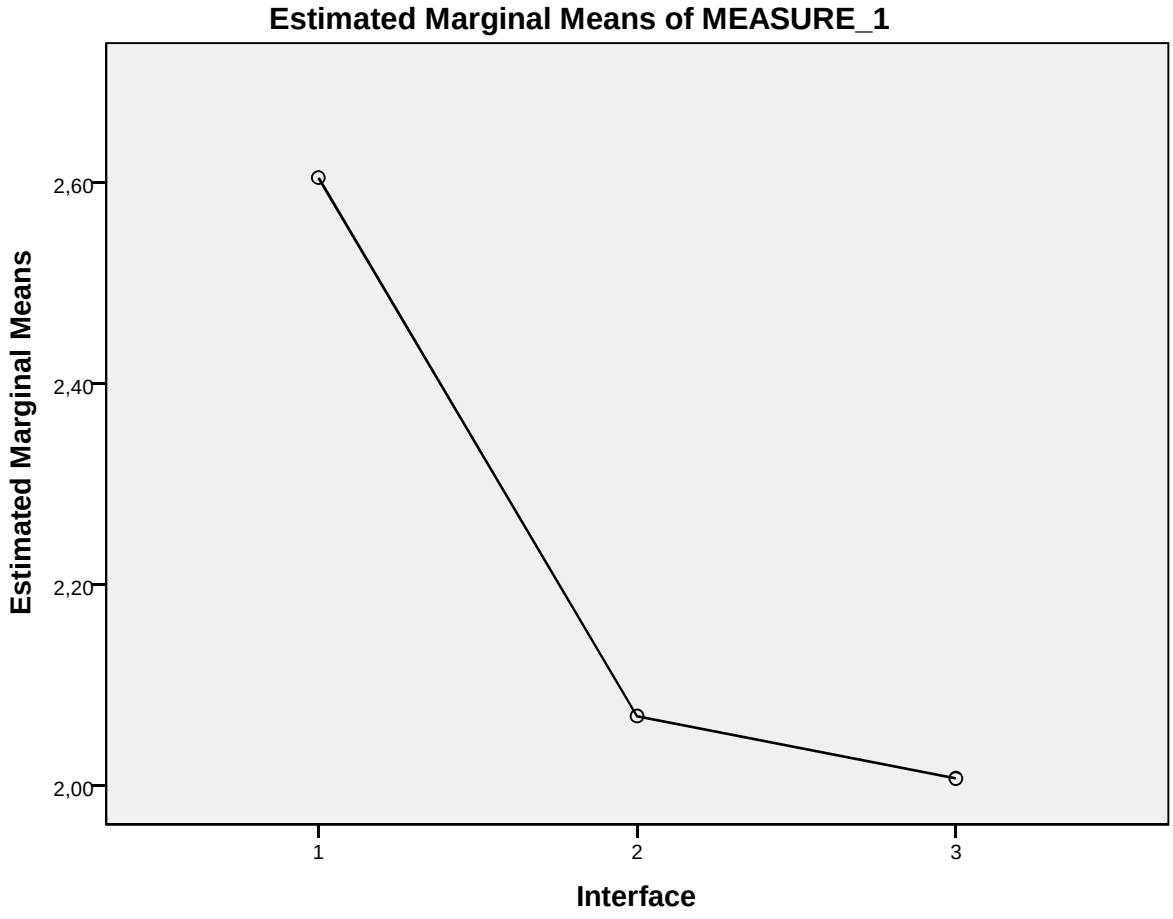

EFFORT MEASURE

```
GLM VAR00001 VAR00003 VAR00006
  /WSFACTOR=Interfaces 3 Polynomial
  /METHOD=SSTYPE(3)
  /PLOT=PROFILE(Interfaces)
  /EMMEANS=TABLES(Interfaces) COMPARE ADJ(BONFERRONI)
  /PRINT=DESCRIPTIVE
  /CRITERIA=ALPHA(.05)
  /WSDESIGN=Interfaces.
```

General Linear Model

```
[DataSet0]
```

Within-Subjects Factors

Measure: MEASURE_1

Interfaces	Dependent Variable
1	VAR00001
2	VAR00003
3	VAR00006

Descriptive Statistics

	Mean	Std. Deviation	N
VAR00001	7.9312	.32686	20
VAR00003	7.4494	.25652	20
VAR00006	7.9132	.56458	20

Multivariate Tests[a]

Effect		Value	F	Hypothesis df	Error df	Sig.
Interfaces	Pillai's Trace	.753	27.502[b]	2.000	18.000	.000
	Wilks' Lambda	.247	27.502[b]	2.000	18.000	.000
	Hotelling's Trace	3.056	27.502[b]	2.000	18.000	.000
	Roy's Largest Root	3.056	27.502[b]	2.000	18.000	.000

a. Design: Intercept
Within Subjects Design: Interfaces

b. Exact statistic

Mauchly's Test of Sphericity[a]

Measure: MEASURE_1

Within Subjects Effect	Mauchly's W	Approx. Chi-Square	df	Sig.	Epsilon[b] Greenhouse-Geisser
Interfaces	.524	11.635	2	.003	.677

Mauchly's Test of Sphericity[a]

Measure: MEASURE_1

Within Subjects Effect	Epsilon[b] Huynh-Feldt	Lower-bound
Interfaces	.711	.500

Tests the null hypothesis that the error covariance matrix of the orthonormalized transformed dependent variables is proportional to an identity matrix.

a. Design: Intercept
Within Subjects Design: Interfaces

b. May be used to adjust the degrees of freedom for the averaged tests of significance. Corrected tests are displayed in the Tests of Within-Subjects Effects table.

Tests of Within-Subjects Effects

Measure: MEASURE_1

Source		Type III Sum of Squares	df	Mean Square	F
Interfaces	Sphericity Assumed	2.984	2	1.492	10.297
	Greenhouse-Geisser	2.984	1.355	2.202	10.297
	Huynh-Feldt	2.984	1.422	2.098	10.297
	Lower-bound	2.984	1.000	2.984	10.297
Error(Interfaces)	Sphericity Assumed	5.506	38	.145	
	Greenhouse-Geisser	5.506	25.744	.214	
	Huynh-Feldt	5.506	27.027	.204	
	Lower-bound	5.506	19.000	.290	

Tests of Within-Subjects Effects

Measure: MEASURE_1

Source		Sig.
Interfaces	Sphericity Assumed	.000
	Greenhouse-Geisser	.002
	Huynh-Feldt	.001
	Lower-bound	.005
Error(Interfaces)	Sphericity Assumed	
	Greenhouse-Geisser	
	Huynh-Feldt	
	Lower-bound	

Tests of Within-Subjects Contrasts

Measure: MEASURE_1

Source	Interfaces	Type III Sum of Squares	df	Mean Square	F	Sig.
Interfaces	Linear	.003	1	.003	.016	.902
	Quadratic	2.981	1	2.981	36.941	.000
Error(Interfaces)	Linear	3.973	19	.209		
	Quadratic	1.533	19	.081		

Tests of Between-Subjects Effects

Measure: MEASURE_1

Transformed Variable: Average

Source	Type III Sum of Squares	df	Mean Square	F	Sig.
Intercept	3617.327	1	3617.327	17942.363	.000
Error	3.831	19	.202		

Estimated Marginal Means

Interfaces

Estimates

Measure: MEASURE_1

Interfaces	Mean	Std. Error	95% Confidence Interval	
			Lower Bound	Upper Bound
1	7.931	.073	7.778	8.084
2	7.449	.057	7.329	7.569
3	7.913	.126	7.649	8.177

Pairwise Comparisons

Measure: MEASURE_1

(I) Interfaces	(J) Interfaces	Mean Difference (I-J)	Std. Error	Sig.[b]	95% Confidence [b]...
					Lower Bound
1	2	.482*	.068	.000	.303
	3	.018	.145	1.000	-.362
2	1	-.482*	.068	.000	-.661
	3	-.464*	.134	.008	-.815
3	1	-.018	.145	1.000	-.398
	2	.464*	.134	.008	.112

Pairwise Comparisons

Measure: MEASURE_1

(I) Interfaces	(J) Interfaces	95% Confidence [b]... Upper Bound
1	2	.661
	3	.398
2	1	-.303
	3	-.112
3	1	.362
	2	.815

Based on estimated marginal means

*. The mean difference is significant at the .05 level.

b. Adjustment for multiple comparisons: Bonferroni.

Multivariate Tests

	Value	F	Hypothesis df	Error df	Sig.
Pillai's trace	.753	27.502[a]	2.000	18.000	.000
Wilks' lambda	.247	27.502[a]	2.000	18.000	.000
Hotelling's trace	3.056	27.502[a]	2.000	18.000	.000
Roy's largest root	3.056	27.502[a]	2.000	18.000	.000

Each F tests the multivariate effect of Interfaces. These tests are based on the linearly independent pairwise comparisons among the estimated marginal means.

a. Exact statistic

Profile Plots

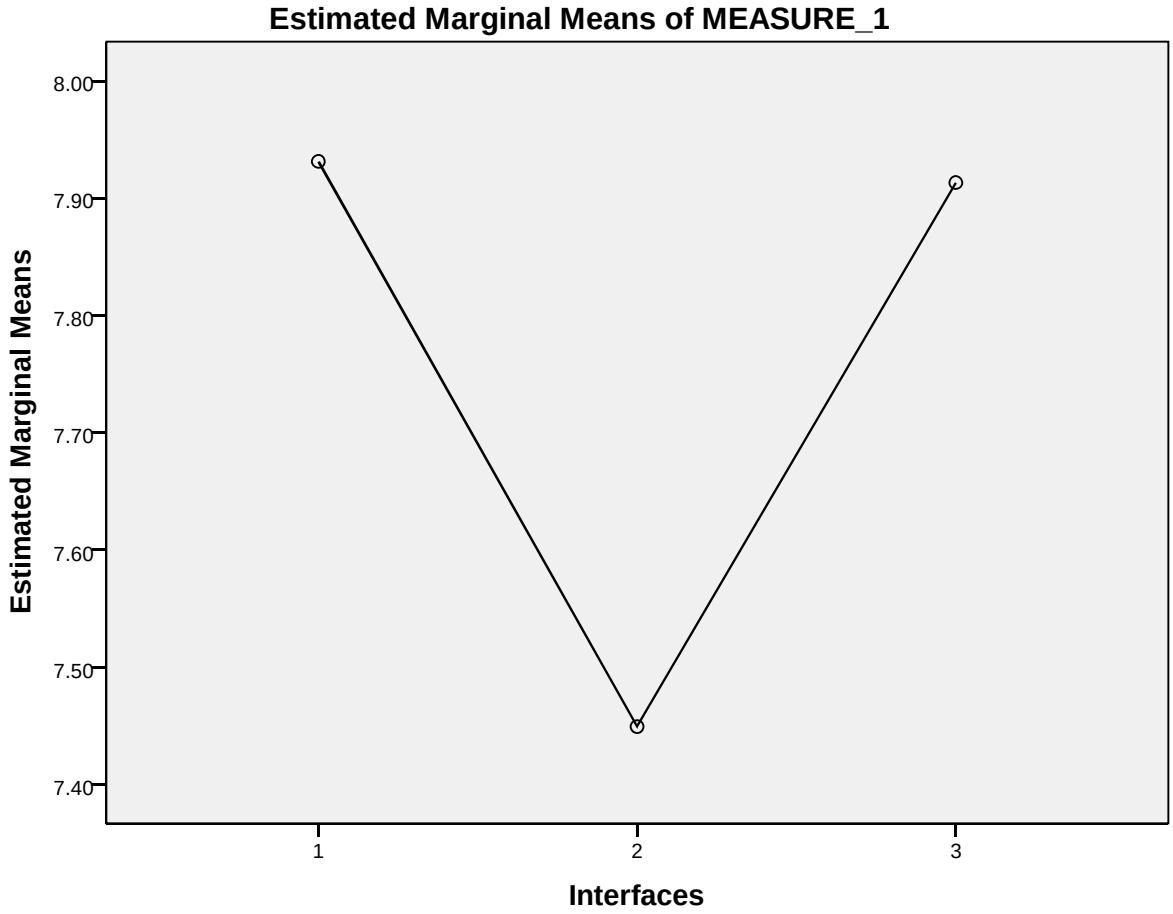
Estimated Marginal Means of MEASURE_1
Estimated Marginal Means
8.00
7.90
7.80
7.70
7.60
7.50
7.40
1
2
3
Interfaces

INFORMATION TRANSMISSION RATE

```
GLM EMG FOR JOY
  /WSFACTOR=Interface 3 Polynomial
  /METHOD=SSTYPE(3)
  /PLOT=PROFILE(Interface)
  /EMMEANS=TABLES(Interface) COMPARE ADJ(BONFERRONI)
  /PRINT=DESCRIPTIVE
  /CRITERIA=ALPHA(.05)
  /WSDESIGN=Interface.
```

General Linear Model

[DataSet0]

Within-Subjects Factors

Measure: MEASURE_1

Interface	Dependent Variable
1	EMG
2	FOR
3	JOY

Descriptive Statistics

	Mean	Std. Deviation	N
EMG	3,1353	,25632	19
FOR	3,4850	,24867	19
JOY	3,4922	,22674	19

Multivariate Tests[a]

Effect		Value	F	Hypothesis df	Error df	Sig.
Interface	Pillai's Trace	,481	7,868[b]	2,000	17,000	,004
	Wilks' Lambda	,519	7,868[b]	2,000	17,000	,004
	Hotelling's Trace	,926	7,868[b]	2,000	17,000	,004
	Roy's Largest Root	,926	7,868[b]	2,000	17,000	,004

a. Design: Intercept
Within Subjects Design: Interface

b. Exact statistic

Mauchly's Test of Sphericity[a]

Measure: MEASURE_1

Within Subjects Effect	Mauchly's W	Approx. Chi-Square	df	Sig.	Epsilon[b] Greenhouse-Geisser
Interface	,766	4,540	2	,103	,810

Mauchly's Test of Sphericity[a]

Measure: MEASURE_1

Within Subjects Effect	Epsilon[b] Huynh-Feldt	Lower-bound
Interface	,879	,500

Tests the null hypothesis that the error covariance matrix of the orthonormalized transformed dependent variables is proportional to an identity matrix.

a. Design: Intercept
Within Subjects Design: Interface

b. May be used to adjust the degrees of freedom for the averaged tests of significance. Corrected tests are displayed in the Tests of Within-Subjects Effects table.

Tests of Within-Subjects Effects

Measure: MEASURE_1

Source		Type III Sum of Squares	df	Mean Square	F
Interface	Sphericity Assumed	1,581	2	,791	12,310
	Greenhouse-Geisser	1,581	1,620	,976	12,310
	Huynh-Feldt	1,581	1,757	,900	12,310
	Lower-bound	1,581	1,000	1,581	12,310
Error(Interface)	Sphericity Assumed	2,312	36	,064	
	Greenhouse-Geisser	2,312	29,165	,079	
	Huynh-Feldt	2,312	31,632	,073	
	Lower-bound	2,312	18,000	,128	

Tests of Within-Subjects Effects

Measure: MEASURE_1

Source		Sig.
Interface	Sphericity Assumed	,000
	Greenhouse-Geisser	,000
	Huynh-Feldt	,000
	Lower-bound	,003
Error(Interface)	Sphericity Assumed	
	Greenhouse-Geisser	
	Huynh-Feldt	
	Lower-bound	

Tests of Within-Subjects Contrasts

Measure: MEASURE_1

Source	Interface	Type III Sum of Squares	df	Mean Square	F	Sig.
Interface	Linear	1,210	1	1,210	14,542	,001
	Quadratic	,372	1	,372	8,208	,010
Error(Interface)	Linear	1,498	18	,083		
	Quadratic	,815	18	,045		

Tests of Between-Subjects Effects

Measure: MEASURE_1

Transformed Variable: Average

Source	Type III Sum of Squares	df	Mean Square	F	Sig.
Intercept	647,653	1	647,653	12830,891	,000
Error	,909	18	,050		

Estimated Marginal Means

Interface

Estimates

Measure: MEASURE_1

Interface	Mean	Std. Error	95% Confidence Interval	
			Lower Bound	Upper Bound
1	3,135	,059	3,012	3,259
2	3,485	,057	3,365	3,605
3	3,492	,052	3,383	3,601

Pairwise Comparisons

Measure: MEASURE_1

(I) Interface	(J) Interface	Mean Difference (I-J)	Std. Error	Sig.[b]	95% Confidence Interval for Difference[b]	
					Lower Bound	Upper Bound
1	2	-,350*	,089	,003	-,586	-,114
	3	-,357*	,094	,004	-,604	-,110
2	1	,350*	,089	,003	,114	,586
	3	-,007	,059	1,000	-,164	,149
3	1	,357*	,094	,004	,110	,604
	2	,007	,059	1,000	-,149	,164

Based on estimated marginal means

*. The mean difference is significant at the ,05 level.

b. Adjustment for multiple comparisons: Bonferroni.

Multivariate Tests

	Value	F	Hypothesis df	Error df	Sig.
Pillai's trace	,481	7,868[a]	2,000	17,000	,004
Wilks' lambda	,519	7,868[a]	2,000	17,000	,004
Hotelling's trace	,926	7,868[a]	2,000	17,000	,004
Roy's largest root	,926	7,868[a]	2,000	17,000	,004

Each F tests the multivariate effect of Interface. These tests are based on the linearly independent pairwise comparisons among the estimated marginal means.

a. Exact statistic

Profile Plots

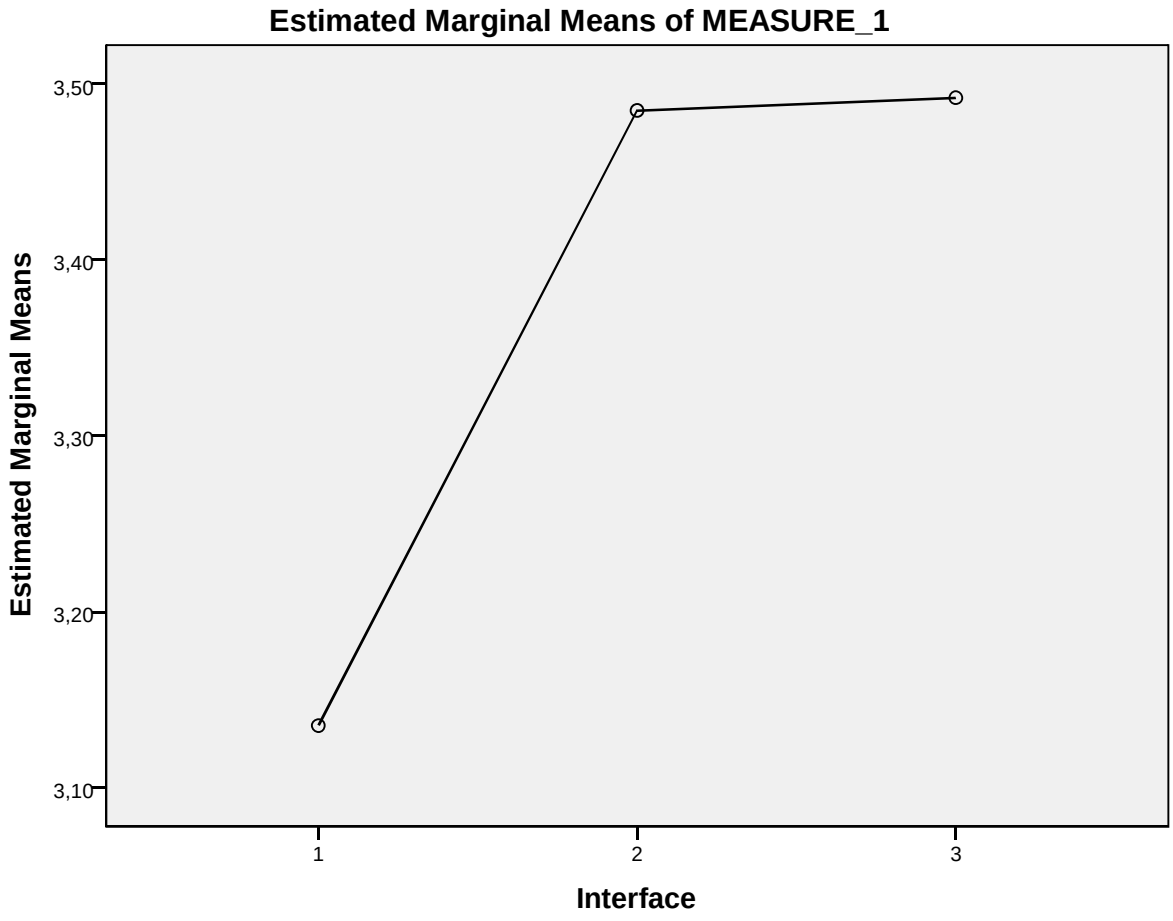

TRACKING ERROR

```
NEW FILE.
DATASET NAME DataSet1 WINDOW=FRONT.
DATASET ACTIVATE DataSet1.
DATASET CLOSE DataSet0.
EXAMINE VARIABLES=EMG FOR JOY
  /PLOT BOXPLOT STEMLEAF HISTOGRAM NPPLOT
  /COMPARE GROUPS
  /PERCENTILES(5,10,25,50,75,90,95) HAVERAGE
  /STATISTICS DESCRIPTIVES EXTREME
  /CINTERVAL 95
  /MISSING LISTWISE
  /NOTOTAL.
```

Explore

```
[DataSet1]
```

Case Processing Summary

	Cases					
	Valid		Missing		Total	
	N	Percent	N	Percent	N	Percent
EMG	102	86,4%	16	13,6%	118	100,0%
FOR	102	86,4%	16	13,6%	118	100,0%
JOY	102	86,4%	16	13,6%	118	100,0%

Descriptives

			Statistic	Std. Error
EMG	Mean		119151,7875	3079,42511
	95% Confidence Interval for Mean	Lower Bound	113043,0364	
		Upper Bound	125260,5385	
	5% Trimmed Mean		117145,0911	
	Median		119276,3975	
	Variance		967251616,2	
	Std. Deviation		31100,66906	
	Minimum		70073,89	
	Maximum		220920,54	
	Range		150846,65	
	Interquartile Range		43775,55	
	Skewness		,874	,239
	Kurtosis		1,061	,474
FOR	Mean		120785,9283	2047,77672
	95% Confidence Interval for Mean	Lower Bound	116723,6902	
		Upper Bound	124848,1665	
	5% Trimmed Mean		119488,3251	
	Median		118215,8835	
	Variance		427725727,4	
	Std. Deviation		20681,53107	
	Minimum		86129,73	
	Maximum		192168,57	
	Range		106038,84	
	Interquartile Range		26805,74	
	Skewness		,923	,239
	Kurtosis		1,140	,474
JOY	Mean		131176,8800	2286,13403
	95% Confidence Interval for Mean	Lower Bound	126641,8050	
		Upper Bound	135711,9549	
	5% Trimmed Mean		130455,0627	
	Median		128530,2508	
	Variance		533093696,7	
	Std. Deviation		23088,82190	
	Minimum		79345,41	
	Maximum		201934,94	
	Range		122589,53	
	Interquartile Range		31617,51	
	Skewness		,467	,239
	Kurtosis		,107	,474

Percentiles

		Percentiles			
		5	10	25	50
Weighted Average(Definition 1)	EMG	75584,0955	83478,5017	92561,4323	119276,3975
	FOR	92338,4472	97221,6833	105728,8786	118215,8835
	JOY	96968,5852	101790,7564	114693,5250	128530,2508
Tukey's Hinges	EMG			92712,9334	119276,3975
	FOR			105747,9976	118215,8835
	JOY			114894,0313	128530,2508

Percentiles

		Percentiles		
		75	90	95
Weighted Average(Definition 1)	EMG	136336,9863	153749,0155	182332,1817
	FOR	132534,6226	144888,1695	167624,6810
	JOY	146311,0310	163233,3910	171641,7079
Tukey's Hinges	EMG	136093,8528		
	FOR	132474,1677		
	JOY	146249,9020		

Extreme Values

			Case Number	Value
EMG	Highest	1	47	220920,54
		2	19	215644,59
		3	88	196844,66
		4	46	196033,17
		5	91	182927,60
	Lowest	1	58	70073,89
		2	67	71268,00
		3	71	72393,74
		4	69	72726,11
		5	85	74874,07
FOR	Highest	1	20	192168,57
		2	45	174706,77
		3	2	174587,77
		4	16	170894,53
		5	42	167795,39
	Lowest	1	72	86129,73
		2	71	87704,81
		3	73	88176,47
		4	64	90773,06
		5	17	92249,24
JOY	Highest	1	76	201934,94
		2	80	190651,90
		3	74	176838,34

Extreme Values

		Case Number	Value
	4	77	175940,62
	5	63	171715,63
Lowest	1	99	79345,41
	2	16	92405,21
	3	102	95797,97
	4	101	95865,46
	5	7	96931,19

Tests of Normality

	Kolmogorov-Smirnov[a]			Shapiro-Wilk		
	Statistic	df	Sig.	Statistic	df	Sig.
EMG	,081	102	,099	,942	102	,000
FOR	,076	102	,156	,948	102	,001
JOY	,079	102	,119	,983	102	,219

a. Lilliefors Significance Correction

EMG

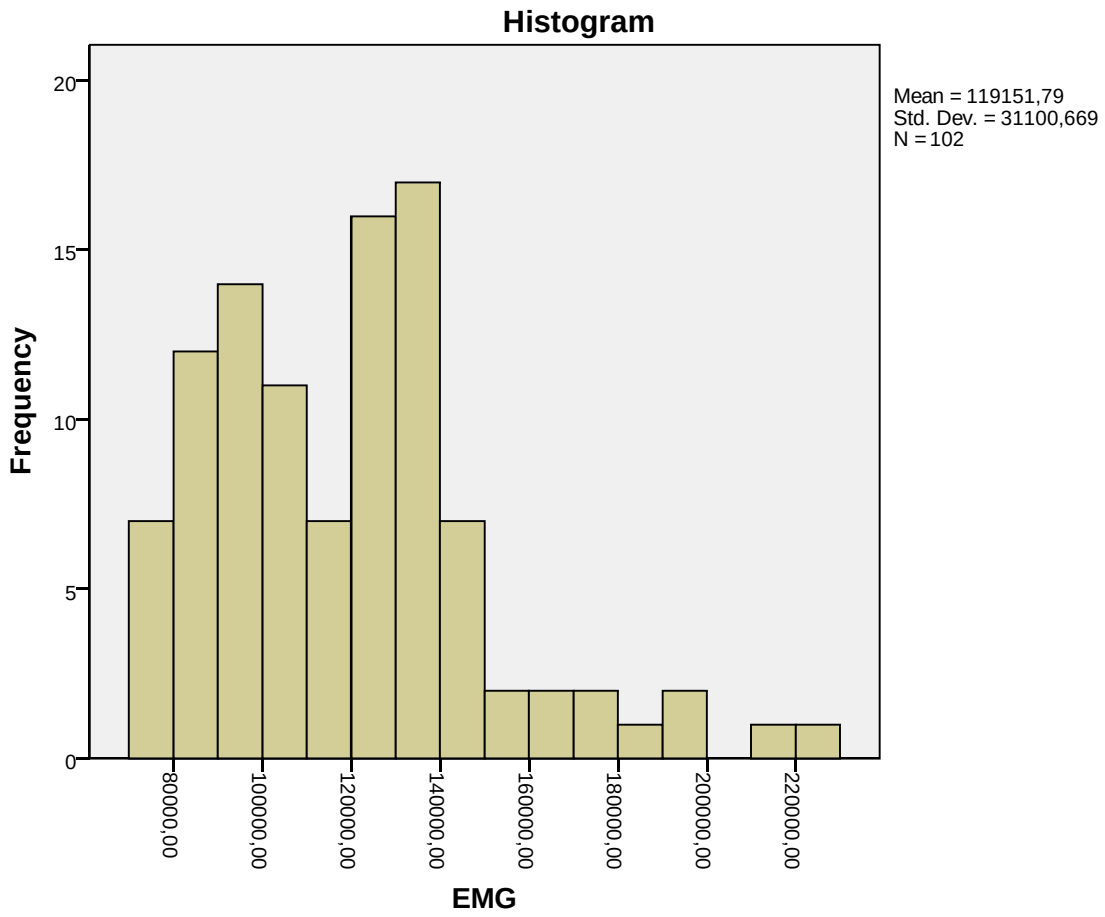

EMG Stem-and-Leaf Plot

Frequency	Stem &	Leaf
7,00	7 .	0122499
12,00	8 .	023355667889
14,00	9 .	01111222446899
11,00	10 .	00134677999
7,00	11 .	1134467
16,00	12 .	1122555666799999
17,00	13 .	00122235567888999
7,00	14 .	1245669
2,00	15 .	05
2,00	16 .	05
2,00	17 .	38
1,00	18 .	2
2,00	19 .	66
2,00 Extremes		(>=215645)

Stem width: 10000,00
Each leaf: 1 case(s)

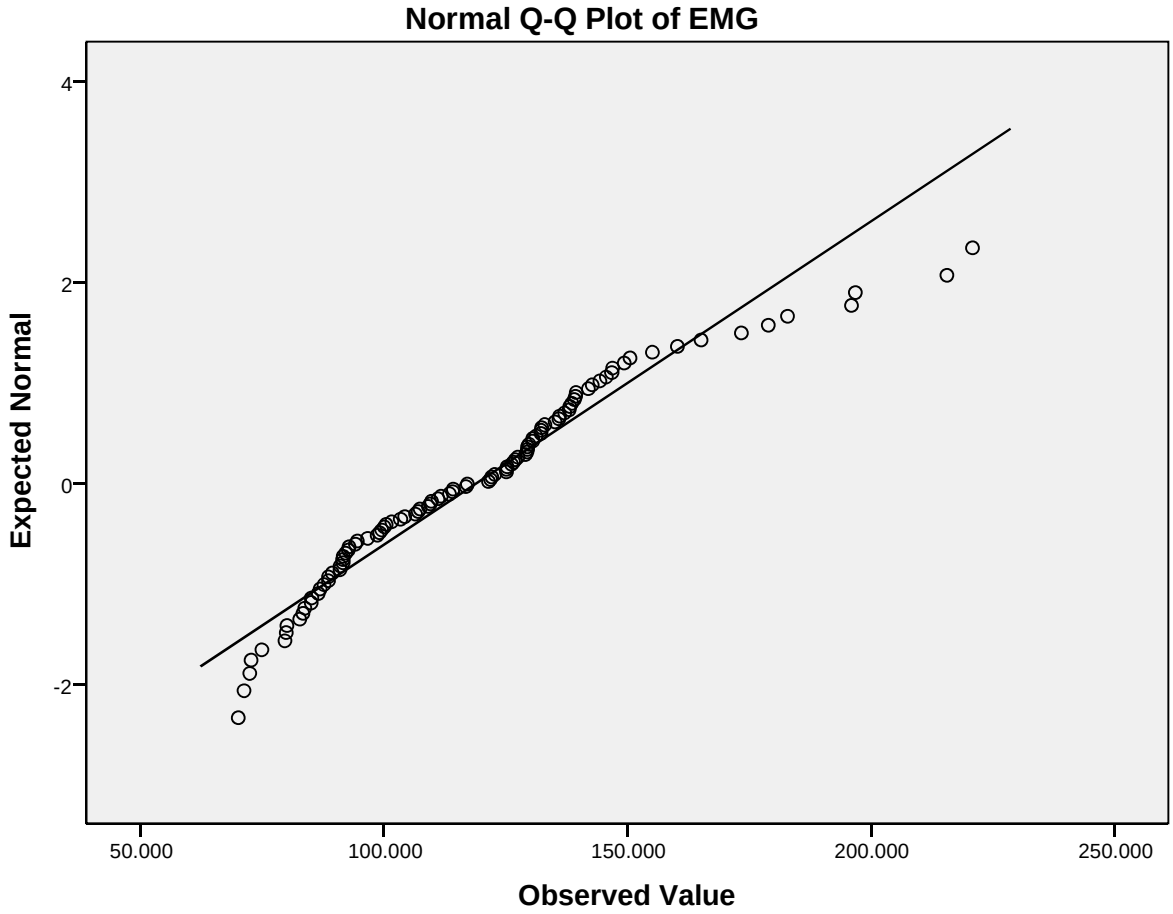
Normal Q-Q Plot of EMG
Expected Normal
4
2
0
-2
50.000
100.000
150.000
200.000
250.000
Observed Value

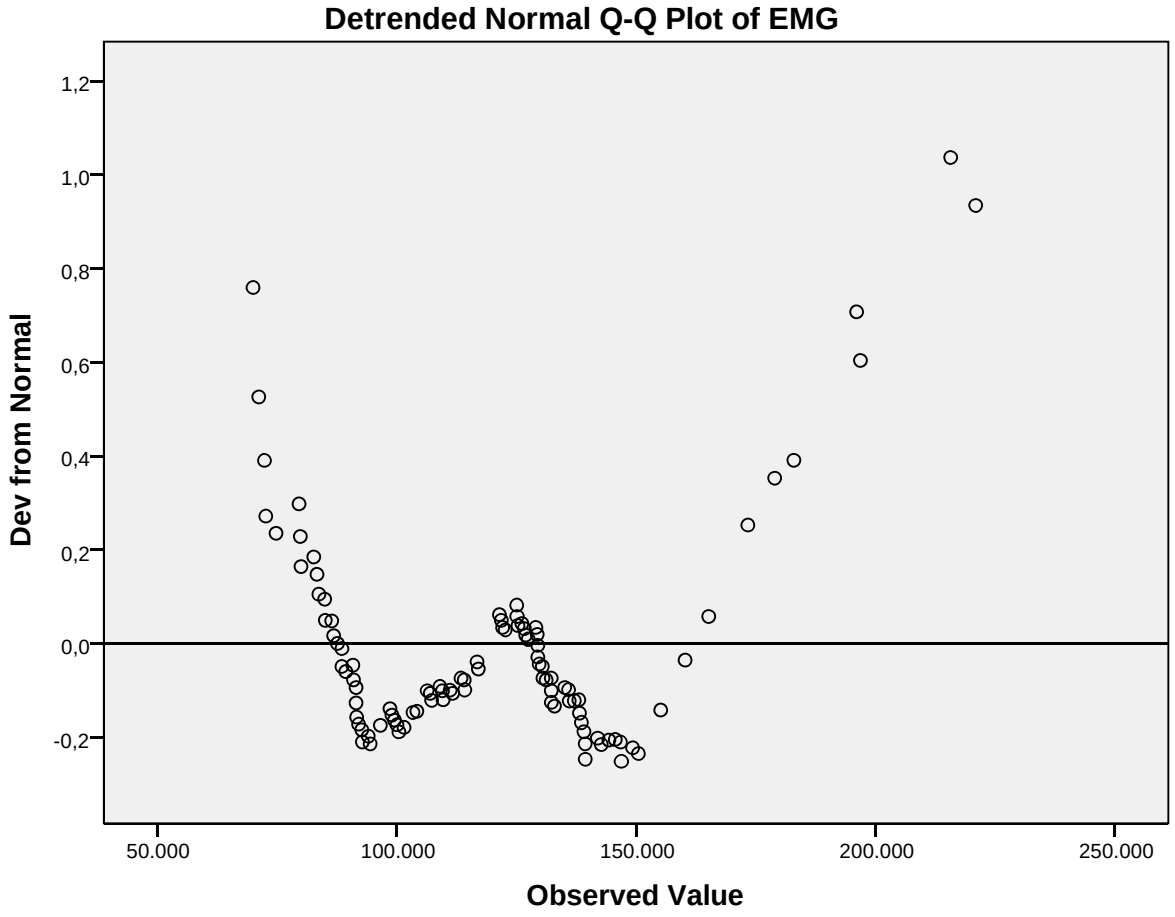
Detrended Normal Q-Q Plot of EMG
Dev from Normal
1,2
1,0
0,8
0,6
0,4
0,2
0,0
-0,2
50.000
100.000
150.000
200.000
250.000
Observed Value

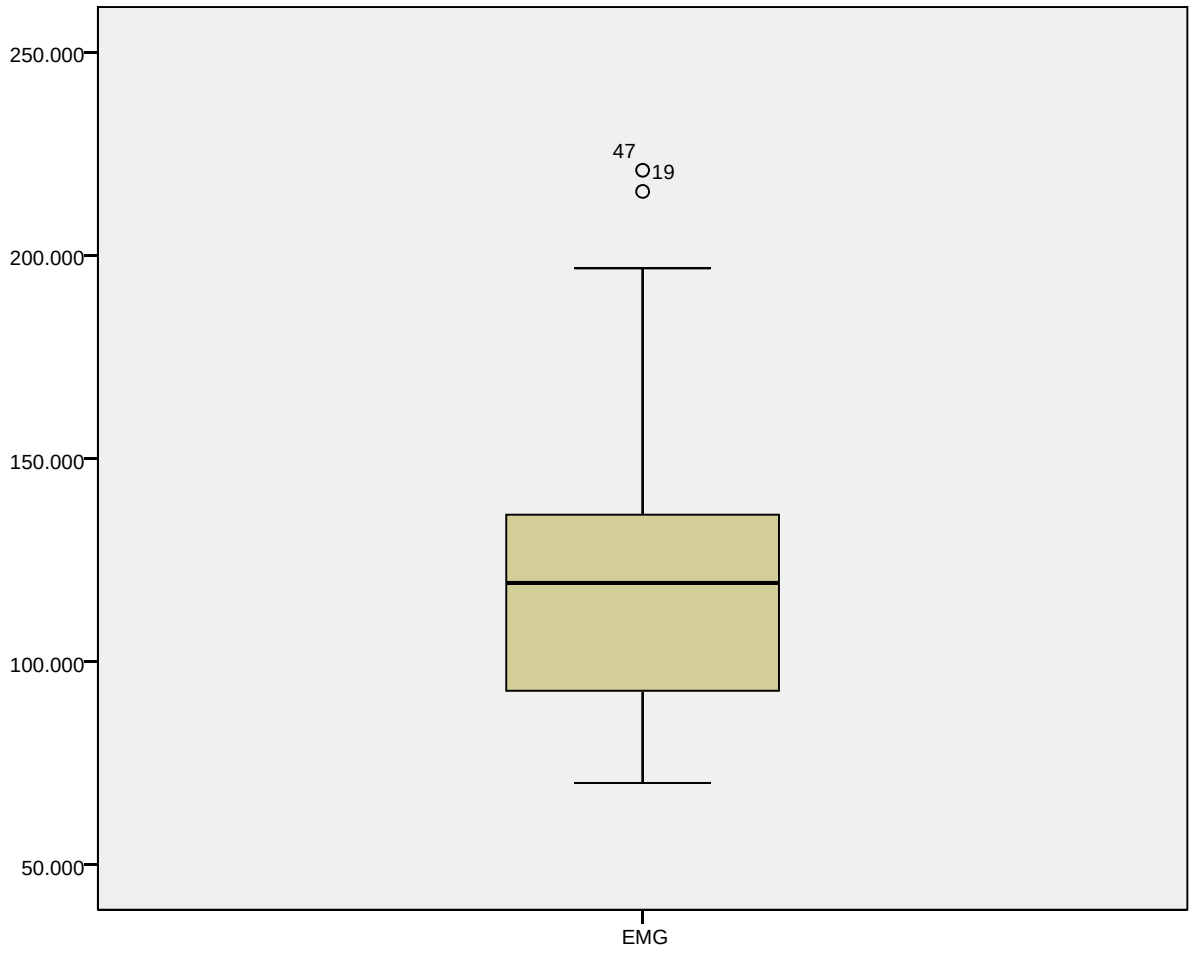

FOR

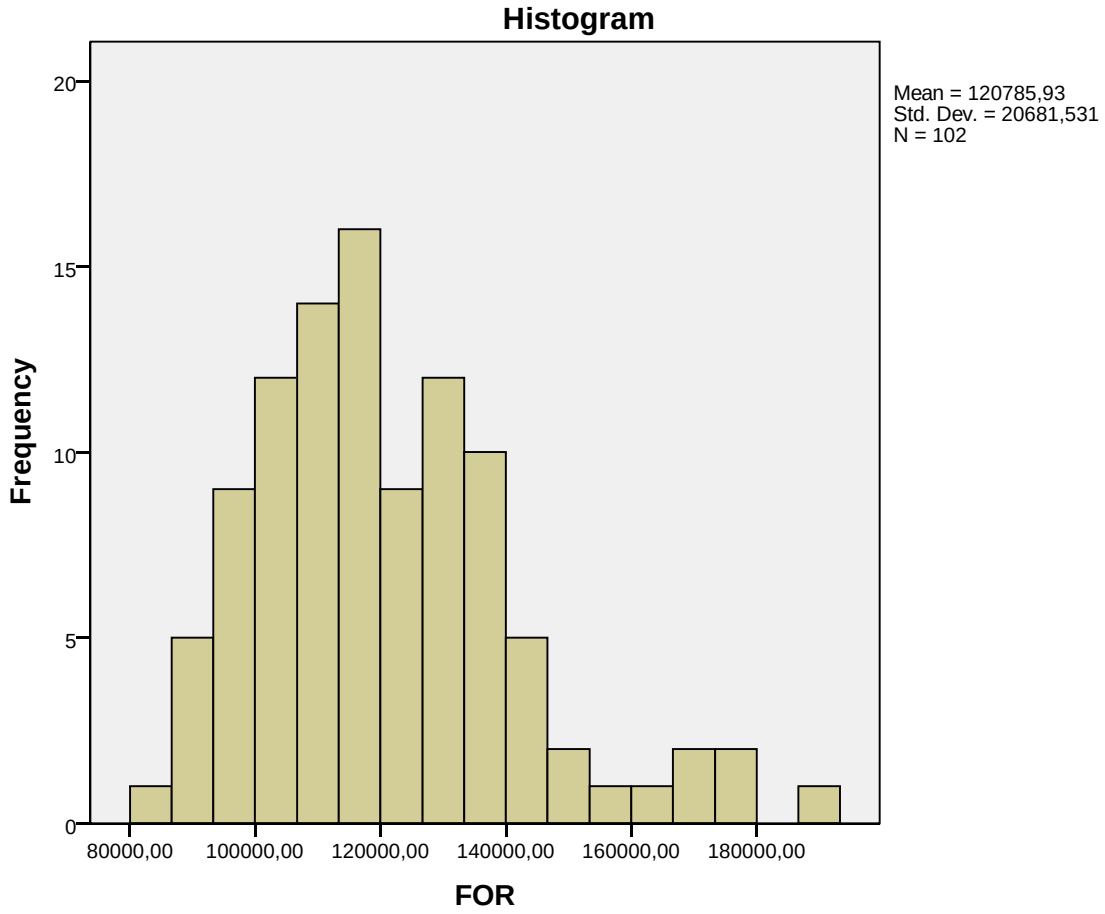

FOR Stem-and-Leaf Plot

Frequency	Stem &	Leaf
3,00	8 .	678
5,00	9 .	02244
7,00	9 .	6778889
9,00	10 .	111112333
10,00	10 .	5567788999
9,00	11 .	011112234
14,00	11 .	55777778888899
8,00	12 .	01233444
8,00	12 .	67778899
7,00	13 .	0012234
8,00	13 .	56677778
4,00	14 .	0134
3,00	14 .	578
,00	15 .	
1,00	15 .	8
,00	16 .	

```
    2,00       16 .  67
    1,00       17 .  0
    3,00 Extremes    (>=174588)

Stem width:  10000,00
Each leaf:       1 case(s)
```

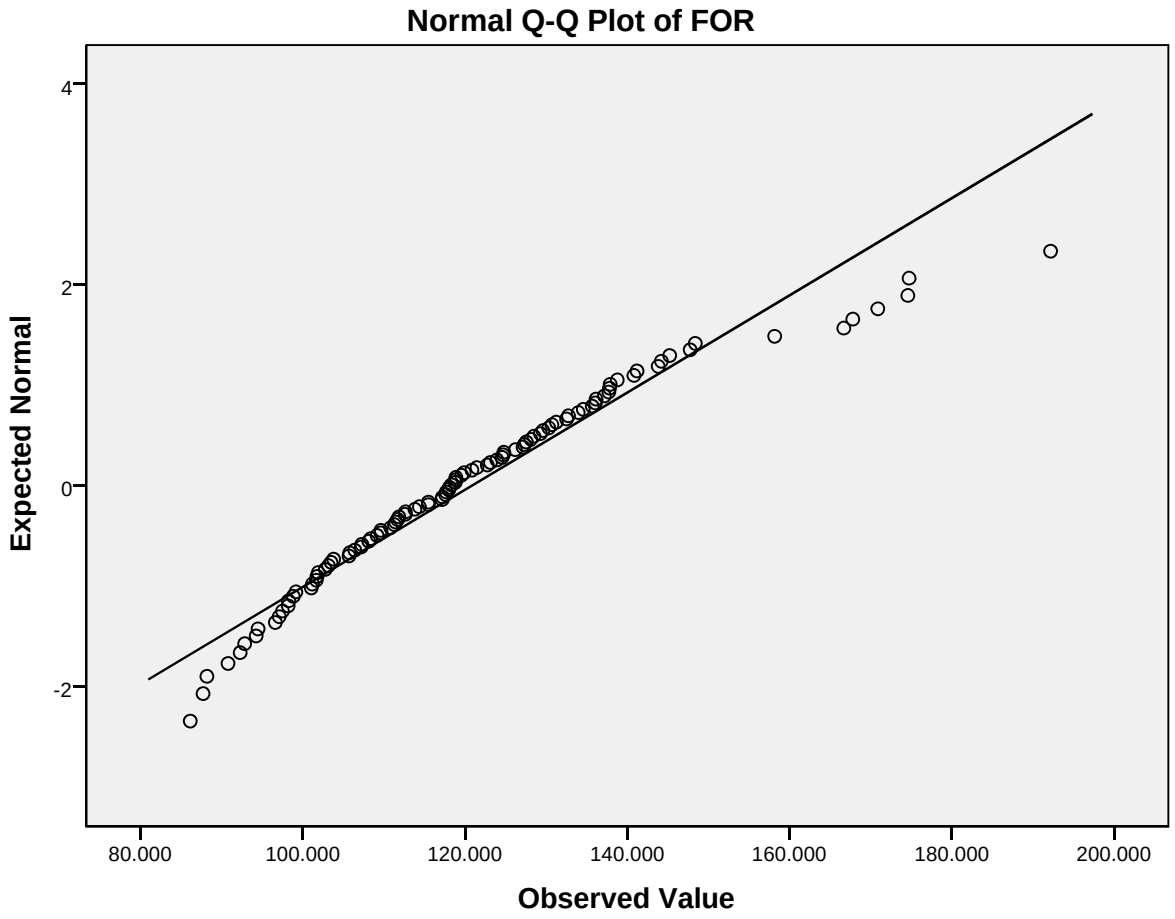

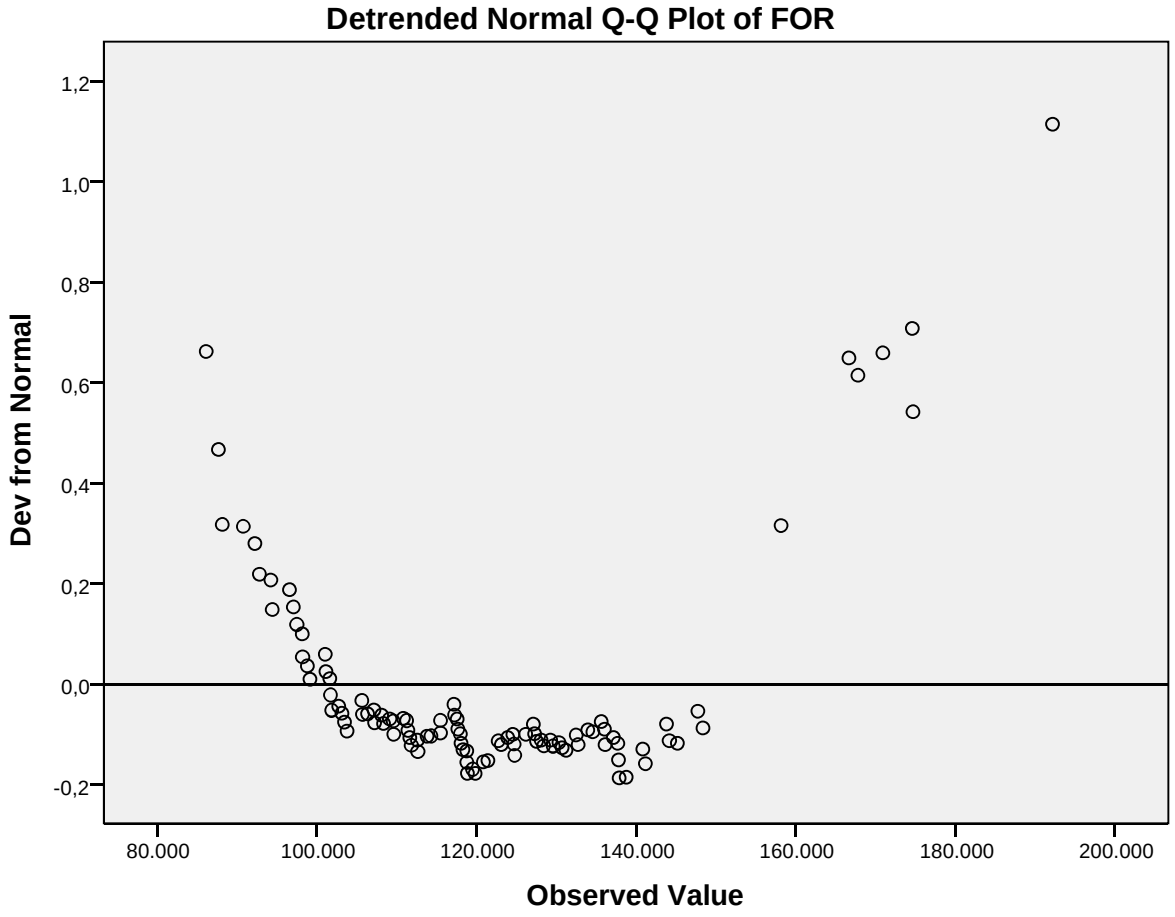
Detrended Normal Q-Q Plot of FOR
Dev from Normal
1,2
1,0
0,8
0,6
0,4
0,2
0,0
-0,2
80.000
100.000
120.000
140.000
160.000
180.000
200.000
Observed Value

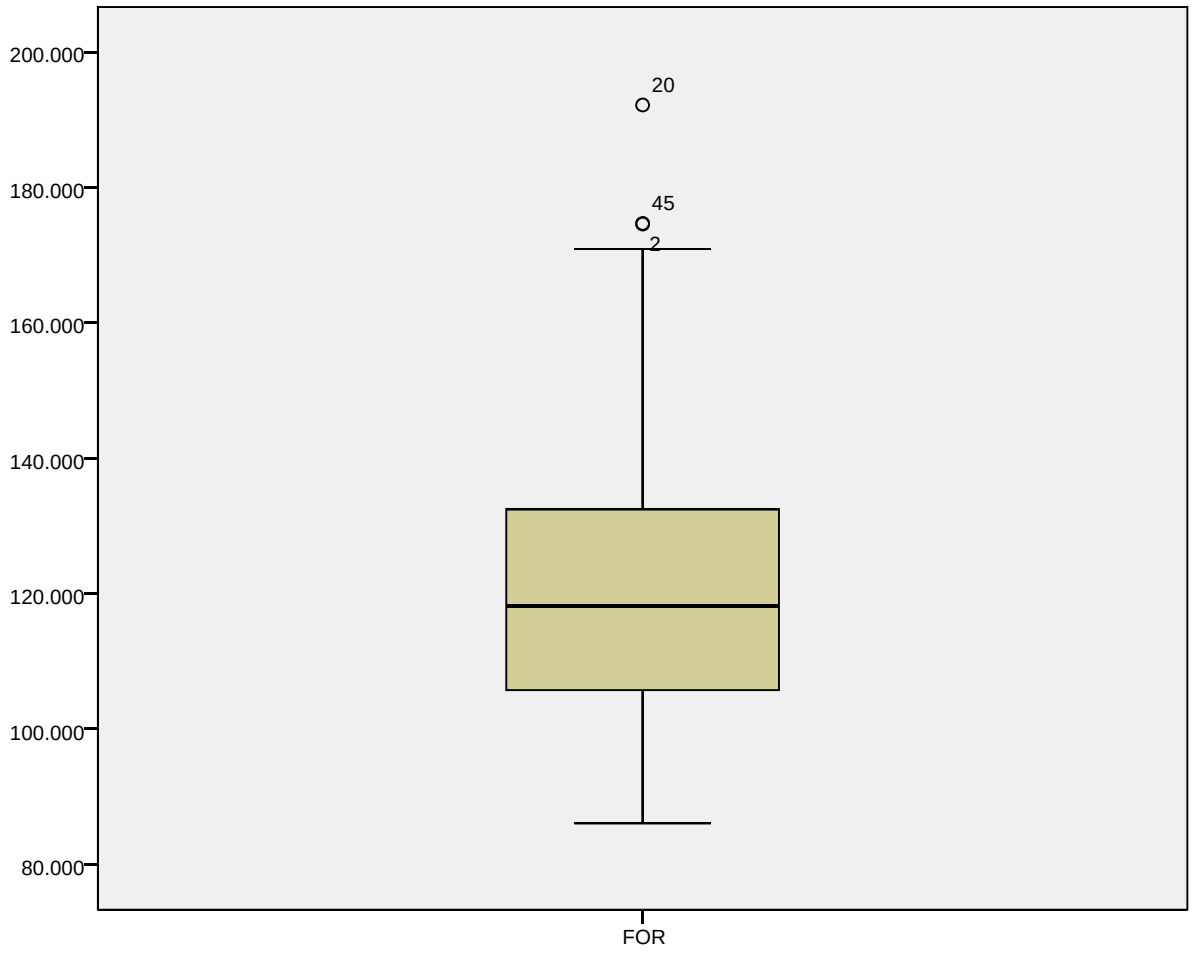

JOY

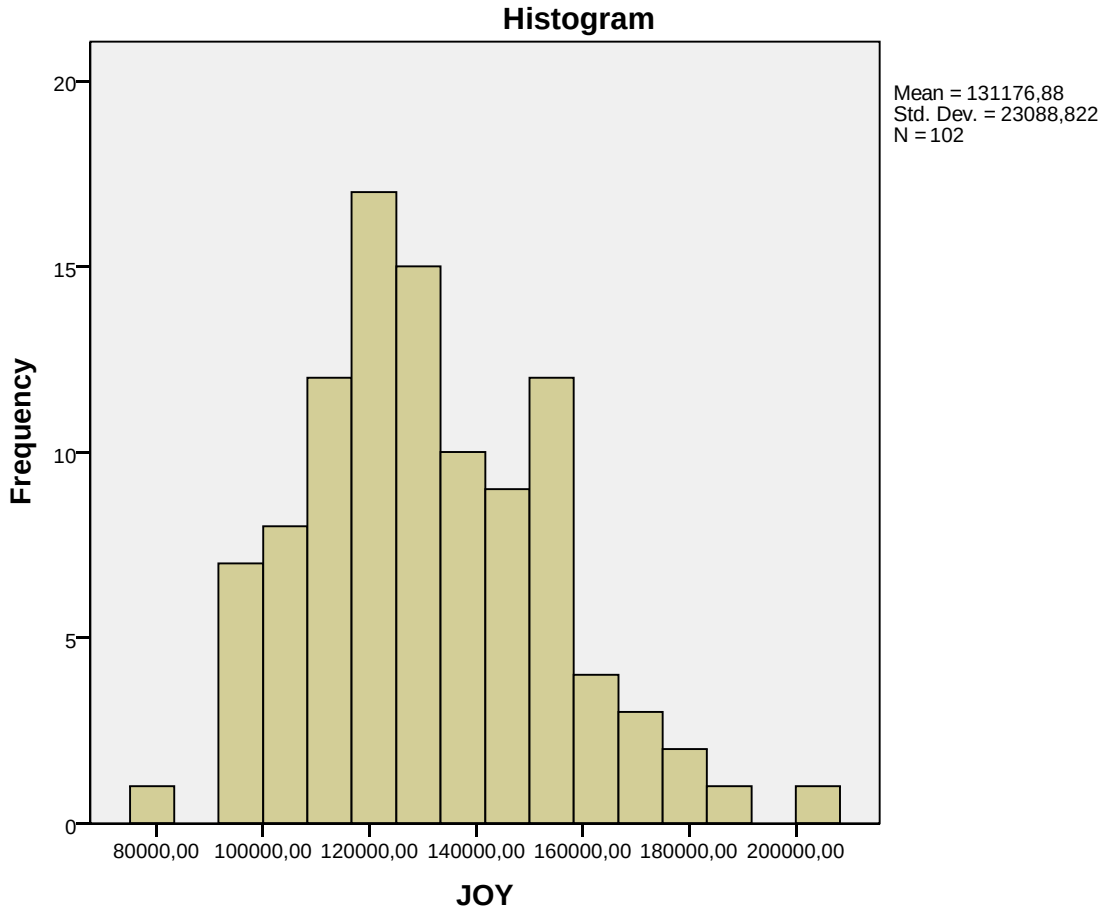

JOY Stem-and-Leaf Plot

Frequency	Stem &	Leaf
1,00	7 .	9
,00	8 .	
7,00	9 .	2556789
8,00	10 .	01223448
18,00	11 .	000113334455667899
20,00	12 .	00012234444667778899
14,00	13 .	00001233477799
11,00	14 .	00223346668
12,00	15 .	011334556777
4,00	16 .	0456
5,00	17 .	01156
,00	18 .	
1,00	19 .	0
1,00 Extremes		(>=201935)

Stem width: 10000,00

Each leaf: 1 case(s)

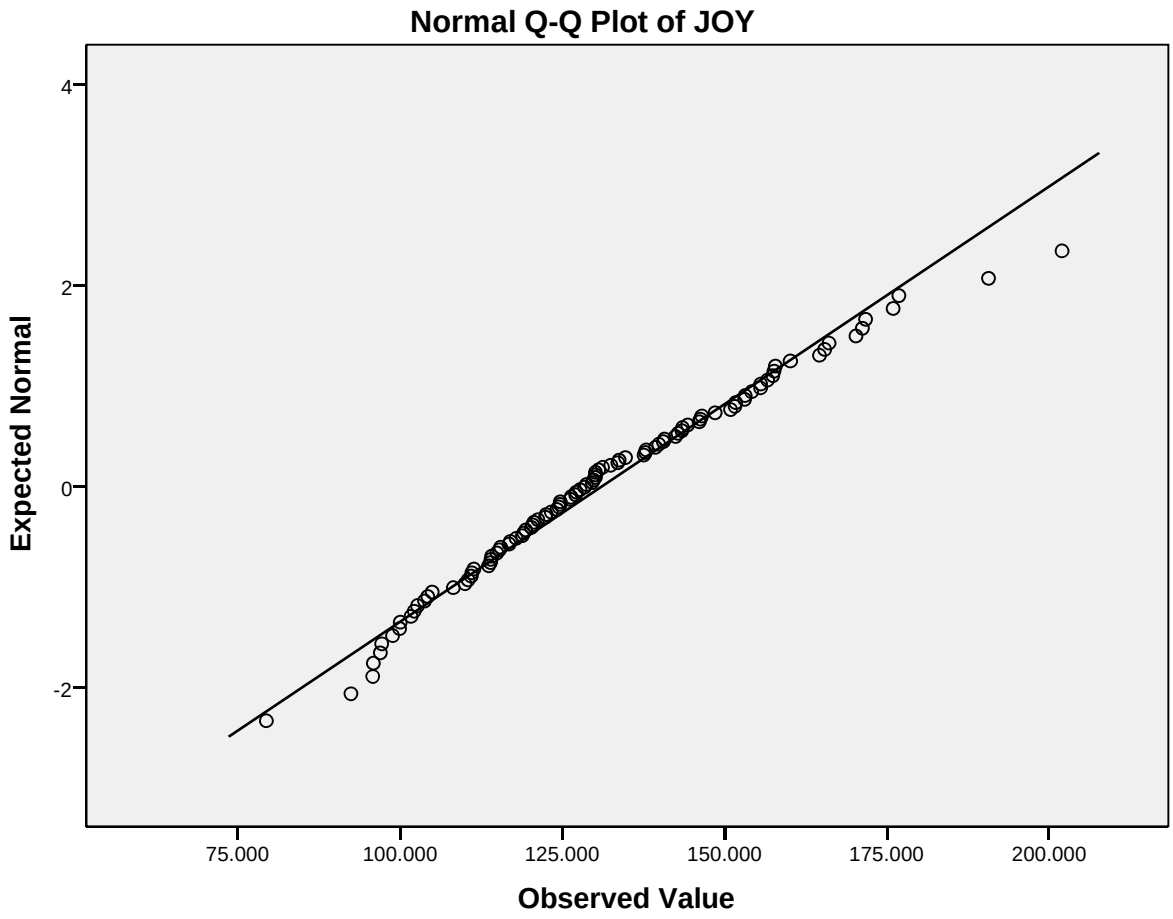

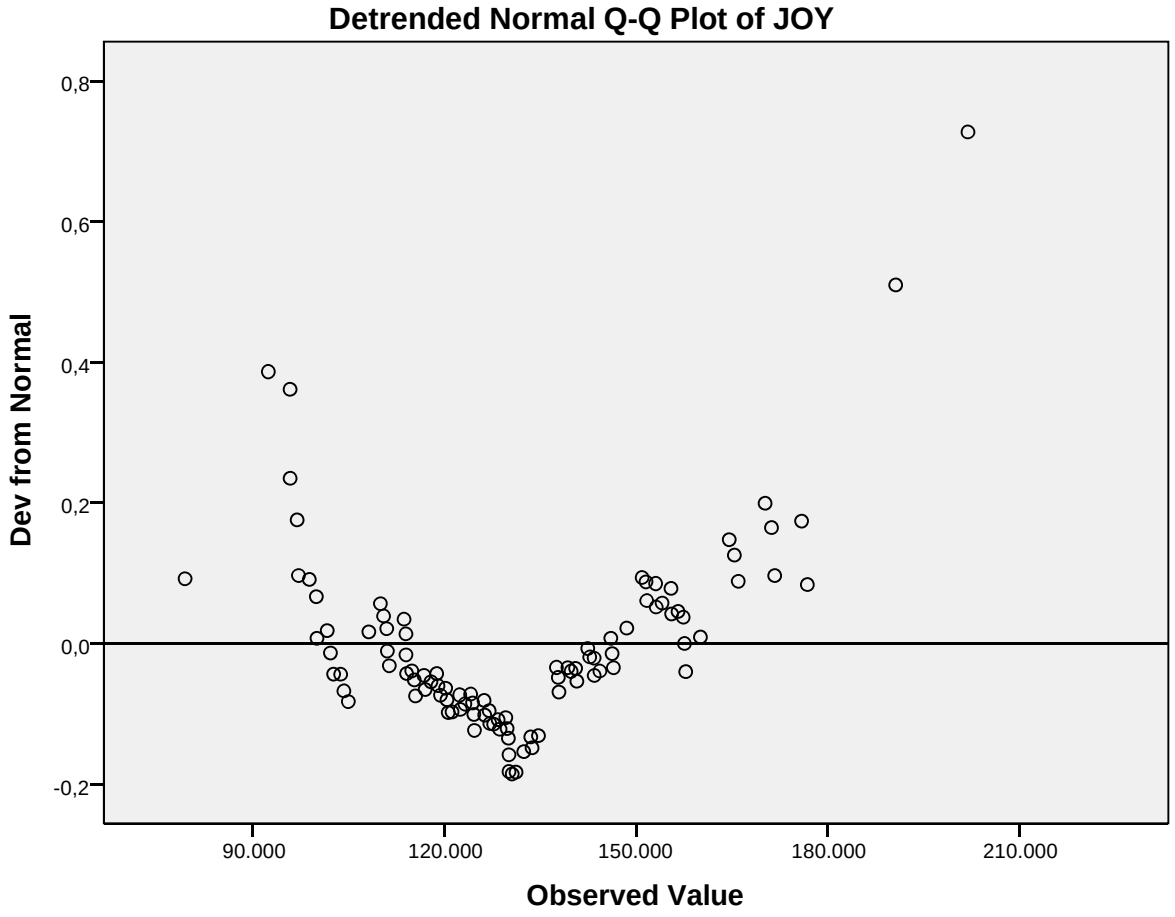
Detrended Normal Q-Q Plot of JOY
Dev from Normal
0,8
0,6
0,4
0,2
0,0
-0,2
90.000
120.000
150.000
180.000
210.000
Observed Value

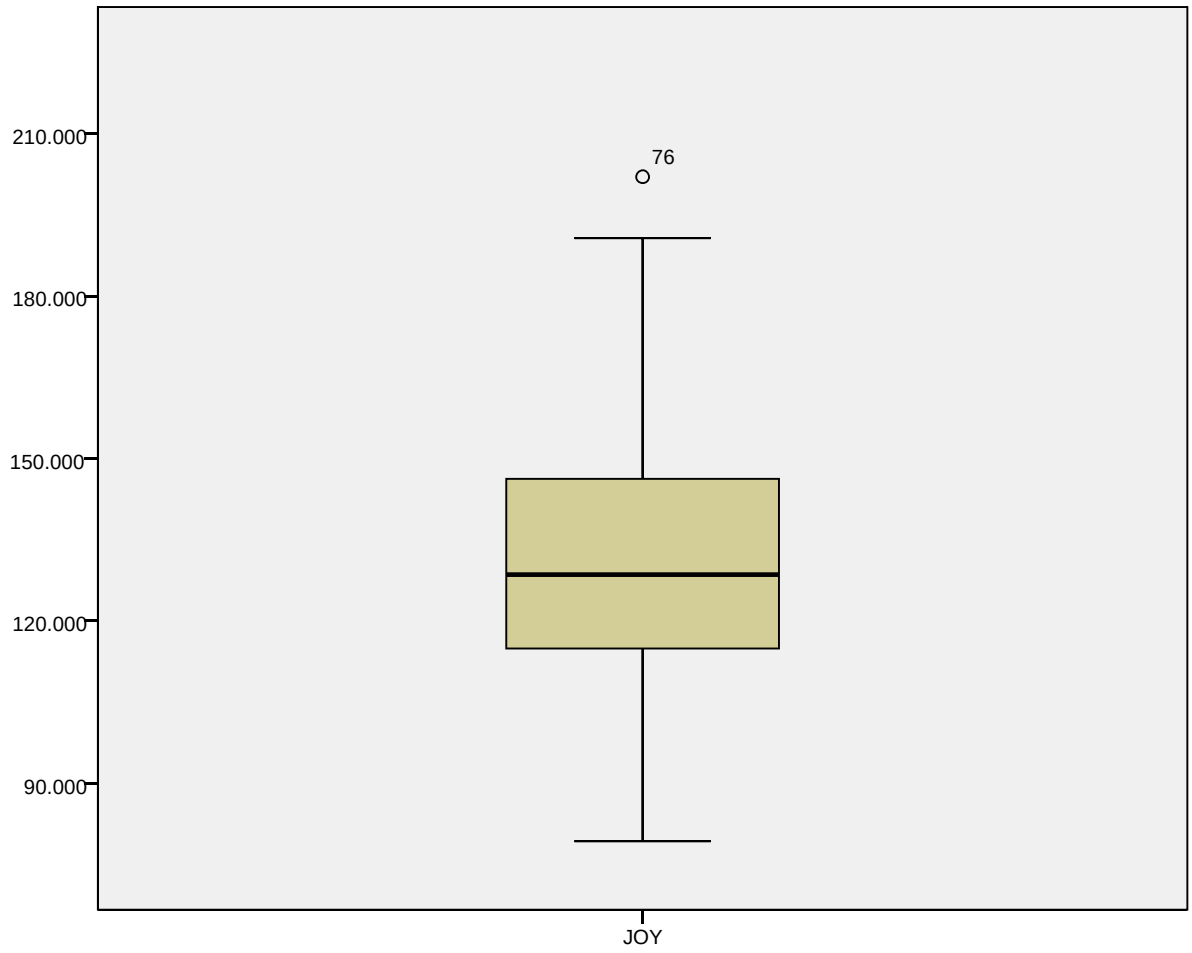


```
GLM EMG FOR JOY
  /WSFACTOR=Interface 3 Polynomial
  /METHOD=SSTYPE(3)
  /PLOT=PROFILE(Interface)
  /EMMEANS=TABLES(Interface) COMPARE ADJ(BONFERRONI)
  /PRINT=DESCRIPTIVE
  /CRITERIA=ALPHA(.05)
  /WSDESIGN=Interface.
```

General Linear Model

```
[DataSet1]
```

Within-Subjects Factors

Measure: MEASURE_1

Interface	Dependent Variable
1	EMG
2	FOR
3	JOY

Descriptive Statistics

	Mean	Std. Deviation	N
EMG	117284,3191	27882,08398	96
FOR	119425,2082	18119,94216	96
JOY	130879,5418	22287,83436	96

Multivariate Tests[a]

Effect		Value	F	Hypothesis df	Error df	Sig.
Interface	Pillai's Trace	,133	7,202[b]	2,000	94,000	,001
	Wilks' Lambda	,867	7,202[b]	2,000	94,000	,001
	Hotelling's Trace	,153	7,202[b]	2,000	94,000	,001
	Roy's Largest Root	,153	7,202[b]	2,000	94,000	,001

a. Design: Intercept
Within Subjects Design: Interface

b. Exact statistic

Mauchly's Test of Sphericity[a]

Measure: MEASURE_1

Within Subjects Effect	Mauchly's W	Approx. Chi-Square	df	Sig.	Epsilon[b] Greenhouse-Geisser
Interface	,849	15,390	2	,000	,869

Mauchly's Test of Sphericity[a]

Measure: MEASURE_1

Within Subjects Effect	Epsilon[b] Huynh-Feldt	Lower-bound
Interface	,884	,500

Tests the null hypothesis that the error covariance matrix of the orthonormalized transformed dependent variables is proportional to an identity matrix.

a. Design: Intercept
Within Subjects Design: Interface

b. May be used to adjust the degrees of freedom for the averaged tests of significance. Corrected tests are displayed in the Tests of Within-Subjects Effects table.

Tests of Within-Subjects Effects

Measure: MEASURE_1

Source		Type III Sum of Squares	df	Mean Square	F
Interface	Sphericity Assumed	10259687836	2	5129843918	8,862
	Greenhouse-Geisser	10259687836	1,738	5904591478	8,862
	Huynh-Feldt	10259687836	1,767	5805824651	8,862
	Lower-bound	10259687836	1,000	10259687836	8,862
Error(Interface)	Sphericity Assumed	1.100E+11	190	578856299.7	
	Greenhouse-Geisser	1.100E+11	165,070	666279526.0	
	Huynh-Feldt	1.100E+11	167,878	655134586.4	
	Lower-bound	1.100E+11	95,000	1157712599	

Tests of Within-Subjects Effects

Measure: MEASURE_1

Source		Sig.
Interface	Sphericity Assumed	,000
	Greenhouse-Geisser	,000
	Huynh-Feldt	,000
	Lower-bound	,004
Error(Interface)	Sphericity Assumed	
	Greenhouse-Geisser	
	Huynh-Feldt	
	Lower-bound	

Tests of Within-Subjects Contrasts

Measure: MEASURE_1

Source	Interface	Type III Sum of Squares	df	Mean Square	F	Sig.
Interface	Linear	8871843881	1	8871843881	11,046	,001
	Quadratic	1387843956	1	1387843956	3,914	,051
Error(Interface)	Linear	76301109707	95	803169575.9		
	Quadratic	33681587232	95	354543023.5		

Tests of Between-Subjects Effects

Measure: MEASURE_1

Transformed Variable: Average

Source	Type III Sum of Squares	df	Mean Square	F	Sig.
Intercept	4.324E+12	1	4.324E+12	9721,471	,000
Error	42253897810	95	444777871.7		

Estimated Marginal Means

Interface

Estimates

Measure: MEASURE_1

Interface	Mean	Std. Error	95% Confidence Interval	
			Lower Bound	Upper Bound
1	117284,319	2845,703	111634,884	122933,754
2	119425,208	1849,359	115753,767	123096,650
3	130879,542	2274,743	126363,607	135395,477

Pairwise Comparisons

Measure: MEASURE_1

(I) Interface	(J) Interface	Mean Difference (I-J)	Std. Error	Sig.[b]	95% Confidence Interval for Difference[b]	
					Lower Bound	Upper Bound
1	2	-2140,889	3068,578	1,000	-9619,353	5337,574
	3	-13595,223*	4090,562	,004	-23564,375	-3626,071
2	1	2140,889	3068,578	1,000	-5337,574	9619,353
	3	-11454,334*	3166,962	,001	-19172,569	-3736,098
3	1	13595,223*	4090,562	,004	3626,071	23564,375
	2	11454,334*	3166,962	,001	3736,098	19172,569

Based on estimated marginal means

*. The mean difference is significant at the ,05 level.

b. Adjustment for multiple comparisons: Bonferroni.

Multivariate Tests

	Value	F	Hypothesis df	Error df	Sig.
Pillai's trace	,133	7,202[a]	2,000	94,000	,001
Wilks' lambda	,867	7,202[a]	2,000	94,000	,001
Hotelling's trace	,153	7,202[a]	2,000	94,000	,001
Roy's largest root	,153	7,202[a]	2,000	94,000	,001

Each F tests the multivariate effect of Interface. These tests are based on the linearly independent pairwise comparisons among the estimated marginal means.

a. Exact statistic

Profile Plots

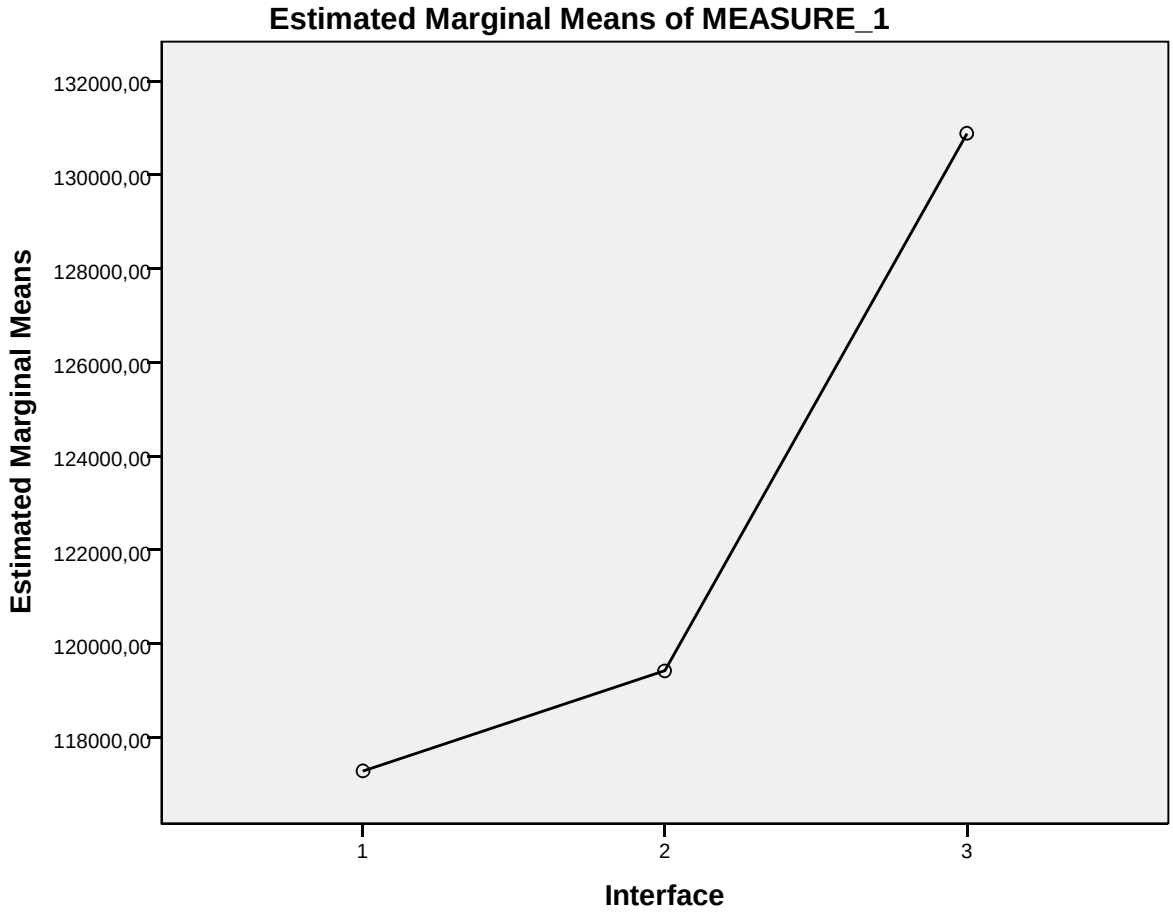
Estimated Marginal Means of MEASURE_1
Estimated Marginal Means
132000,00
130000,00
128000,00
126000,00
124000,00
122000,00
120000,00
118000,00
1
2
3
Interface